RECEPTOR KINASE INTERACTIONS IN BACTERIAL CHEMOTAXIS REVEALED BY PULSED DIPOLAR ESR SPECTROSCOPY

A Dissertation

Presented to the Faculty of the Graduate School

of Cornell University

In Partial Fulfillment of the Requirements for the Degree of

Doctor of Philosophy

by

Jaya Bhatnagar

August 2009

RECEPTOR KINASE INTERACTIONS IN BACTERIAL CHEMOTAXIS REVEALED BY PULSED DIPOLAR ESR SPECTROSCOPY

Jaya Bhatnagar, Ph. D.

Cornell University 2009

Bacterial chemotaxis refers to the movement of bacteria under influence of attractants and repellents. This signal transduction pathway is characterized by incredible gain, sensitivity and co-operativity. The extra-cellular domains of receptors transmit the signal from outside the cell into the cytoplasm where it is further processed by the signaling complex of histidine kinase CheA, coupling protein CheW and cytoplasmic domains of receptors. Structural determination of individual protein components and their protein complexes is necessary to gain insight into the mechanism. In this work, we have used site-directed spin labeling and long-range distance restraints from Pulsed dipolar ESR spectroscopy to predict the structure of a ternary complex formed by CheA, CheW and the signaling domain of the receptor. We have developed a novel method to refine the structures of protein complexes from the distance restraints provided by pulsed dipolar ESR. Apart from determining the position of receptor in the ternary complex, our efforts have been directed towards understanding the change in orientations of CheA and CheW in the presence of receptor.

On a macroscopic scale, CheA, CheW and receptors form dense clusters at the poles of cell. We observed that CheA also self-associates in solution to some extent. We speculate that this self-association property of CheA may play a crucial role in

clustering of chemotaxis proteins in cell. We have successfully identified this binding interface with disulphide cross-linking and novel application of pulsed dipolar ESR signals that report on local spin concentrations.

BIOGRAPHICAL SKETCH

Jaya Bhatnagar was born and brought up in India. She completed her Masters in Integrated Chemistry from Indian Institute of Technology, Bombay in 2004. After coming to Cornell, she started to work on a collaborative project between research labs of Prof. Crane and Prof. Freed. The aim of the project was to determine the structure of a key ternary protein complex involved in chemotaxis signaling pathway. Among various biophysical and biochemical methods used to elucidate the structure, she extensively used pulsed dipolar Electron Spin Resonance Spectroscopy in her research work. In the initial part of the project, she also developed a novel method that performs rigid body refinement based on long range distance restraints. Numerous experimental ESR restraints were collected and used as input to the rigid body refinement program to predict the structure of the ternary complex. She also studied aggregation properties of histidine kinase CheA and identified a specific interface through which CheA self-associates.

I dedicate this work to my parents

ACKNOWLEDGMENTS

I would like to express my gratitude to all the people who helped and influenced me during my five years of PhD studies. I believe that it is crucial to find happiness both in professional and personal spheres of life and I consider myself very fortunate that at Cornell, I got this perfect combination.

I am very grateful to Brian and Prof. Freed for letting me work on the Chemotaxis project and for being amazing mentors. When I started this project, I felt very lost and absolutely had no idea about what will be in store for me since I did not have any background in biochemistry. But now, after five years, I feel sincerely grateful to Brian for giving me the initial push and encouraging me to learn all the new things. Throughout my time in the lab, I enjoyed every moment of this work. (Well, except for harvesting the cells which I still hate to do!) On a serious note, because of being a part of this lab, I have developed a strong interest in working with proteins, which I want to pursue in future.

I would like to thank Peter Borbat for his guidance and for teaching me many concepts about pulsed ESR.

As a graduate student, I spent most of the time in Brian's lab working with proteins and I feel very fortunate that I have made some very good friends in the process. In the initial period of my time in the lab, I am thankful for Gaby for teaching me the lab techniques and Bhumit for his patience in making me understand the concepts of biochemistry from the very scratch. Any other person would have simply given up on me!

When I look back over my time in the lab, I remember many happy memories/funny stories in the lab. I would miss my giggling partner Abiola, with whom I shared a wide range of conversations: from silly things to serious discussions

about life. Sudhamshu or Suddu has been a good friend and helped me a lot when I was applying for jobs. I would remember him the most for his silly comments after listening to which sometimes will leave me completely speechless without an answer, but each time will make me laugh really hard! I want to thank Bhumit and Mike for many enjoyable conversations and inspiring me with their optimistic attitude. They both have really good sense of humor which kept the atmosphere of the lab lively. I have always enjoyed the company of Anand, who over a short period of time became a good friend of mine. I want to thank him for always giving me company for the coffee trips to Mann library and sharing generously with me all the stored eatables in the desk of his drawer. It has been a pleasure to know Xiaoxiao, Doowon, Pete, Ria, Joanne, Tom and Ken too.

I was fortunate to have a very close friend circle outside the lab without whom I cannot imagine my stay at Cornell. All my friends: Debo, Som, Kalyan, Deepti, Lekha, Rusty, and Amrita have supported me in the ups and down of my graduate life at Cornell. I still can not forget the incident when Rusty, Kalyan and Lekha came all the way to NY city just to give me a big surprise. Debo and Lekha have been incredible apartment-mates and I thank them for making so many delicious meals. I am inspired by Debo who always has a smile on her face, Lekha who is very simple and straightforward and Deepti who finds great pleasure from little things in life. I admire Rusty for his extraordinary lively nature, for his ability to enjoy life with so much of energy. He has an inherent talent for being funny and telling jokes at slightest instance and is clearly the funniest person I have met so far. Rusty also has a sensitive shade to his personality and I thank him for supporting me during my low times by offering his company on my trip to NJ.

I thank Som for being a very sensitive and caring friend, for having several interesting scientific discussions with me, for listening to all day to day lab events:

minor or major, and the associated frustration or joy associated with each of them, for trying his best to teach me to play tennis (yes, I failed to learn), for always inviting me for dinner on the day of his cooking turn, and most importantly, for tolerating my indecisive nature! He would patiently listen to my confusing thought process and help me to pick the option that would be best for me. For this, and for many other things I would always be grateful to him.

My friendship with Kalyan has been the oldest among all my friends in Ithaca. He has constantly entertained me with his sarcastic humor of which I have been a huge fan. I am thankful to him for always being there for me, for giving me wise advices, for helping me to look at the practical side of things, for being a good listener, and to sum it all, for always taking care of me like a family member.

Over the last two years, I got the opportunity to know Amrita Hazra, the bubbly girl in the Begley's lab and found an amazing friend in her. I thank her for giving me courage and hope in my depressing moments and her incredible ability to make me smile and forget my troubles and for being such a remarkable person herself.

Finally, I would like to express my gratitude towards my parents, sister and brother-in-law who made this day possible for me. It is their constant support and faith in me that encouraged me to perform better and strive for success in life. It is their understanding nature and emotional support that motivated me to come so far from home and pursue graduate studies at Cornell.

TABLE OF CONTENTS

LIST OF FIGURES

LIST OF TABLES

CHAPTER 1

INTRODUCTION

1.1 Introduction to Chemotaxis

Chemotaxis refers to the phenomenon by which bacteria move under the influence of chemicals which can be either attractants or repellants. To date, at least three modes of motility have been identified: twitching, gliding and flagella-dependent[1].Each of these modes shares a general control mechanism which is highly conserved among all the species. The signal transduction of chemotaxis has been studied most extensively in the enteric bacteria *Escherichia coli* since its discovery in 1975[2]. The motility of *E.coli* is determined by the sense of rotation of its flagella. In a chemically isotropic environment, the bacterial motion is composed of "runs", where the bacterium moves forward with its flagella bundled together, and "tumbles" where this bundle falls apart and the bacterium moves in a new direction. In the presence of attractants, the runs in the direction of increasing ligand concentration get extended and the bacterium moves favorably towards attractants. In *E.coli*, the runs and tumbles are characterized by counter-clockwise and clockwise rotation of the flagella respectively.

Chemotaxis, like most of the signal transduction pathways in bacteria is a "two-component" system where CheA is the sensor kinase and CheY is the respons regulator. The external signal is detected by the extra-cellular domains of the methyl-accepting proteins (MCP) or chemoreceptors. Thereafter, the signal is integrated and processed inside the cell by a complex of proteins formed by the signaling domain of chemoreceptors, adaptor protein CheW and CheA. The former two proteins regulate the kinase activity of CheA. In *E.coli*, the kinase gets autophosphorylated in presence

of repellents, which is followed by the transfer of the phosphate group to the response regulator CheY(Figure 1.1).

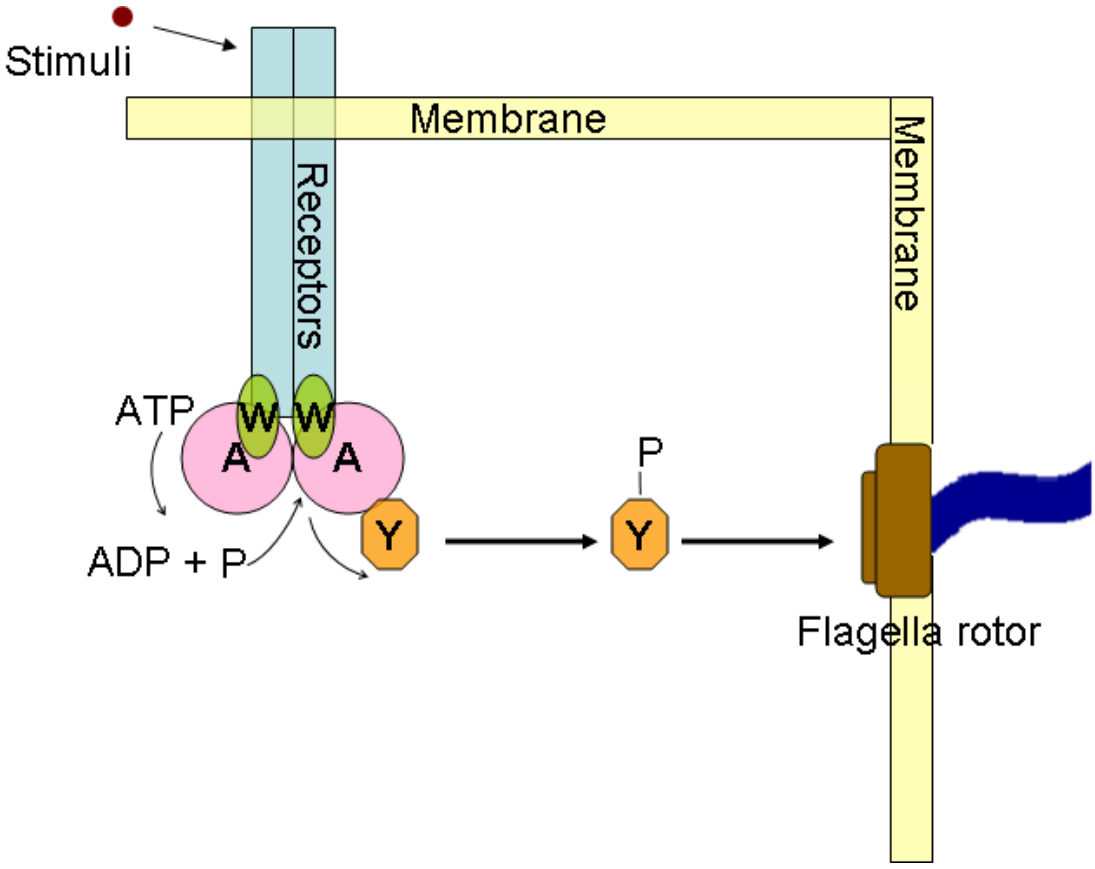

Figure1.1. Schematic diagram of the Chemotaxis pathway. The extracellular part of receptor sense the external stimuli and transmit the signal into the cytoplasm. The signaling domain of receptor interacts with CheA and CheW. Activation of kinase results in autophosphorylation and transfer of phosphate group to response regulator CheY.

Phosphorylated CheY then interacts with the flagella rotor which leads to the clockwise rotation of the flagella. This complete relay comprises the excitation part of

the chemotaxis pathway. For the bacteria to be able to continuously sense changes in ligand concentration, it is essential that the concentration of phosphorylated CheY reduces to the basal level over time. This process is called adaptation and is determined by the methylation state of receptors. The adaptation mechanism affects the kinase activity in a manner that balances out the effect due to stimuli. For instance in *E.coli*, while the presence of repellents increases the kinase activity (kinase "on" state) on one hand, on the other, it also results in methylation of receptors which leads to decrease in kinase activity (kinase "off" state) over time. The timescales of excitation and adaptation process are drastically different. Excitation is very fast and occurs in a fraction of second[3], while adaptation takes longer time, anywhere between several seconds to minutes depending upon the concentration of ligand[4,5].

The result of interaction of phosphorylated CheY with the flagella rotor is unique to the organism, for example in *B.subtilis*, it causes smooth swimming of the bacteria[6]. Chemotaxis proteins from a hypertheromophilic organism *T.maritima* share more identity with their homologues in *B.subtilis* than in *E.coli* suggesting that the chemotaxis system is more similar to *B.subtilis*[7].

The chemotaxis pathway is particularly remarkable for its high sensitivity, gain and cooperativity. In *E.coli*, the stimulus signal is amplified by 50 times [8]and the bacteria are able to respond to ligand concentrations varied between nanomolar to millimolar range[9]. Due to this reason, chemotaxis has remained an attractive signaling pathway for study.

1.2 Molecular components of the ternary complex

The key to understanding the regulation of kinase activity lies in elucidating the structure of the ternary complex formed with CheW and receptors. But before we investigate the whole complex, it is necessary to understand the properties of the

individual components. Fortunately, a lot of structural information is available for each of them. CheA has five domains, labeled P1 to P5 and each has a separate function (Figure 1.2). The P1 domain contains the conserved histidine which gets phosphorylated, the P2 domain docks CheY for phosphate transfer to CheY, P3 is the dimerization domain, P4 is the kinase domain which binds ATP and P5 is the regulatory domain. In 1999, the structure of a CheAΔ289 (domains P3-P4-P5 together) revealed relative orientations of the three domains and different subunit conformations in the dimer suggested flexibility around the hinges that connect the three domains[10]. The structures of P1 [11,12] and P2 domains[13] have been determined in isolation. The structure of P2 domain in complex with CheY has also been determined.[14].

CheW is composed of two β barrel like domains and is structurally similar to the regulatory domain (P5) of CheA. CheW is unique in possessing many hydrophobic surfaces which perhaps allows it to have multiple protein interactions. The ends of the two subdomain are also potential binding interfaces due to the presence of hydrophobic residues. Chemoreceptors are homodimers and the cytoplasmic region is composed of four-helical bundles arranged in coiled-coil domain manner [18] (Figure 1.3).

The signaling domain region of the receptor is highly conserved among all species and is known to interact with CheA and CheW[20]. Extensive biochemical [21], crystallographic [18 22] and cryo-EM tomography studies [23,24 25] have determined that receptors associate as trimer of dimers in solution as well as in the cell.

1.3 CheA, CheW and Receptors form dense clusters in cells

Immunoelectron microscopy, indirect immunofluorescence light microscopy[26], i*n vivo* fluorescence microscopy [27 28] and cryo-EM tomography [29 25] have shown that CheA, CheW and receptors form dense clusters at the poles of the cell. Receptor

clustering increases in the presence of CheW and certain constructs of CheA[28], but the exact nature of interactions that drive this clustering is not known. As mentioned before, the only mode of interaction known with certainty is the trimers of dimer arrangement of receptors in cells. In Chapter 3, we investigate the self-association property of histidine kinase CheA which we believe may contribute to clustering in the higher order complexes of CheA, CheW and Receptors. We have used Pulsed dipolar Electron Spin Resonance spectroscopy [30 31 32 33] (PDS) and disulphide cross-linking studies to investigate the surface by which CheA aggregates.

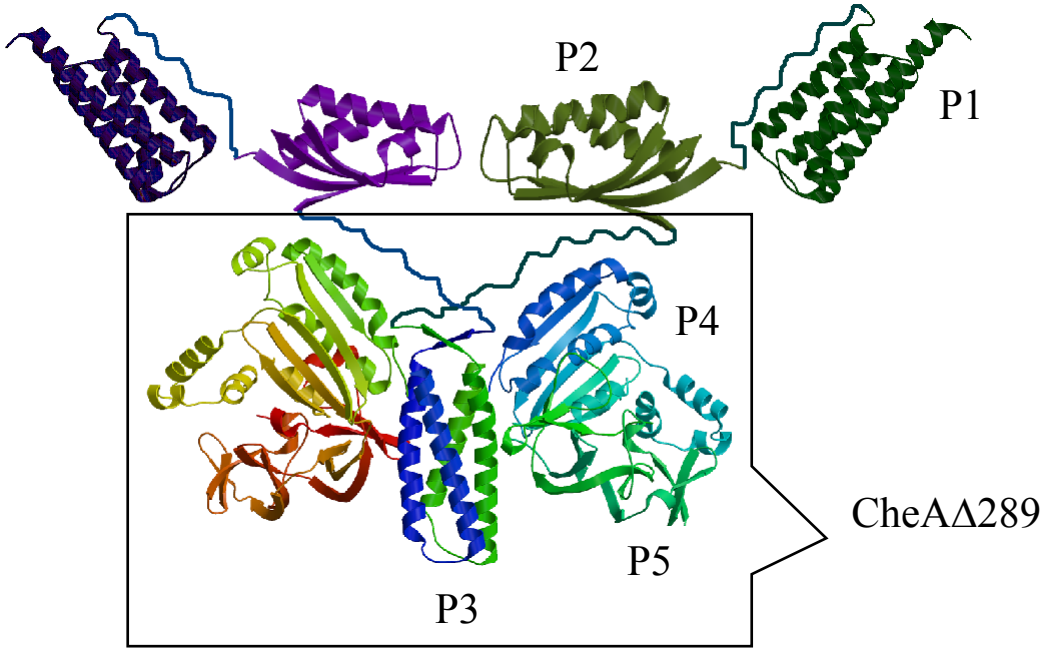

Figure 1.2. Structure of CheA dimer. P1 and P2 domains are linked to the CheAΔ289 (P3-P4-P5 domains together) via long flexible linkers.

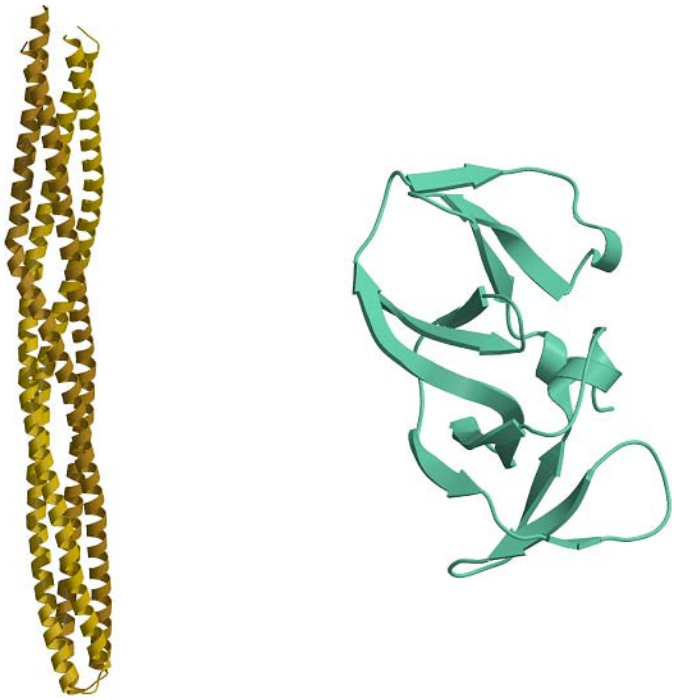

Figure 1.3 Structure of cytoplasmic signaling domain of receptor dimer and CheW from *T.maritima*. (Adapted from Figure 1 of reference [19] and Figure 3 of reference[17])

1.4 Architecture of ternary complex of CheA, CheW and Receptors

Numerous studies have shown that CheW binds strongly to CheAΔ289 specifically through the P5 domain[17,34-36]. The binding interface is formed by sub-domain 2 of CheW and subdomain 1 of P5 domain (Figure 1.4).

Protection studies[34], NMR chemical shift experiments [16] , fluorescence anisotropy binding experiments[38], and genetic studies [39]have mapped out surfaces or specific sites on CheA and CheW that are proposed to interact directly with receptor. The hydrophobic core at the inter-subdomain region buries the maximum hydrophobic surface and is proposed to be a binding site for receptor[16]. However for CheA, a rather broad receptor interaction surface involving four sites on P3, P4 and P5 domains has been identified[34].

Based on the knowledge of these interaction surfaces between CheA, CheW and receptors, over the past few years, different models of the ternary complex as well as the arrangement of the higher order complexes have been suggested[17,34,40]. Electron microscopy on soluble complexes has revealed low resolution structures composed of 24 receptor monomers, 4 CheA monomers and 6 CheW monomers[41]. In Chapter 4 and 5, we propose a new detailed structural model of this ternary complex based on experimental distance restraints obtained from Electron Spin Resonance Spectroscopy and disulphide crosslinking studies. We report how CheA domains and CheW change their relative position/orientation while transforming from a binary to ternary complex after binding with the receptor. Specifically, in the initial set of experiments (Chapter 4) we monitor how the distances between domains in the two subunits of the CheA dimer (or CheW while bound to CheA) change in the presence of receptor.

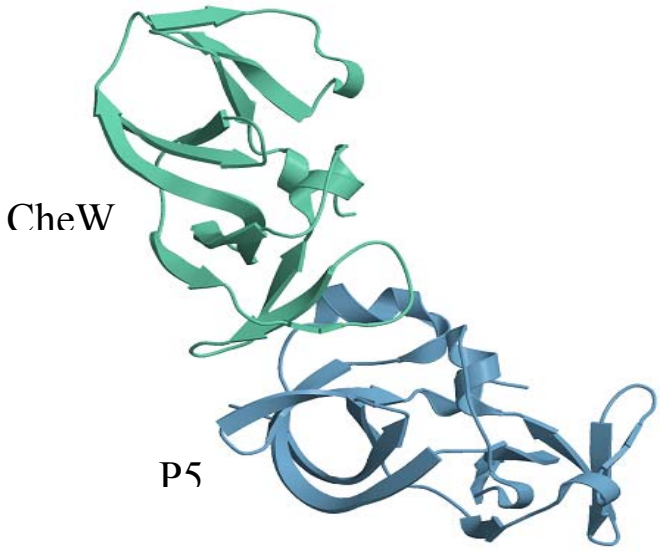

Figure 1.4. Structure of complex of CheW with CheAΔ354 as determined by crystallography. (Adapted from Figure 3 of reference[37]) P4 domain has been omitted for clarity.

In the second set of experiments (discussed in Chapter 5), we directly measure distances between receptor and the CheA/CheW complex. In the final step, we combine all the distance restraints to perform a rigid body refinement and propose a structure of the whole complex.

EM tomography has identified a regular hexagonal pattern of electron density in wild type as well as in cells over-expressing receptor[23,29,42,43]. It has been shown that the electron density at the vertex of the hexagon can easily accommodate a trimer of dimers of receptors. Additional density close to the signaling region of receptors has been attributed to CheA and CheW, but interestingly, it was only found beneath every alternate vertex. If this low resolution density is to be believed, the geometry of the receptors/CheA/CheW lattice does impose serious constraints as to how the three proteins probably interact with each other. However, another study has reported a continuous density for these proteins[43]. In Chapter 6, we propose two possible models ("open-space" and "close-packed") of arrangement of these proteins which satisfy these constraints.

In the next section, the attributes and advantages of the PDS spectroscopic technique has been discussed.

1.5 Pulsed Dipolar Electron Spin Resonance Spectroscopy(PDS)

PDS is a powerful technique for structural determination of protein complexes[30-33]. The underlying principle is the dipolar interaction between a coupled pair of electron spins through which the distance between them can be determined. The electron spin is introduced into the protein by reacting the cysteine residues with a chemical reagent, most commonly MTSSL (1-Oxyl-2,2,5,5- tetramethylpyrolinyl-3-methyl)-methane sulphonate), which has an unpaired electron (Figure 1.5). The

procedure is referred to as site directed spin labeling (SDSL) and is conveniently simple.

A distance measurement between coupled electron spins by ESR involves either of two pulsed techniques: Double Electron Electron Resonance (DEER) [30,44,45]and Double Quantum Coherence (DQC)[33,46]. Since DEER requires weaker pulses as compared to DQC, the experiment is easier to set up, and this technique was used for all distance measurements in this thesis. This technique is discussed in more detail in the following sub-section. At this point, the next immediate issue that needs to be addressed is the relation between distance measurements and structural determination of protein complexes. In Chapter 2, we propose a novel method that uses distance constraints and performs rigid body refinement to predict the structure of a protein complex[47].

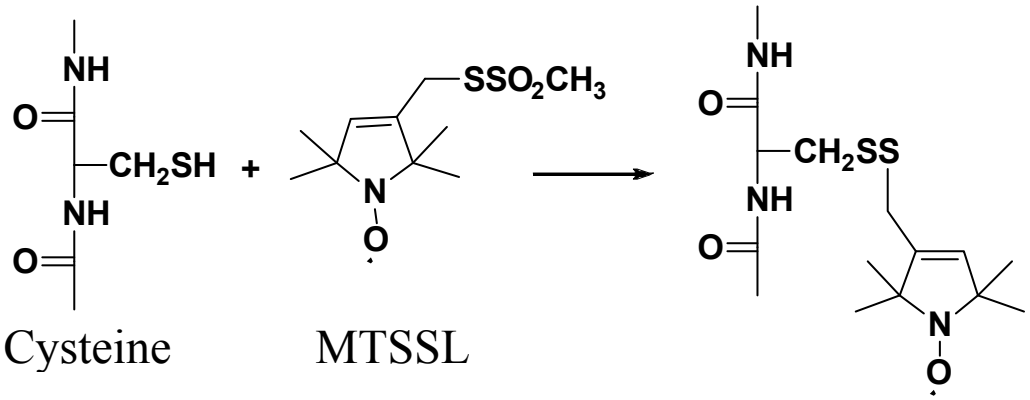

Figure 1.5. Schematic diagram of procedure of protein spin labeling with MTSSL

1.6 Double Electron Electron Resonance (DEER)

The distance measurement experiments with pulsed dipolar ESR are conducted on frozen samples and are based on measurement of dipolar coupling between a pair of electron spins. The dipolar coupling between a pair of electron spins [30]separated by distance r in frequency units is:

$$A(r,\theta) = \omega_{dd}(1-3\cos^2\theta) \tag{1}$$

With $\omega_{dd} = \gamma_e{}^2\hbar / r^3$ and θ is the angle between the external magnetic field and the vector joining the two electrons (Figure 1.6)

Double electron electron resonance experiments can be conducted in either 3[48] or 4 pulse forms[49]. In the 3 pulse form, the two pulse primary echo is detected while a third pumping pulse is applied (Figure 1.7).

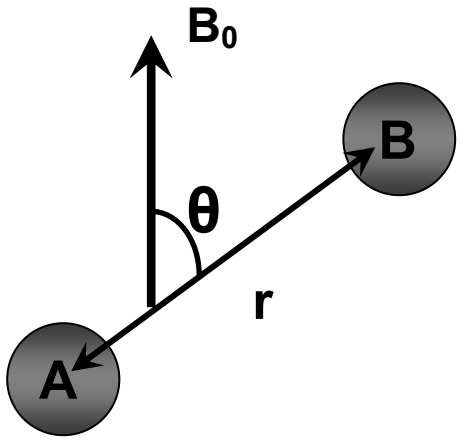

Figure 1.6. Dipolar coupling between a pair of electron spins A and B. The spins are separated by a distance r and θ is the angle between external magnetic field B_0 and the vector joining the two spins.

Spins A and B are separated by a distance r and are magnetically coupled to each other. The primary echo sequence is applied to spins A which resonate at frequency ω_A. The pumping pulse is applied at a frequency ω_B which is very different than ω_A and excites spins B. The π pulse at frequency ω_B inverts the coupling with spins A and results in the change in the frequency of spins A. This leads to modulation of spin-echo amplitude[48]in the following manner:

$$V(t) = V_0(1 - p(1 - \cos A(r,\theta)t)) \qquad \text{for } 0<t<\tau \qquad (2)$$

where V_0 is the echo amplitude in absence of pumping pulse and p is the probability of flipping spins B. For an isotropic distribution of magnetic tensors A and B relative to the vector joining them, the overall signal is decaying and oscillatory in nature:

$$V(t) = V_0(1 - p(1 - \nu(\omega_d t)) \qquad (3)$$

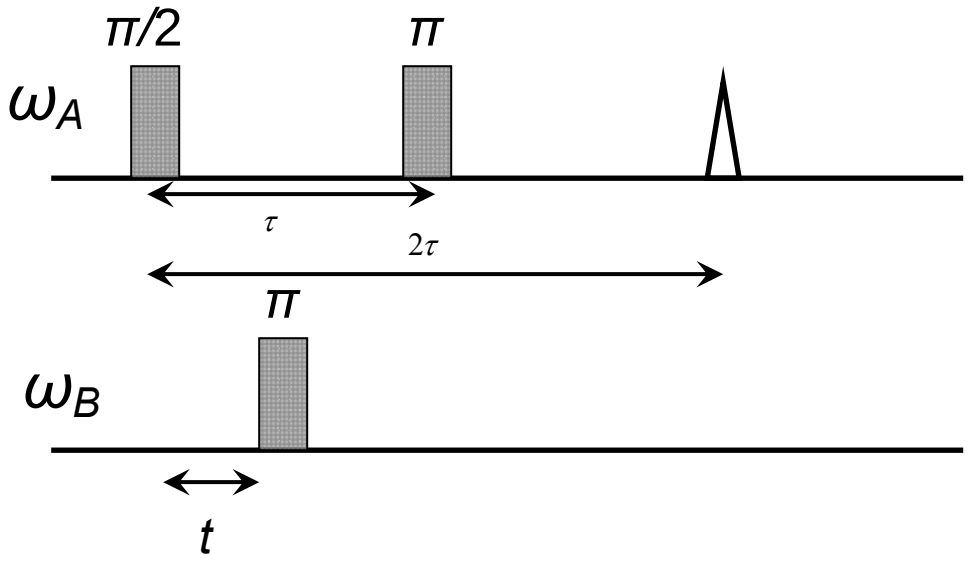

Figure 1.7. Schematic diagram of a 3 pulse DEER sequence. Spins resonating at frequency ω_A form echo at time 2τ while pumping pulse at frequency ω_B is inserted at time t.

Where $\nu(\omega_d t) = \int_0^{\Pi/2} \cos[\omega_d(1 - 3\cos^2\theta)t]d(\cos\theta)$ (4)

The intermolecular dipolar coupling [30]between spins A and B is a simple exponential decay:

$$V_{inter}(t) = \exp(-kt) \tag{5}$$

where $k^{-1} = 1.0027(10^{-3} / pC)$ and C is the spin concentration

The overall DEER signal is a product of intermolecular and intramolecular dipolar signals. For a homogeneous solution, the intermolecular contribution is a simple decay (Equation 5) and is subtracted out from the overall signal to obtain just the intramolecular dipolar signal.

REFERENCES

1. Butler, S. M. & Camilli, A. (2005). Going against the grain: Chemotaxis and infection in Vibrio cholerae. *Nature Reviews Microbiology* **3**, 611-620.
2. Adler, J. (1975). Chemotaxis in bacteria. *Annual Review of Biochemistry* **44**, 341-356.
3. Segall, J. E., Manson, M. D. & Berg, H. C. (1982). Signal-processing times in bacterial chemotaxis. *Nature* **296**, 855-857.
4. Spudich, J. L. & Koshland, D. E. (1975). Quantitation of sensory response in bacterial chemotaxis. *Proceedings of the National Academy of Sciences of the United States of America* **72**, 710-713.
5. Berg, H. C. & Tedesco, P. M. (1975). Transient-response to chemotactic stimuli in Escherichia-coli. *Proceedings of the National Academy of Sciences of the United States of America* **72**, 3235-3239.
6. Bischoff, D. S., Bourret, R. B., Kirsch, M. L. & Ordal, G. W. (1993). Purification and characterization of Bacillus-subtilis CheY. *Biochemistry* **32**, 9256-9261.
7. Swanson, R. V., Sanna, M. G. & Simon, M. I. (1996). Thermostable chemotaxis proteins from the hyperthermophilic bacterium Thermotoga maritima. *Journal of Bacteriology* **178**, 484-489.
8. Segall, J. E., Block, S. M. & Berg, H. C. (1986). Temporal comparisons in bacterial chemotaxis. *Proceedings of the National Academy of Sciences of the United States of America* **83**, 8987-8991.
9. Mesibov, R., Ordal, G. W. & Adler, J. (1973). Range of attractant concentrations for bacterial chemotaxis and threshold and size of response over

this range-Weber law and related phenomena. *Journal of General Physiology* **62**, 203-223.

10. Bilwes, A. M., Alex, L. A., Crane, B. R. & Simon, M. I. (1999). Structure of CheA, a signal-transducing histidine kinase. *Cell* **96**, 131-141.
11. Zhou, H. J., Lowry, D. F., Swanson, R. V., Simon, M. I. & Dahlquist, F. W. (1995). NMR-sudies of the phosphotransfer domain of the histidine kinase CheA from Escherichia coli-assignments, secondary structure, general fold, and backbone dynamics. *Biochemistry* **34**, 13858-13870.
12. Quezada, C. M., Gradinaru, C., Simon, M. I., Bilwes, A. M. & Crane, B. R. (2004). Helical shifts generate two distinct conformers in the atomic resolution structure of the CheA phosphotransferase domain from Thermotoga maritima. *Journal of Molecular Biology* **341**, 1283-1294.
13. McEvoy, M. M., Muhandiram, D. R., Kay, L. E. & Dahlquist, F. W. (1996). Structure and dynamics of a CheY-binding domain of the chemotaxis kinase CheA determined by nuclear magnetic resonance spectroscopy. *Biochemistry* **35**, 5633-5640.
14. Welch, M., Chinardet, N., Mourey, L., Birck, C. & Samama, J. P. (1998). Structure of the CheY-binding domain of histidine kinase CheA in complex with CheY. *Nature Structural Biology* **5**, 25-29.
15. Li, Y., Hu, Y. F., Fu, W. Y., Xia, B. & Jin, C. W. (2007). Solution structure of the bacterial chemotaxis adaptor protein CheW from Escherichia coli. *Biochemical and Biophysical Research Communications* **360**, 863-867.
16. Griswold, I. J., Zhou, H. J., Matison, M., Swanson, R. V., McIntosh, L. P., Simon, M. I. & Dahlquist, F. W. (2002). The solution structure and interactions of CheW from Thermotoga maritima. *Nature Structural Biology* **9**, 121-125.

17. Park, S. Y., Borbat, P. P., Gonzalez-Bonet, G., Bhatnagar, J., Pollard, A. M., Freed, J. H., Bilwes, A. M. & Crane, B. R. (2006). Reconstruction of the chemotaxis receptor-kinase assembly. *Nature Structural & Molecular Biology* **13**, 400-407.

18. Kim, K. K., Yokota, H. & Kim, S. H. (1999). Four-helical-bundle structure of the cytoplasmic domain of a serine chemotaxis receptor. *Nature* **400**, 787-792.

19. Pollard, A. M., Bilwes, A. M. & Crane, B. R. (2009). The Structure of a Soluble Chemoreceptor Suggests a Mechanism for Propagating Conformational Signals. *Biochemistry* **48**, 1936-1944.

20. LeMoual, H. & Koshland, D. E. (1996). Molecular evolution of the C-terminal cytoplasmic domain of a superfamily of bacterial receptors involved in taxis. *Journal of Molecular Biology* **261**, 568-585.

21. Studdert, C. A. & Parkinson, J. S. (2004). Crosslinking snapshots of bacterial chemoreceptor squads. *Proceedings of the National Academy of Sciences of the United States of America* **101**, 2117-2122.

22. Kim, S. H., Wang, W. R. & Kim, K. K. (2002). Dynamic and clustering model of bacterial chemotaxis receptors: Structural basis for signaling and high sensitivity. *Proceedings of the National Academy of Sciences of the United States of America* **99**, 11611-11615.

23. Weis, R. M., Hirai, T., Chalah, A., Kessel, M., Peters, P. J. & Subramaniam, S. (2003). Electron microscopic analysis of membrane assemblies formed by the bacterial chemotaxis receptor Tsr. *Journal of Bacteriology* **185**, 3636-3643.

24. Lefman, J., Zhang, P. J., Hirai, T., Weis, R. M., Juliani, J., Bliss, D., Kessel, M., Bos, E., Peters, P. J. & Subramaniam, S. (2004). Three-dimensional electron microscopic Imaging of membrane invaginations in Escherichia coli

overproducing the chemotaxis receptor Tsr. *Journal of Bacteriology* **186**, 5052-5061.

25. Zhang, P. J., Khursigara, C., Hartnell, L. & Subramaniam, S. (2007). Molecular architecture of receptor arrays in intact E.coli cells determined using cryo electron tomography. *Microscopy and Microanalysis* **13**, 36-37.
26. Maddock, J. R. & Shapiro, L. (1993). Polar location of the chemoreceptor complex in the Escherichia coli cell. *Science* **259**, 1717-1723.
27. Sourjik, V. & Berg, H. C. (2000). Localization of components of the chemotaxis machinery of Escherichia coli using fluorescent protein fusions. *Molecular Microbiology* **37**, 740-751.
28. Kentner, D., Thiem, S., Hildenbeutel, M. & Sourjik, V. (2006). Determinants of chemoreceptor cluster formation in Escherichia coli. *Molecular Microbiology* **61**, 407-417.
29. Zhang, P. J., Khursigara, C. M., Hartnell, L. M. & Subramaniam, S. (2007). Direct visualization of Escherichia coli chemotaxis receptor arrays using cryo-electron microscopy. *Proceedings of the National Academy of Sciences of the United States of America* **104**, 3777-3781.
30. Borbat, P. P. & Freed, J. H. (2007). Measuring distances by pulsed dipolar ESR spectroscopy: Spin-labeled histidine kinases. *Two-Component Signaling Systems, Pt B* **423**, 52-+.
31. Jeschke, G. & Polyhach, Y. (2007). Distance measurements on spin-labelled biomacromolecules by pulsed electron paramagnetic resonance. *Physical Chemistry Chemical Physics* **9**, 1895-1910.
32. Schiemann, O. & Prisner, T. F. (2007). Long-range distance determinations in biomacromolecules by EPR spectroscopy. *Quarterly Reviews of Biophysics* **40**, 1-53.

33. Borbat, P. P. & Freed, J. H. (2000). Double-Quantum ESR and Distance Measurements. In *Distance Measurements in Biological Systems by EPR* (Berliner, L. J., Eaton, G. R. & Eaton, S. S., eds.), Vol. 19, pp. 383-459. Kluwer Academic/Plenum Publishers, New York.

34. Miller, A. S., Kohout, S. C., Gilman, K. A. & Falke, J. J. (2006). CheA kinase of bacterial chemotaxis: Chemical mapping of four essential docking sites. *Biochemistry* **45**, 8699-8711.

35. Zhao, J. H. & Parkinson, J. S. (2006). Mutational analysis of the chemoreceptor-coupling domain of the Escherichia coli chemotaxis signaling kinase CheA. *Journal of Bacteriology* **188**, 3299-3307.

36. Zhao, J. S. & Parkinson, J. S. (2006). Cysteine-scanning analysis of the chemoreceptor-coupling domain of the Escherichia coli chemotaxis signaling kinase CheA. *Journal of Bacteriology* **188**, 4321-4330.

37. Park, S. Y., Quezada, C. M., Bilwes, A. M. & Crane, B. R. (2004). Subunit exchange by CheA histidine kinases from the mesophile Escherichia coli and the thermophile Thermotoga maritima. *Biochemistry* **43**, 2228-2240.

38. Boukhvalova, M. S., Dahlquist, F. W. & Stewart, R. C. (2002). CheW binding interactions with CheA and Tar - Importance for chemotaxis signaling in Escherichia coli. *Journal of Biological Chemistry* **277**, 22251-22259.

39. Liu, J. D. & Parkinson, J. S. (1991). Genetic evidence for interaction between the CheW and Tsr proteins during chemoreceptor signaling by Escherichia coli. *Journal of Bacteriology* **173**, 4941-4951.

40. Shimizu, T. S., Le Novere, N., Levin, M. D., Beavil, A. J., Sutton, B. J. & Bray, D. (2000). Molecular model of a lattice of signalling proteins involved in bacterial chemotaxis. *Nature Cell Biology* **2**, 792-796.

41. Francis, N. R., Wolanin, P. M., Stock, J. B., DeRosier, D. J. & Thomas, D. R. (2004). Three-dimensional structure and organization of a receptor/signaling complex. *Proceedings of the National Academy of Sciences of the United States of America* **101**, 17480-17485.

42. Khursigara, C. M., Wu, X. W. & Subramaniam, S. (2008). Chemoreceptors in Caulobacter crescentus: Trimers of receptor dimers in a partially ordered hexagonally packed array. *Journal of Bacteriology* **190**, 6805-6810.

43. Briegel, A., Ding, H. J., Li, Z., Werner, J., Gitai, Z., Dias, D. P., Jensen, R. B. & Jensen, G. J. (2008). Location and architecture of the Caulobacter crescentus chemoreceptor array. *Molecular Microbiology* **69**, 30-41.

44. Milov, A. D., Maryasov, A. G. & Tsvetkov, Y. D. (1998). Pulsed electron double resonance (PELDOR) and its applications in free-radicals research. *Applied Magnetic Resonance* **15**, 107-143.

45. Jeschke, G. (2002). Distance measurements in the nanometer range by pulse EPR. *Chemphyschem* **3**, 927-932.

46. Borbat, P. P. & Freed, J. H. (1999). Multiple-quantum ESR and distance measurements. *Chemical Physics Letters* **313**, 145-154.

47. Bhatnagar, J., Freed, J. H. & Crane, B. R. (2007). Rigid body refinement of protein complexes with long-range distance restraints from pulsed dipolar ESR. *Two-Component Signaling Systems, Pt B* **423**, 117-+.

48. Milov, A. D., Salikhov, K. M. & Shirov, M. D. (1981). Application of double resonance method to electron spin echo in a study of the spatial distribution of paramagnetic centers in solids. *Soviet Physics-Solid State* **23**, 565.

49. Pannier, M., Veit, S., Godt, A., Jeschke, G. & Spiess, H. W. (2000). Dead-time free measurement of dipole-dipole interactions between electron spins. *Journal of Magnetic Resonance* **142**, 331-340.

CHAPTER 2

RIGID BODY REFINEMENT OF PROTEIN COMPLEXES*

2.1 INTRODUCTION

Elucidation of the structures of protein complexes is often critical for understanding molecular mechanism and function. This is no more evident than for two-component signaling systems where transient associations of proteins mediate the propagation of information. Despite numerous successes, the structure determination of complexes remains a challenge because of the difficulty in growing crystals for X-ray crystallography or in obtaining enough suitable small distance and orientation restraints by NMR. Techniques such as Electron Microscopy[1], small-angle X-ray scattering [2] and small-angle neutron scattering [3] can provide molecular envelopes for complexes but suffer from lack of contrast and resolution. In addition, a number of useful approaches map molecular interfaces by measuring perturbations to interfacial residues, such as changes in cross-linking reactivity, accessibility, or NMR chemical shifts. While these methods provide points of contact between partners, relative orientations can be difficult to discern. Finally, distance measurements between specifically labeled positions on associating molecules are possible with FRET and ESR. The former relies on resonance energy transfer between a donor excited state [1] and an acceptor ground state, the latter relies on the direct dipolar coupling between two spins.

[1] Reprinted from Methods in Enzymology, Vol 423, Jaya Bhatnagar, Jack H. Freed and Brian R. Crane, Rigid body refinement of protein complexes, 117-133, Copyright (2007), with permission from Elsevier.

In each case, probe positioning is often achieved with site-directed cysteine substitution, but whereas FRET requires two different types of labels, ESR requires only one, usually a nitroxide derivative. Also, ESR provides the distance directly, since it does not require calibrations nor does it have uncertain parameters. In addition, the distribution in distance, P(r), can readily be obtained. Pulsed ESR techniques like Double Electron Electron Resonance (DEER) and Double Quantum Coherence (DQC) are capable of measuring biologically relevant distances in the range 1-8 nm between spin labels[4].

Such long range pairwise distance restraints can, in principle, be processed to formulate precise structures. Related methodologies have already been applied to FRET derived distances[5,6]. In the present study, we have developed a simple and convenient method for modeling the structure of a binary complex by rigid body refinement of known sub-structures, using as restraints the intermolecular distances derived from pulsed ESR. Also, by testing simulated restraints, we produced a set of guidelines to optimize spin label location, number of labels, and measurement error schemes for achieving reasonable model accuracies. Our method is general enough to be applied to any type of distance restraints provided a reasonable estimate of uncertainty associated with the particular measurement is known.

2.2 METHOD

2.2.1 Rigid body Minimization with CNS

The software package Crystallography and NMR System (CNS) developed by Brunger et al. [7]is primarily designed for structure determination using data from X-ray Crystallography or Nuclear Magnetic Resonance (NMR) spectroscopy. However, the minimization algorithms can readily be applied to other types of structural restraints. Our incorporation of ESR measured distances into CNS is quite similar to that for

distances derived from Nuclear Overhauser Effect (NOE) data in structure refinement. Distances, (d) were input in the form of a table, each line of which specifies the pair of atoms between which the d has been measured, and the error limits d_{minus} and d_{plus}, which represent the minimum and maximum allowed distances associated with that measurement. CNS provides six possible restraining functions associated with NOE derived distances: biharmonic function, square-well function, soft-square function, symmetry function, 3D NOE-NOE function and high dimensional function. We have applied the soft square potential [7] to generate the energy term (E_{ESR}), which is then minimized by conjugate gradient refinement based on the agreement between measured distances 'd' and model distance 'R'. Taking default values for most of the constants[2], a simplified version of the function has the form:

$$E_{ESR} = S \times \begin{cases} a + (b/\Delta) + \Delta \; ; & R > d + d_{plus} + r_{sw} \\ \Delta^2 \; ; & R < d + d_{plus} + r_{sw} \end{cases} \qquad (1)$$

$$\text{where } \Delta = \begin{cases} R - (d + d_{plus}) \; ; & d + d_{plus} < R \\ 0 \; ; & d - d_{minus} < R < d + d_{plus} \\ d - d_{minus} - R \; ; & R < d - d_{minus} \end{cases}$$

We assign 'd' as the ESR measured distance between C_β atoms of the corresponding amino acid residues at which the spin label is attached, R is the corresponding distance in the model, d_{plus} and d_{minus} are the positive and negative errors associated with each distance, r_{sw} is a constant with default value 0.5 Å, a and b are determined by the program such that E_{ESR} is a smooth function at point $R = d + d_{plus} + r_{sw}$. S is a scale factor that weights the ESR energy relative to the van der waals energy. A similar soft square potential has also been used to model constraints for a system of transmembrane helices [8] and is analogous to a global penalty function

[2] Softexp=1;Exp=2,C=1;c =1

developed by Knight et al [6] for modeling FRET derived restraints. However, an additional property of the restraining function in CNS is that it becomes linear for large deviations between experimental and model restraints. This allowance maintains numerical stabilities[9].

2.2.2 Initial conformation of the complex

Gradient-descent optimization methods like conjugate gradient minimization converge to a global minimum of the system if the starting conformation is not very different from the correct structure. Various computational procedures have been developed to model initial conformations for refinement, provided distance restraints are available[8];[10]. For our first case study of the complex between chemotaxis proteins CheA and CheW, we test initial conformations determined randomly with those generated with matrix distance geometry from both X-ray crystallography and pulsed ESR as discussed in our previous work[11]. With our second case, the protein alpha-synuclein (αS), we compare refinements beginning with either the NMR-determined structure or random orientations of the two synuclein helices.

2.2.3 Evaluation Criterion

In case 1, the separate structures of CheW and the P5 domain of CheA were taken from the crystal structure of CheW and the CheA domains P4-P5, where CheW predominantly binds to the CheA domain, P5 [11]. The final conformation of the complex after rigid body minimization was evaluated by comparing the ESR-refined complex to the coordinates of P4:P5:CheW crystal structure. The tight binding between CheW and CheAΔ289 (domains P3,P4,P5 collectively called CheAΔ289 ; K_b=100 nM) makes it unlikely that crystal packing forces significantly alter the association mode of the complex[12]. The measure of agreement was assigned as the

root-mean-square deviation (RMSD) in the position of C_α atoms of CheW in the final refined structure with respect to the crystal structure after least square fitting of the P5 domains from both the structures[13].

In case 2, we aimed to reproduce the orientation of two anti parallel helices of α-synuclein when bound to micelles, for which a secondary but not tertiary NMR structure has been determined [14,15]. Inter-helical distances measured by ESR give information about relative orientation of the helices, which cannot be determined with certainty from NMR data alone. For comparison, the quality of the ESR-refined structure was evaluated by superimposing one of the two α-synuclein helices with the NMR structure of the molecule bound to micelles [14] and then calculating the RMSD between the ESR refined second helix and that from the NMR structure.

2.3 RESULTS

2.3.1 Case Study 1

CheA:CheW complex

CheW forms a complex with the histidine kinase CheA that is necessary for assembly with chemorecepters. To construct the structure of the CheA:CheW complex, twelve intermolecular distances were measured between nitroxide spin labels on four residues (N553C, S568C, E646C and D579C) of the P5 domain of *T.maritima* CheAΔ289 (which contains domains P3-P4-P5) and three residues (S15C, S72C and S80C) on *T.maritima* CheW (Figure 2.1).

Positioning of the labels was achieved by site directed cysteine mutagenesis followed by reaction with (1-oxyl-2,2,5,5-tetramethylpyrolinyl-3-methyl)-methanethiosulfonate (MTSSL).

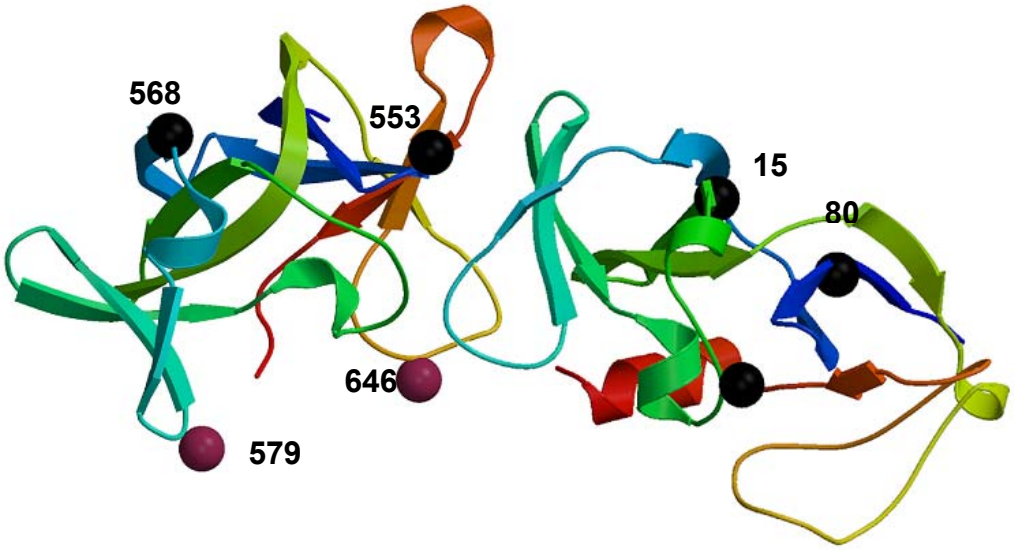

Figure 2.1 Crystal structure of CheW-P5 complex showing positions of spin label sites (balls) along the polypeptide. Both proteins shown as ribbon representations colored blue to red from N to C terminus. Sites producing the most aberrant ESR restraints compared to the crystal structure shown in red.

An initial conformation of the complex was predicted by using a matrix distance geometry method, and it was found to agree with a root mean square deviation (RMSD) in C_α atom positions of about 16 Å when compared with the crystal structure of the complex. Rigid-body refinement using CNS reduced the RMSD to 11 Å. The total energy function in the refinement of CNS is a sum of $E_{EMPIRICAL}$ and $E_{EFFECTIVE}$ terms[7]. This force field is similar to the Bundler penalty function used to model transmembrane helices against sparse distance constraints[8]. $E_{EMPIRICAL}$ describes the energy of the molecule as a function of atomic coordinates (for example energy associated with bonds, angles, dihedral angles etc), whereas $E_{EFFECTIVE}$ refers to restraining energy terms associated with agreement of the model to the ESR data, that is, it equals E_{ESR} given by equation (1). In rigid body refinement only energy terms that reflect van der Waals contacts contribute to $E_{EMPIRICAL}$.

The convergence was tested by randomly orienting CheW in various positions and evaluating the refined complex. Within rigid body displacements of 15 Å and rotations of 30 degrees the same final conformation was found (within an RMSD difference of ~3 Å). In the following sections we investigate how parameterization of the refinement affects the quality of the final solution. By adding restraints comprising distances taken from the crystal structure with errors derived from the standard deviations observed in the ESR measurements, we also explore how the number and nature of distance restraints affect the modeling results. In particular, we present guidelines to aid selection of potential spin labeling sites on the protein components within a general complex.

Error Allocation Scheme

A pulsed ESR experiment with a pair of nitroxide spin labels measures the separation between the nitroxyl groups of the spin labels; which can have considerable orientational freedom with respect to the protein backbone and with respect to each other because of their flexible tethers. In the absence of information about the spin label orientation, we have assigned the ESR experimental distance to coincide with the C_β position of the native amino acid residue. If the spin label tethers point away from each other in the complex, the model distances will underestimate the nitroxide separations. In fact, the ESR measured distances are almost always larger than those predicted by C_β separations (Table 2.1). In contrast, if the spin label tethers project toward each other in the complex, then the spin-spin separation will be overestimated by C_β separations. However, when globular domains associate, there is a bias against facing labels because they tend to reside on protein surfaces that participate in the interface. To compensate for overall longer experimental distances, on average, we have found that an asymmetric uncertainty model is effective. In our previous work,

[11]we presented a distance-dependent error allocation scheme. However, better results are obtained by setting d_{minus} = 5 Å and d_{plus} = 1 Å for all restraints which are the boundaries within which most of the experimental distances are over or underestimated by C_β separations (Table 2.1).

Table 2.1. Comparison of ESR-measured distances to C $_{\beta\beta}$ separations between corresponding residues in the P5-CheW crystal structure

Residue P5-CheW	*Distance between C_β atoms in crystal structure(R_{crys})*	*ESR measured distances (R_{esr})*	R_{esr}- R_{Crys}
568-80	44.5	47	2.5
579-80	44.5	54.5	10
	(Å)	(Å)	(Å)
553-15	34.9	37	2.1
646-15	31.8	43.7	11.9
568-15	55.4	54.5	-0.9
579-15	52	61	9
553-72	28.3	27	-1.3
646-72	27.5	32.5	5
568-72	47.9	49	1.1
579-72	41	46	5
553-80	23.6	26	2.4
646-80	26.8	39.5	12.7

Similar magnitudes in error are consistent with other spin labeling studies[10]; [16] which may also benefit from asymmetric error boundaries. However, four out of twelve distances do not meet this criteria due to reasons related to the location of spin label site on the protein surface. The reasons for such inaccuracies in distance measurements are discussed in a later section.

Weighting scheme for contact parameters

For ESR restraints to determine the final configuration, $E_{EFFECTIVE}$ must account for a considerable percentage of the total energy. This can be achieved by simply increasing the scale factor (S) in the input file associated with E_{NOE}, or in our case E_{ESR}. With the ceiling constant assigned to 10^5, the scale factor was increased from 75 to 75,000 in steps of 100 and the RMSD in C_α positions were evaluated. Predictably, the convergence improves progressively as the scale factor increases (S = 75 yields an RMSD = 16.38 Å; S = 75,000 an RMSD = 11.06 Å). Above S = 75,000 there is no further improvement.

Type and number of restraints

Applying all twelve experimental intermolecular distance restraints between CheW and P5 domain, while setting d_{minus} = 5 Å and d_{plus} = 1 Å, the best structure that could be achieved has an RMSD on C_α positions of 11.06 Å compared to the crystal structure. To evaluate the effect of additional arbitrarily chosen distance restraints, four new label sites on CheW were successively added to the refinement. Each new site generated four new distances to the P5 labels. The standard deviation of the parameter (R_{esr} -R_{crys}) as defined in Table 1 is 5 Å. In order for the new distances to mimic the experimental ones, the standard deviation obtained above was added to the C_β separations. Then, for each successive addition of a label site on CheW, the RMSD

in positions of the C_α atoms in the final structure was calculated and the results were plotted against total number of restraints. Two error schemes d_{minus} = 5 Å, d_{plus} = 1 Å (Figure 2.2 (A)) and d_{minus} = 5 Å, d_{plus} = 5 Å (Figure 2.2 (B)) were used for comparison. The procedure was also repeated for five different initial conformations of the complex. The results indicate that irrespective of the initial conformation prior to refinement, addition of random distance restraints leads to an improved RMSD of 8-12 Å but beyond 20 and 24 restraints with d_{minus} = 5 Å d_{plus} = 1 Å and d_{minus} = 5 Å d_{plus} = 5 Å respectively, there is no improvement. It is interesting to note that Knight et al [6] also reported that model accuracies of only 10 Å RMSD can be obtained with twenty or more FRET restraints.

Addition of more accurate restraints

As illustrated above, about twenty distance restraints with standard deviation of 5 Å from the crystal-structure derived distances are sufficient to produce model accuracies of about 10 Å. The inability of additional restraints to obtain better results suggested that convergence is limited by inaccuracies in the experimental distances. With the initial configuration taken from distance geometry, even the addition of 28 accurate crystal-derived distances (setting d_{minus} = 1 Å and d_{plus} = 1 Å) to twelve experimental distances (setting d_{minus} = 5 Å and d_{plus} = 5 Å) only improved the final agreement to a limited degree (from RMSD 15.4 Å to 10.5 Å); thus a few distances with large inconsistencies appear to dominate the more accurate restraints.

Comparison of twelve experimental distances with crystal separations revealed that 2 of the distances were highly skewed with average deviations up to 12.7 Å (Table 2.1). If we take the same set of 28 crystal-structure derived distances and 12 experimental distances, and the observed ESR distances are deleted two at a time

beginning with the most deviant ones, the RMSD drastically reduces from 10.5 Å to 6.2 Å and then becomes constant at 2.6 Å (Figure 2.3).

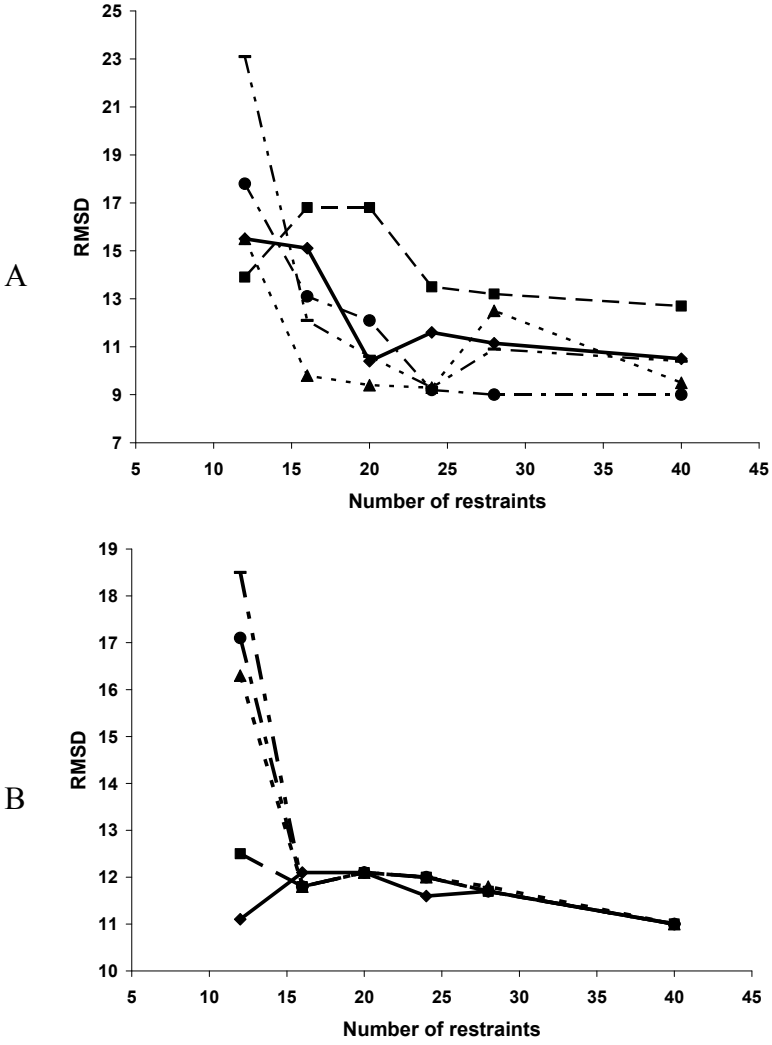

Figure 2.2. The effects of different error schemes and simulated restraints on refinement accuracy. RMSDs for the refined CheW/P5 complex are shown for five different initial conformations of the complex ■, ◆, ▲, ●, _. Two different error schemes: (A) d_{minus} = 5 Å, d_{plus} = 1 Å and (B) d_{minus} = 5 Å, d_{plus} = 5 Å.

Adding only the two highly skewed measurements to the crystal-structure derived restraints produces a worse RMSD than the entire set of experimental restraints, emphasizing the deleterious effects of these aberrant measurements.

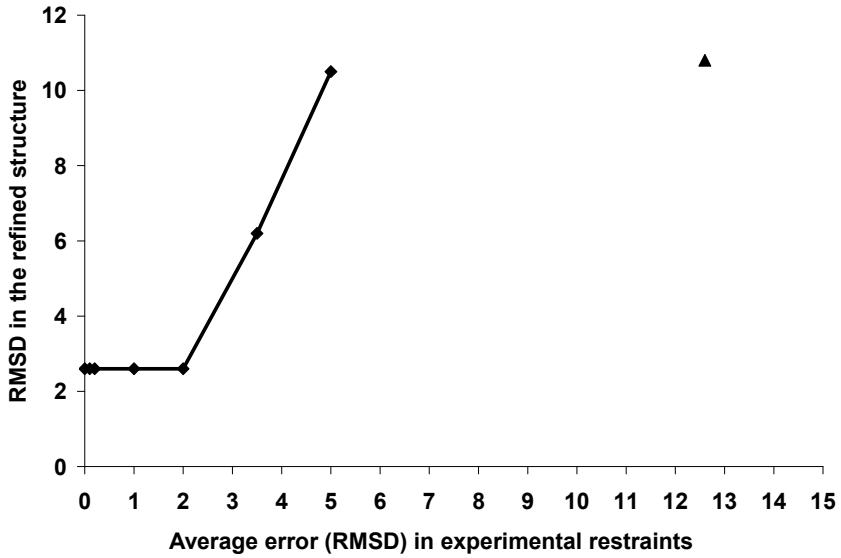

Figure 2.3. The effect of aberrant measurements on refinement accuracy in the presence of additional restraints derived from the crystal structure. From a set of 28 crystal distances with ± 1 Å and experimental distances with ± 5 Å, the most deviant ESR distances were deleted two at a time (◆). Addition of only the two most deviant distances to the crystal distances give slightly higher RMSD compared to the overall set of experimental distances (▲).

However, in the absence of the simulated restraints, the deletion of the 2 most deviant distances from the set of 12 experimental distances increased the RMSD from 11 Å to 16 Å. This is probably because the refinement now suffers from under determination which suggests that more experiments need to be done in this case. Alternatively, since the total energy associated with distance restraints is the sum of individual contributions, improved convergence may result from a weighting scheme based on experimental to model agreement that adjusts on successive iterations to reduce the weight of the contribution of aberrant measurements. Simply, if the

difference between a measurement and its predicted distance by the refined complex is deviant by more than two standard deviations, as given by the distribution of residuals from all the measurements, then the measurement should be removed and the refinement repeated. As we discuss below, due to surface site mobility, labels interfering with complex formation and other conformational effects, it is reasonable to encounter some outliers in these experiments.

If experimental restraints are deleted successively in the absence of simulated restraints, the RMSD increases as expected. However, the additional increase in RMSD is more sensitive to removal of the shortest, rather than the longest distance (Figure 2.4). This suggests that longer experimental distances in the CheA:CheW system are more inaccurate than shorter ones.

Effect of spin label position

Site directed spin labeling (SDSL) is a convenient method to attach ESR probes to cysteine residues on proteins[17]; however it is unclear how the pattern of sites affect the refinement apart from the considerations that a solvent exposed residue is more likely to react with the spin label, and that spin labels in the interfacial region may disrupt complex formation.

To test the effect of label position on predicting the CheA:CheW solution complex, CheW was broadly divided into three sections, front, middle and back, and from each of these sections, one amino acid residue was randomly selected as a label site. Additional distance restraints from these sites to P5 were measured as before while setting d_{minus} = 5 Å and d_{plus} = 1 Å. This procedure was repeated seven more times, selecting a random site in each section each time, and finally the RMSD on C_α positions after refinement was averaged for all the eight cases per section.

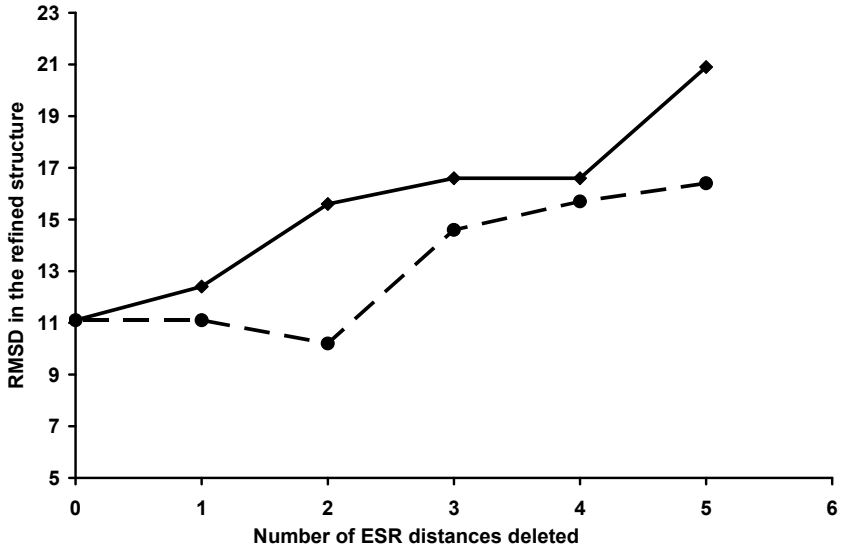

Figure 2.4. Long vs short restraints in refinement of CheA/CheW complex. Successive deletions of distances beginning with the shortest (◆) or the longest (●) restraints.

The trend in RMSD values (Figure 2.5) showed a slight preference for locating the new sites in the middle and back sections of the protein (from 11.99 Å to 11.14 to 10.7 Å respectively).

We also considered the effect of adding four more CheW sites (16 new restraints). The selection of sites was organized the following six ways:

1. All from front section (residues I60, S45, N54, S37)
2. All from middle section (E90, K67, D139, I34)
3. All from back section (V101, K123, N107, N113)
4. Two from front and two from middle section
5. Two from middle and two from back section
6. Two from back and two from front section

For the first three cases, the RMSD from the refined structure shows slightly better agreement to the crystal structure when sites in the distal end of CheW are selected compared to sites closer to the P5 interface.

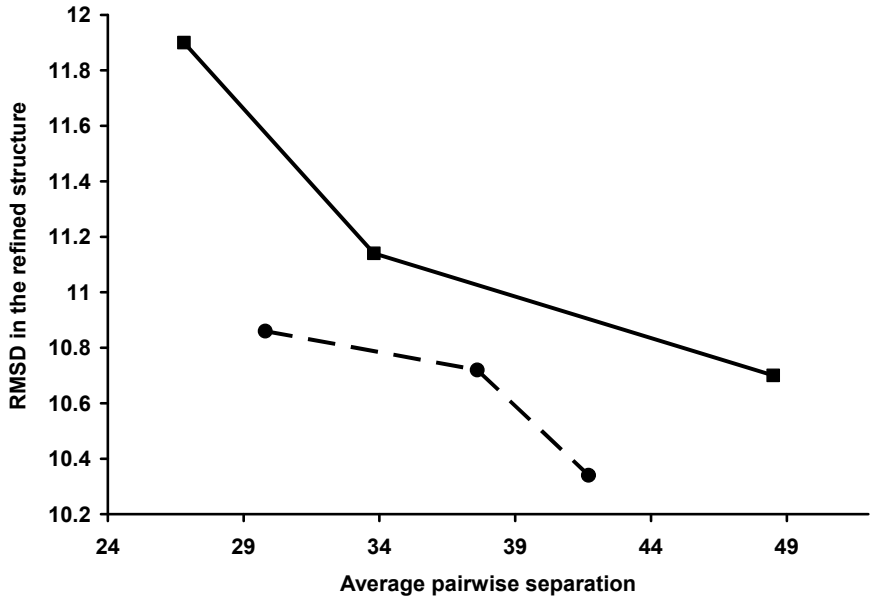

Figure 2.5 Variation of RMSD with average pairwise separation of the label sites with addition of one new spin label (■) and four spin labels on CheW(●).

For scenarios 4-6, the selection of two residues from each section of CheW was done in eight different ways and the final RMSD was averaged for all the eight cases. Plotting the final RMSD in the final structure versus the average pair-wise separation of each new label from sites on P5 demonstrates that only minimal improvement in RMSD are seen no matter how the sites are chosen (Figure 2.5).

However, we can conclude that more restraints result in a lower RMSD, and longer restraints play a crucial role only when the total number of restraints is less than sixteen. As more restraints are added, the locations of sites on the surface of CheW have little effect on the refined complex.

2.3.2 Case Study 2

Helix orientations of α-synuclein bound to micelles

NMR studies on the protein alpha-synuclein (αS) have shown that when bound to sodium dodecyl sulphate (SDS) micelles, the protein adopts a conformation of two separate anti-parallel helices (helix 1 residues: 3-37; helix 2 residues: 45-92) connected by an ordered linker[14,15]. Pulsed ESR has been used to determine inter-helix distances between spin labels at various positions on the two helices when the protein is bound to both SDS and lyso-1-palmitoylphosphotidylglycerol (LPPG) micelles[18]. In total, thirteen inter-helical dipolar couplings were measured and from them the average distance (R_{avg}) and its root mean square deviation (RMSD) were evaluated. We tested the ability of our refinement procedure to orient the two helices relative to each other under the assumption that each helix behaves as a rigid body. To generate two rigid bodies, the helices were separated between residues 40 and 41 in the linker. To account for the covalent bonding between residues 40-41, additional restraints were added between residues 40 – 41, 39 – 41 and 40 – 42 (C_i-N_k, $C_{\alpha i}$-$C_{\alpha k}$, C_i-C_k, $C_{\alpha i}$-N_k, N_i-N_k and C_i-$C_{\alpha k}$, for i=40; k=i+1and k=i+2, for i=39; k=i+2). In this scheme the restraints were calculated by summing the bond lengths connecting the two atoms of interest and d_{plus} was set to 0 because any distance measured through space is shorter than that measured along the summed bond lengths. For a hypothetical case where no information is available regarding the conformation of the turn residues, the d_{minus} error was given more flexibility by assigning d_{minus} = 1 Å for distances between adjacent residues and d_{minus} = 8 Å for distances between non-adjacent residues.

For SDS bound α-synuclein (with the exception of two distances, between V3C/E61C and E13C/H50C), eleven inter-helical ESR distances, taken as their reported R_{max} values were incorporated into the refinement. The RMSD in label position obtained from P(r) measurements were taken as estimates for the d_{minus} error.

As the ESR measurements likely overestimate R as in the CheA/CheW case, d_{plus} was set to a smaller value, but was increased to reflect changes in d_{min} (d_{plus} =1 Å for 5 Å < $d_{minus} \leq$ 8 Å , d_{plus} = 2 Å for 9 Å < $d_{minus} \leq$ 15 Å and d_{plus}= 5 Å for $d_{minus} \geq$ 15 Å). Combining all the restraints, and starting with what was available from the NMR structure, the refinement places the ends of the two rigid helices close to each other, (the length of amide bond C_{40} - N_{41} is 2.2 Å compared to ideal bond length 1.3 Å). When the helical fragment from 1-40 is superimposed on its position in the NMR structure, the anti-parallel partner helix (residues 41 -103) is rotated by an angle $\Phi \sim 30°$ with respect to its position in the NMR structure (Figure 2.6). However, the angle separating the two helical axes (θ) is better determined. Thus, the ESR refinement is unable to distinguish which side of the helices faces each other, and this generates inaccuracy in Φ. This is not surprising, as the errors in the spin label position are larger than the width of a helix. We noted that the absolute orientation of the two helices can be determined if precise restraints on the conformation of linker residues are known by other means. If rigid restraints are added for the conformation of residues within the loops, the agreement with the NMR structure is excellent.

2.4 DISCUSSION

In this study we have described a simple and readily implemented method for refining association modes of protein complexes from ESR restraints. Agreement with crystal data improves with number of ESR restraints until approximately twenty restraints are available, additional restraints beyond this number result in little further improvement due to errors associated with the knowledge of the label position. A recent study reported agreement between C_β-C_β distances and ESR distance restraints with mean errors up to 6 Å[19]. These errors are similar in magnitude to those accounted

for by our asymmetric error scheme in CheA/CheW case study. Molecular modeling approaches like

Monte Carlo simulations and molecular dynamics have been found to be useful in lowering the uncertainty associated with spin-label positions[19];[20];[21].

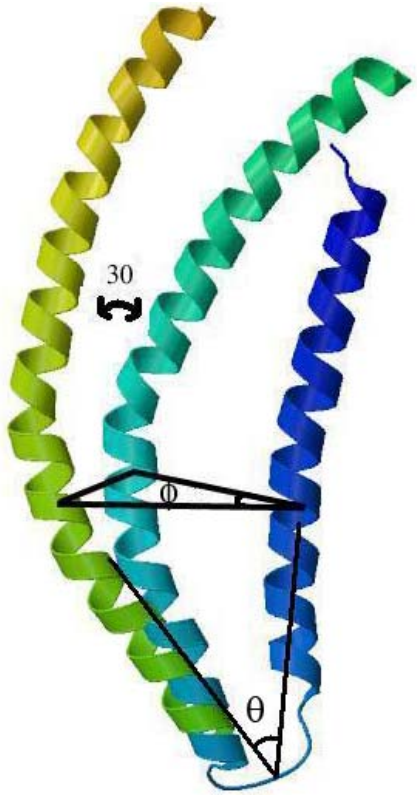

Figure 2.6 Orientation of two anti-parallel α-synuclein helixes (residues 3-34 and 44-94) as derived from NMR structure (blue). Superposition of N terminal of helix from the rigid body refined structure, places the second helix rotated by angle of 30 ° with respect to the NMR structure.

2.4.1 Type of restraints

We investigated how positioning of the spin labels influences convergence of varying accuracies. Addition of longer simulated restraints appeared most effective in

driving convergence to the target model, provided the total number of restraints was less than 16. However, removal of the shortest experimental distances has more deleterious effect in the absence of simulated restraints. This apparent contradiction may derive from the longer experimental restraints being unusually aberrant due to conformational properties of these sites in the CheA:CheW system. In addition, any real differences between the solution and crystal complex would be expected to be greatest at sites farthest from the high affinity interface. Nonetheless, our combination of studies suggest that spin labeling 4 or 5 sites on each protein at positions distributed as far apart as possible on the structures of the individual components is a reasonable strategy for covering the distance space.

2.4.2 Inaccuracies in distance measurement

Apart from the technical limitations of the experimental method in measuring accurate distances, local conformational changes in the protein structure, backbone dynamics and the flexibility of the spin label lead to ambiguity in measurements. The two most deviant intermolecular distances in the CheW/P5 complex were those measured from site 646 on P5 domain (P5/CheW: 646-15, 646-80). In the crystal structure of the complex, P5-646 is very close to the binding interface with CheW, and thus the label conformation may be unusually perturbed in the complex. In addition, the 646 site resides in a loop which may impart more than usual flexibility (Figure 2.1). Aberrant distances involving P5 site 579 may also be caused because this residue resides in a loop with few neighbor contacts and hence may be more mobile.

2.4.3 The Spatial Resolution of ESR-derived structures

Case 2 demonstrates that this method as implemented is less effective at orienting secondary structure elements within a protein than defining association

modes within the complex. It follows, that even with a large number of measurements it may be difficult to precisely define conformational changes involving small to medium amplitude shifts in secondary structure positions. This limitation could be overcome by more rigid spin labels whose positions on the protein surface are fixed and well defined. In this regard, metal complexes may be an attractive alternative to nitroxide-based labels[22].

In conclusion, pulsed dipolar ESR combined with site-directed spin labeling can reconstitute structures of protein-protein complexes with reasonable accuracies provided structures of the individual components are well-defined. CNS-based rigid-body refinement is a straightforward and accessible method for generating complexes from the distance restraints. Further improvements may be possible with a weighting scheme that identifies and adjusts the contribution of outliers during the course of refinement.

REFERENCES

1. Frank, J. (1996). Three dimensional electron microscopy of macromolecular assemblies, Academic Press, San Diego, CA.
2. Kratky. O, G. O. (1982). Small Angle X-ray Scattering, Academic Press, London.
3. Higgins. J.S, B. H. C. (1994). Small Angle Neutron Scattering, Clarendon Press, Oxford.
4. Chiang, Y. W., Borbat, P. P. & Freed, J. H. (2005). The determination of pair distance distributions by pulsed ESR using Tikhonov regularization. *J. Magn. Reson.* **172**, 279-295.
5. Mukhopadhyay, J., Sineva, E., Knight, J., Levy, R. M. & Ebright, R. H. (2004). Antibacterial peptide microcin J25 inhibits transcription by binding within and obstructing the RNA polymerase secondary channel. *Mol. Cell* **14**, 739-751.
6. Knight, J. L., Mekler, V., Mukhopadhyay, J., Ebright, R. H. & Levy, R. M. (2005). Distance-restrained docking of rifampicin and rifamycin SV to RNA polymerase using systematic FRET measurements: Developing benchmarks of model quality and reliability. *Biophys. J.* **88**, 925-938.
7. Brunger, A. T., Adams, P. D., Clore, G. M., DeLano, W. L., Gros, P., Grosse-Kunstleve, R. W., Jiang, J. S., Kuszewski, J., Nilges, M., Pannu, N. S., Read, R. J., Rice, L. M., Simonson, T. & Warren, G. L. (1998). Crystallography & NMR system: A new software suite for macromolecular structure determination. *Acta Crystallographica Section D-Biological Crystallography* **54**, 905-921.

8. Sale, K., Faulon, J. L., Gray, G. A., Schoeniger, J. S. & Young, M. M. (2004). Optimal bundling of transmembrane helices using sparse distance constraints. *Protein Sci.* **13**, 2613-2627.

9. Brunger, A. T., Adams, P. D. & Rice, L. M. (1999). Annealing in crystallography: a powerful optimization tool. *Prog. Biophys. Mol. Biol.* **72**, 135-155.

10. Faulon, J. L., Sale, K. & Young, M. (2003). Exploring the conformational space of membrane protein folds matching distance constraints. *Protein Sci.* **12**, 1750-1761.

11. Park, S. Y., Borbat, P. P., Gonzalez-Bonet, G., Bhatnagar, J., Pollard, A. M., Freed, J. H., Bilwes, A. M. & Crane, B. R. (2006). Reconstruction of the chemotaxis receptor-kinase assembly. *Nature Structural & Molecular Biology* **13**, 400-407.

12. Park, S. Y., Quezada, C. M., Bilwes, A. M. & Crane, B. R. (2004). Subunit exchange by CheA histidine kinases from the mesophile Escherichia coli and the thermophile Thermotoga maritima. *Biochemistry* **43**, 2228-2240.

13. McRee, D. E. (1999). XtalView Xfit - A versatile program for manipulating atomic coordinates and electron density. *J. Struct. Biol.* **125**, 156-165.

14. Ulmer, T. S., Bax, A., Cole, N. B. & Nussbaum, R. L. (2005). Structure and dynamics of micelle-bound human alpha-synuclein. *J. Biol. Chem.* **280**, 9595-9603.

15. Bussell, R., Ramlall, T. F. & Eliezer, D. (2005). Helix periodicity, topology, and dynamics of membrane-associated alpha-Synuclein. *Protein Sci.* **14**, 862-872.

16. Rabenstein, M. D. & Shin, Y. K. (1995). Determination of the Distance between 2 Spin Labels Attached to a Macromolecule. *Proc. Natl. Acad. Sci. U. S. A.* **92**, 8239-8243.

17. Hubbell, W. L. & Altenbach, C. (1994). Investigation of Structure and Dynamics in Membrane-Proteins Using Site-Directed Spin-Labeling. *Curr. Opin. Struct. Biol.* **4**, 566-573.

18. Borbat, P., Ramlall, T. F., Freed, J. H. & Eliezer, D. (2006). Inter-helix distances in lysophospholipid micelle-bound alpha-synuclein from pulsed ESR measurements. *J. Am. Chem. Soc.* **128**, 10004-10005.

19. Sale, K., Song, L. K., Liu, Y. S., Perozo, E. & Fajer, P. (2005). Explicit treatment of spin labels in modeling of distance constraints from dipolar EPR and DEER. *J. Am. Chem. Soc.* **127**, 9334-9335.

20. Schiemann, O., Piton, N., Mu, Y. G., Stock, G., Engels, J. W. & Prisner, T. F. (2004). A PELDOR-based nanometer distance ruler for oligonucleotides. *J. Am. Chem. Soc.* **126**, 5722-5729.

21. Borbat, P. P., McHaourab, H. S. & Freed, J. H. (2002). Protein structure determination using long-distance constraints from double-quantum coherence ESR: Study of T4 lysozyme. *J. Am. Chem. Soc.* **124**, 5304-5314.

22. Rodriguez-Castaneda, F., Haberz, P., Leonov, A. & Griesinger, C. (2006). Paramagnetic tagging of diamagnetic proteins for solution NMR. *Magn. Reson. Chem.* **44**, S10-S16.

CHAPTER 3

SELF ASSOCIATION OF THE HISTIDINE KINASE CHEA AND CHEW FROM *T.maritima* STUDIED BY PULSED ESR SPECTROSCOPY

3.1 INTRODUCTION

Bacteria sense and respond to changes in their environment via a complex signal transduction pathway that involves transmembrane chemoreceptors, the histidine kinase CheA and the coupling protein CheW as major components of the sensory apparatus. Cellular studies in *E.coli* as well as in other bacteria have shown that these proteins are organized into higher order assemblies or clusters at the poles of the cell[1-5]. Recent whole-cell tomography of these clusters reveal them to form a hexagonal lattice on the cytoplasmic side of the membrane, with the long, rod-shaped receptors thought to be projecting down from the membrane to associate a layer of CheA and CheW at their tips[4,6,7]. This complex assembly is essential to generate the sensitivity, gain and dynamic range exhibited by the chemotaxis system. Substantial information is available about the individual components of the ternary complex of CheA, CheW and receptors. The crystal structure of the cytoplasmic signaling domain from the *E.coli* serine receptor Tsr [8] and subsequent cross-linking, genetic, and reconsitution studies [9-12] indicate that a trimer-of-dimers forms among the *E.coli* receptors. Tomographic reconstructions of overexpressed full-length Tsr receptors [7,13-15] confirm a trimer-of-dimers assembly state for the isolated receptors, and the 3-fold symmetry is consistent with observed hexagonal lattices[6,7,13,14]. These lattice structures are remarkably conserved across a wide range of bacteria[6]. Unlike Tsr, signaling domains from a hyperthermophilic organism *T.maritima* do not form trimers in

crystals, but rather pack as a hedgerow of dimers[16,17]. Such an association mode may reflect interactions between receptors on the edges of the cluster hexagon.

At the tips of the receptors lie CheA and CheW, but relatively little is known about how they assemble within the lattice. The histidine kinase CheA is a homodimer, with each subunit consisting of five distinct functional domains, from P1 to P5. P1 contains the histidine that is the site of autophosphorylation, P2 docks CheY, (the phosphocarrier protein that receives phosphate from P1), P3 dimerizes CheA, P4 (the kinase domain) binds ATP, and P5 (the regulatory domain) couples CheA to CheW and receptors. Whereas P3, P4 and P5 are linked together and form a somewhat rigid construct referred to as CheAΔ289[18], the substrate-binding domain (P1) and CheY-docking domain (P2) are joined to each other and the latter to CheAΔ289 via long variable linkers that give them high mobility, at least in purified samples[16,19,20]. The regulatory domain P5 and CheW are structurally similar, each made of two intertwined SH3-like β-barrel domains, designated as subdomain 1 and 2 in CheW. The end of each β-barrel in both CheW and P5 domain contains conserved, exposed, hydrophobic residues. Consistent with the genetic and biochemical studies[21-25], the structure determined by Electron Spin Resonance (ESR)spectroscopy and the crystal structure of CheW in complex with CheAΔ354 (domains P4 and P5 only) revealed that the proteins bind in a pseudo-symmetric interaction with the hydrophobic end of P5 subdomain 1 binding the hydrophobic end of CheW subdomain 2[16]. With application of site-directed spin labeling and pulsed-dipolar ESR, this association mode was demonstrated in the context of CheΔ289, where one CheW binds each subunit of the CheΔ289 dimer. Less is known about how CheA and CheW bind to the chemoreceptors, but direct biophysical data is mounting. Protection and fluorescence studies have highlighted a rather wide receptor docking surface on CheA[24], and critical receptor-interaction residues on CheW have been identified by biochemical and

genetic studies[23,26,27]. *In vivo* florescence microscopy studies reveal that receptors aggregate via their cytoplasmic domains and the clustering enhances in the presence of both CheW and selected domains of CheA[3]. This suggests that: either CheA and/or CheW indirectly induces a change in the nature of intrinsic receptor self association, or CheA and/or CheW directly act as a linker on groups of receptor and thereby increase clustering. In the latter case, one might expect that either CheA or CheW self-associate through a specific interface.

In one of the initial models of the sensory apparatus[28], CheA monomers were suggested to play a major role in propagating conformational changes not only within the homo-dimer, but also to monomer units of nearby CheA dimers. In crystal structures of CheAΔ289 alone[18] and in complex of CheAΔ354 with CheW[16], subdomain 2 of P5 makes a symmetric interaction with a neighboring P5 domain in a manner that closely mimics the contact between CheW and the P5 subdomain 1 (Figure 3.1). Notably, this region is conserved among all CheA sequences and mutants near or at this surface show reduction in the ability of attractant to deactivate CheA even though single-site substitutions at this interface are still functional for chemotaxis[22]. Also, in the NMR studies, failure to get resolved resonances from the CheAΔ289 construct was partly attributed to transient associations between different dimers[29]. Based on these observations, we proposed that a P5-P5 contact may be an important interaction within the kinase-receptor clusters[16]. We have now probed the association properties of *T.maritima* CheA in solution by Pulsed Dipolar ESR Spectroscopy (PDS) [30-33]and mapped interacting surfaces by cross-linking studies. We herein report that dimers of CheAΔ289 do self-associate to a minor degree in solution, and the interface through which these associations occur is essentially the same as the one that participates in the forementioned crystal contacts. Furthermore, the binding of CheW to CheA does not appear to affect CheA self-association.

We found that similar to CheAΔ289, CheW also self associates in solution to some extent to form dimers. In past, no self association properties have been reported for CheW. We have recorded dipolar signals from spin labeled CheW proteins which confirms the presence of higher order associations for CheW. The amplitude of the signals were weak and correspond to only 10-15% of the maximum dipolar signals. The signals from CheW dimers disappeared in presence of CheAΔ289 indicating that the binding with latter is considerably stronger than interaction between dimers.

3.2 RESULTS

3.2.1 Size-exclusion chromatography indicates that CheA dimers form tetramers

The CheA kinases from both *E.coli* and *T.maritima* are predominantly dimers in solution[34-36]. Nevertheless, CheA and CheAΔ289 from *T.maritima*, in addition to having a strong affinity for dimer formation, also have a tendency to self associate and form higher state oligomers in solution. The elution profile from gel filtration chromatography (Superdex 200 column) of wild type CheAΔ289 shows the majority species to be a dimer (molecular weight 84kDa), along with a small population of higher state oligomers (Figure 3.2).

These oligomers are likely to be tetramers (dimer of dimers) of CheAΔ289 because of their elution volume and the fact that CheA dimers, purposely cross-linked through engineered disulfide bonds, elute at the same position. Along with the wild type protein, about twenty cysteine variants of CheAΔ289 also show tetramer formation, both with and without covalent cross-linking. For some preparations, a small fraction of the protein formed even larger aggregates and eluted in the void volume of the column.

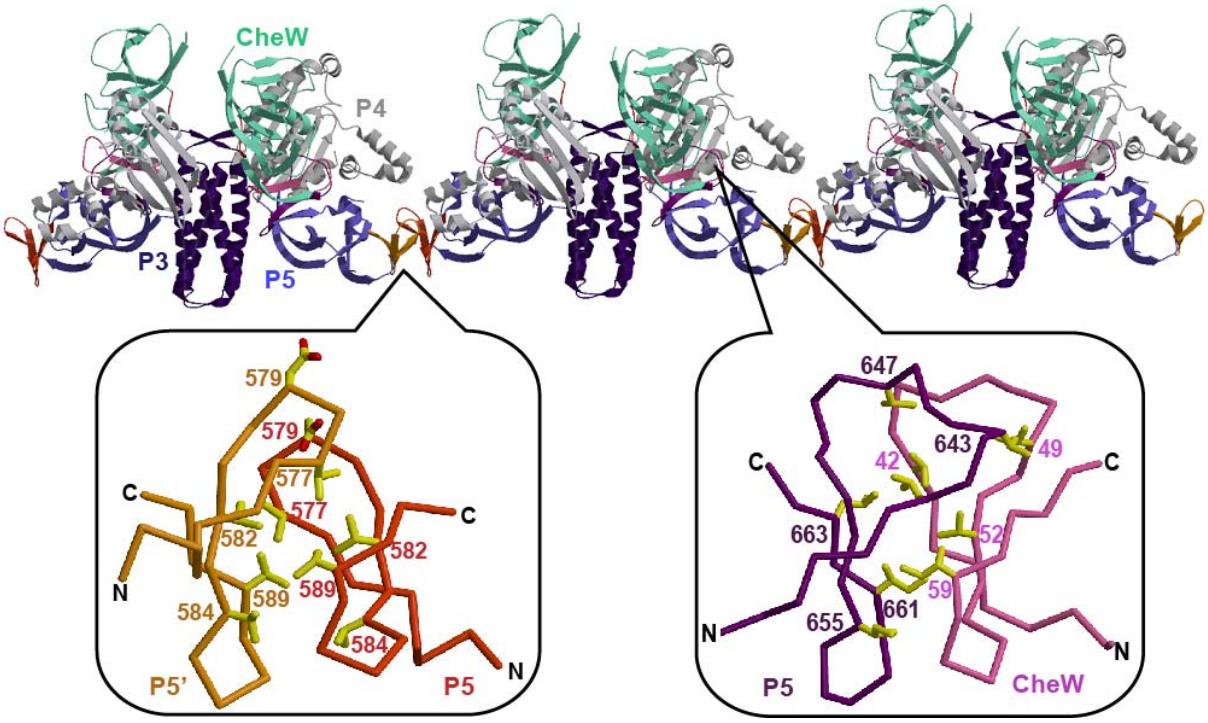

Figure 3.1 Similarity of binding interface between CheW and P5 domain, and between two P5 domains from adjacent CheA dimers. (Figure has been adapted from Figure 4 of reference[16].

3.2.2 Size-exclusion chromatography indicates that CheW associate in dimers

We observed that CheW forms weak affinity dimers in solution. The elution profile from gel filtration chromatography (Superdex 75)of wild type CheW as well as five different cysteine mutants of CheW showed a major peak(Figure 3.3) for a monomer (elution volume about 177 ml), but also a minor peak corresponding to that of CheW dimer (elution volume about 150ml).

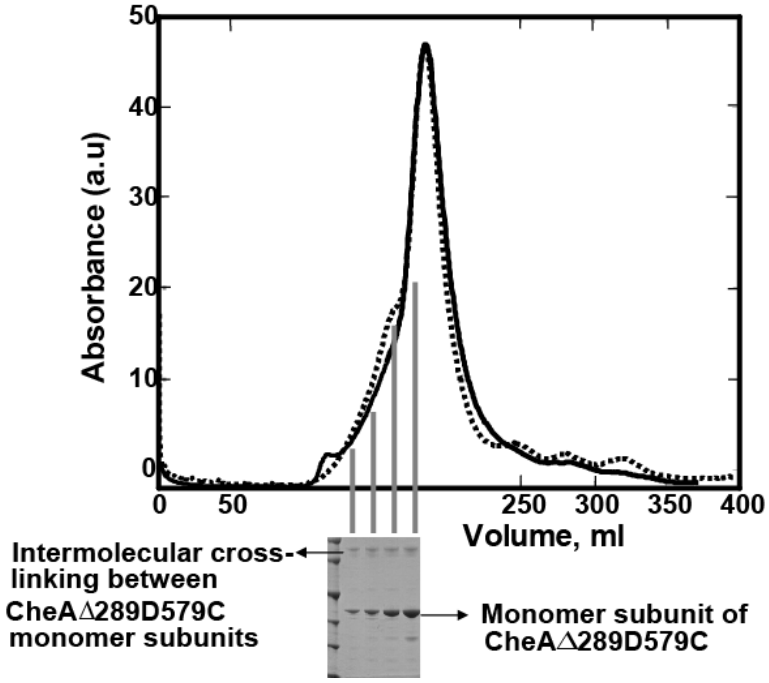

Figure 3.2. Initial evidence for CheA aggregation from size-exclusion chromatography. Overlay of gel filtration profiles of wild type CheAΔ289 (——) and D579CCheAΔ289 (·····)show the dominant peak corresponding to the molecular weight of dimer, while a small shoulder at 163 ml indicates higher order associations. The SDS PAGE analysis of selected fractions close to the peak shoulder from CheAΔ289 variant D579C produces higher molecular weight bands (~84kD) which correspond to the two cross-linked monomer subunits of CheAΔ289D579C.

3.2.3 DEER experiments

a) Non-specific dipolar signals from spin-labeled CheAΔ289

The DEER signal (V(t)), which reflects both the frequency and strength (amplitude) of the dipolar interaction is a product of intramolecular (within CheAΔ289 dimer, V_{intra}) and intermolecular (V_{inter}) dipolar contributions (Equation 2 in Materials and Methods). In a homogenous protein solution, the intermolecular contribution leads

to a simple exponential decay from which the local spin concentration can be calculated (Equation 6).

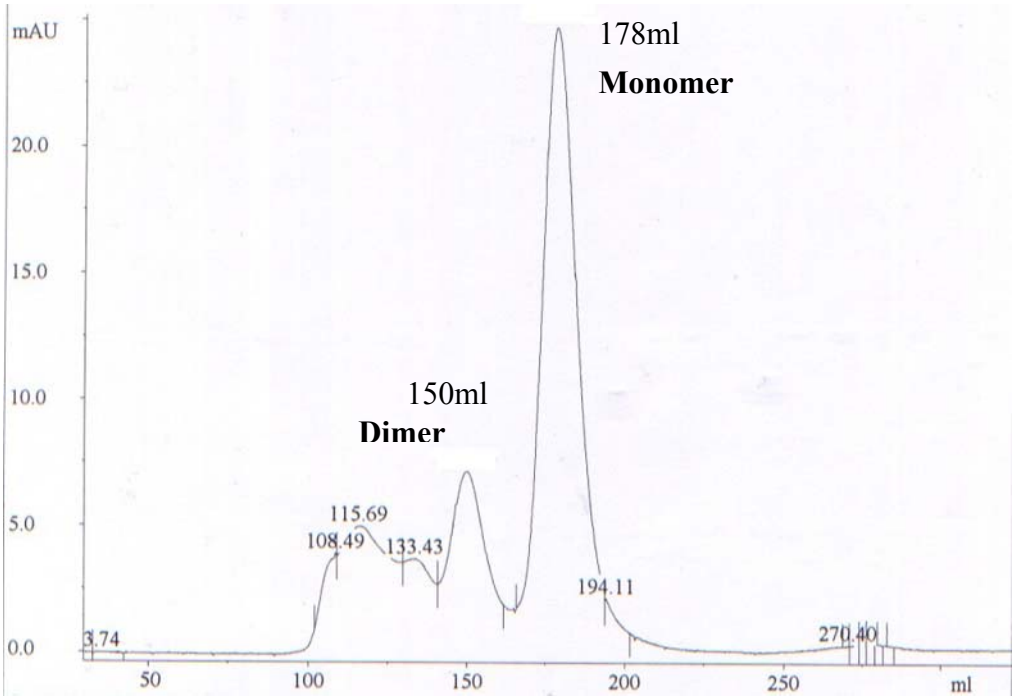

Figure 3.3 Elution profile of spin labeled CheWS80C from gel filtration chromatography.

This decay modifies both the signal of interest (i.e V_{intra}) and the constant background. The latter is thus visible as a monotonically decaying baseline. In the logarithmic plot of the signal amplitude vs time, this contribution leads to a slope of V(t) (also referred as baseline, Equation 6). In dipolar experiments with several spin labeled cysteine variants of CheAΔ289, we consistently observed that the apparent spin concentration calculated from a DEER experiment (Equation 6) was by a factor of 4-5 higher compared to that expected based on protein concentration. This points to a possibility of aggregation as elaborated in the discussion section. In such a case, the

local spin concentration within a 1.5-7 nm radius from a given spin pair is greater than that average spin concentration and hence the increase slope of ln(V(t)) vs time reports on a local concentration, which is greater than the average. To directly confirm the presence of aggregates, we performed magnetic dilution experiments, in which unlabeled protein systematically replaces those molecules with spin labels. At a sufficiently high level of magnetic dilution, the local concentration will be decreased and only the contribution from a random distribution over the sample remains. When the normalized amplitudes from successively diluted samples are compared to each other a reduction in the slope indicates association/aggregation at higher concentrations.

We performed magnetic dilution experiments with spin-labeled sites on all the three domains of CheAΔ289. Not only did changes in the dipolar signal on dilution indicate higher order associations of CheA in solution, but notably the behavior was not the same for each labeled position (Figure 3.4).

In particular, upon magnetic dilution we noticed a significant reduction in the intermolecular signals from spin labels on P4 (Figure 3.5(a)) and those sites which are located at the peripheral end of the P5 domains (Figure 3.5(b)). Nearly no effect was observed for those spins located close to or on the P3 domain (Figure 3.5(c), (d)). Given the structure of the CheA dimer (Figure. 3.4), this result suggests that the dimers are associating via their more peripheral domains (P4 and P5). In the aggregates, the P3 domains, which reside at the center of the dimers, must be separated by at least 70 Å[30] leading to only a small contribution from aggregation. (Note that there is a distinct intramolecular signal from the symmetric spins across the P3 domain within one dimer, as is evident from the strong oscillatory shape of Figure. 3.6)

b) Specific dipolar signals from spin-labeled CheAΔ289

We have measured dipolar distances between several spin labeled sites on CheAΔ289. With the exception of D579C on the P5 domain, the dipolar signals from all the Cys-substituted CheAΔ289 variants gave average distances of separation that agree well with the intramolecular distances measured between the C_β coordinates of the native residues in the crystal structure of CheAΔ289 dimer (Table 3.1).

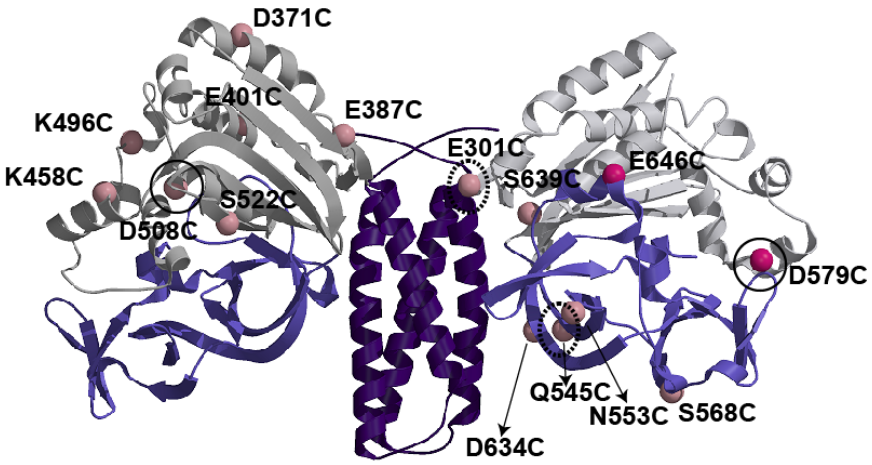

Figure 3.4. Position of spin label sites on the crystal structure of CheAΔ289 which were tested in cross-linking and magnetic dilution experiments. For cross-linking experiments, sites on P4 and P5 domain are shown on different monomer subunits for the sake of clarity and are represented by spheres. From a set of fourteen sites, only E646C and D579C on P5 domain (represented by dark-pink spheres) were found to form disulphide bond readily. Magnetic dilution experiments were performed with four spin-labeled sites (E301C, Q545C, D508C and D579C) on CheAΔ289. Sites D508C and D579C (spheres marked with solid black circles) are located at the periphery of the complex and show drastic reduction in baseline when unlabeled CheAΔ289 protein is added. In contrast, only minor changes were observed for E301C and Q545C (spheres marked with dashed black circle), as they are located near the core of the protein.

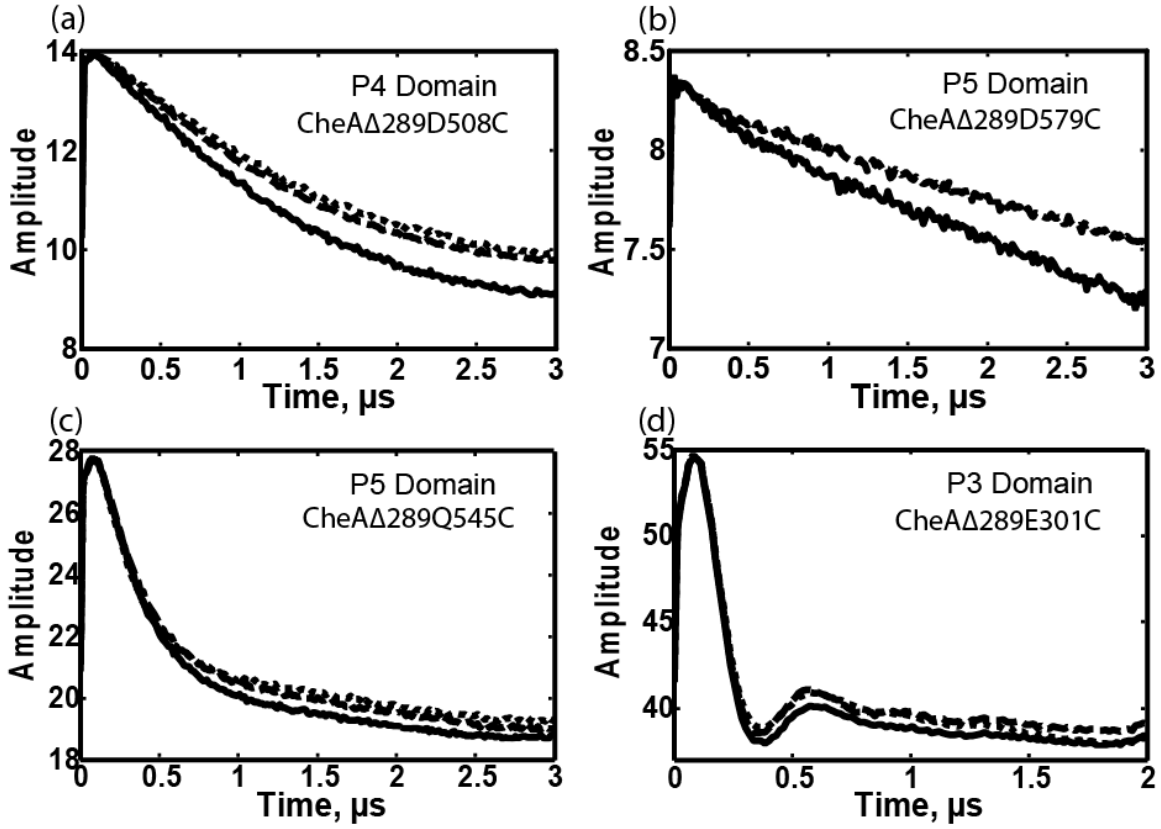

Figure 3.5. Magnetic dilution experiments were carried out with four (E301C, D508C, Q545C and D579C) spin labeled sites on CheAΔ289. While the first two sites belong to domain P3 and P4 respectively, the latter two are located on different ends of P5 domain. In all samples, the concentration of spin labeled protein was kept constant at 25μM. The solid line (——) in each of the plot shows the DEER signal obtained from spin labeled CheAΔ289. Wild type protein was added in three (– – · denoted by 3X) and five times·(·····5 X) excess of the concentration of spin labeled CheAΔ289. Stoichiometric amounts of wild type CheW was added in all samples.

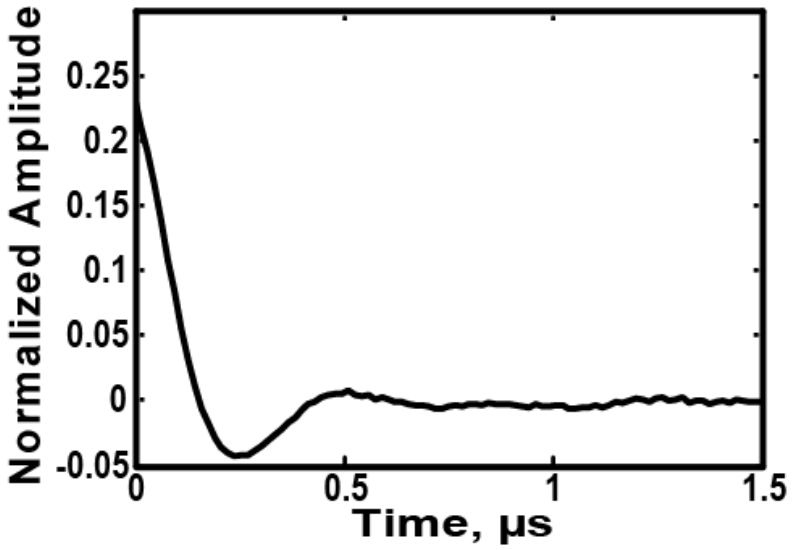

Figure 3.6. A characteristic intra-molecular dipolar signal on the CheA P3 domain. Strong oscillating dipolar signal from site E301C after baseline correction. This site is located at the top of P3 domain and the signal represents the width of the dimerization domain.

However, with D579C, in addition to a very long distance that cannot be measured directly (consistent with the separation of these symmetric sites within the dimer (103 Å)), we observed a weak dipolar signal representing a definite short distance (inset in Figure 3.7(b)). Residue 579 is located at the peripheral end of the P5 domain (subdomain 2), hence the presence of this additional short distance, argues in favor of a spin-spin coupling that results from two CheA dimers associated via an interface that brings the two 579 positions close together. The short distance component increased from 15 to 30% of maximum dipolar signal amplitude when the protein concentration was changed from 50 to 100 µM, which would be expected for a biomolecular association.

Table 3.1. Comparison of distance averages from ESR with C_β separations of corresponding sites in the structure of CheAΔ289.

	R_{avg} from ESR (Å)	C_β separations from the crystal structure of CheAΔ289 (Å)
P3 domain		
301	27	22
318	28	20
331	29	18
P4 domain		
371	50	65
387	59	49
401	50	52
508	60	72
P5 domain		
545	44	41
553	63	64
568	62	74
634	40	31
639	45	32
646	58	60

However, further increase in the concentration of spin-labeled CheAΔ289D579C failed to increase the short distance component. At such high concentrations of protein, more non-specific aggregation of the dimers occurs, and thus, these other modes of association may compete with the specific association through the P5 domains. In the presence of CheW, the short distance signal persisted, but due to the weak nature of the signal, it is difficult to quantitatively conclude whether CheW has a positive or negative impact on the self-association behavior of CheAΔ289 as detected at the 579 site. The distributed nature of the DEER signal from CheAΔ289E646C prevented us from distinctly separating the short distance component.

c) Specific dipolar signals from spin-labeled CheW

Pulsed dipolar spectroscopy on CheW proteins individually spin labeled at sites 9, 31, 80, 137 and 139 produced dipolar signals between sites that confirmed the presence of CheW dimer. In most of the cases, for almost the same protein concentration, the strength of the signal was very weak, corresponded to only 10-15% of the maximum dipolar amplitude. The exception was site 80, where the amplitude of the signal was as high as 50% of the expected full amplitude (Figure 3.8).

Distance distributions have been calculated for all the sites, except sites 31 and 139. In these two cases, the low signal to noise prevented us from processing the data further. For site 9, the increase in protein concentration by a factor of 1.6 improved the dipolar amplitude by the corresponding factor. However, with site 80, the increase in protein concentration by 5 times only increased the amplitude by factor of 2.3. Possible reason for this discrepancy could come from the uncertainty in the baseline correction for the DEER signal.

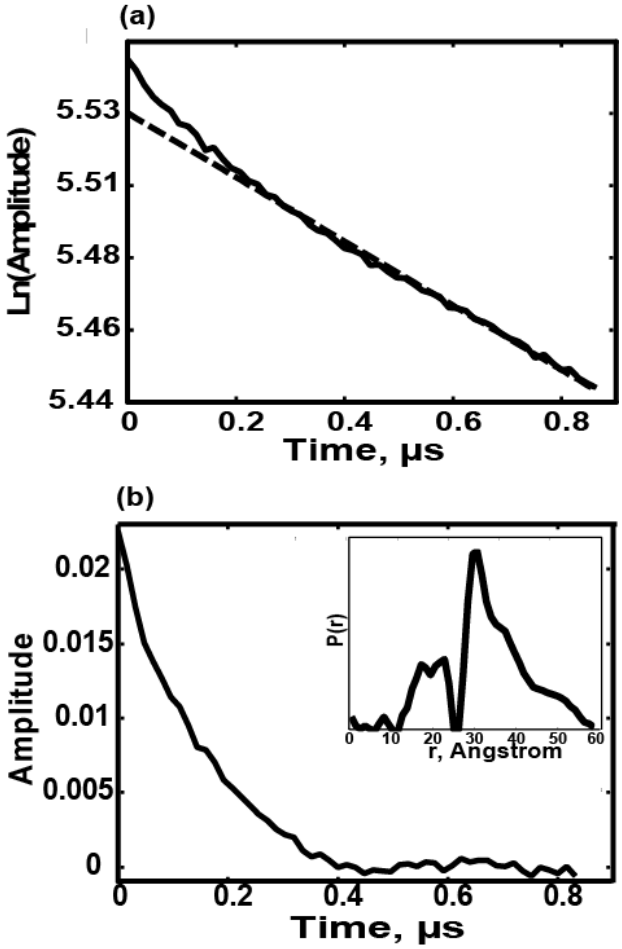

Figure 3.7. Direct evidence for dimer-to-dimer contacts from dipolar ESR. DEER signal from spin labeled site D579C on CheAΔ289 indicates presence of a minor amount of short distance along with major long distance. a) In the logarithmic plot of signal against time, the solid curve represents the signal derived from short separations sitting on a large baseline (the dotted line) which is approximated by a linear function. b) The signal after baseline correction clearly shows the presence of a weak but definite short distance. It should be noted that any contribution from the very long distance of 103 Å corresponding to C_β separations within the dimer is implicitly subtracted out as a part of the baseline. The inset shows the distance distribution from the remaining signal corresponding to shorter distances.

Also, the addition of 225 μM wild type CheW to 125 μM spin labeled CheWS80C reduced the dipolar amplitude by 30% which is consistent with a reduction in the population of CheW dimers.

We found that the short distance from spin-labeled CheWE31C dimer disappears in presence of wild type CheAΔ289. Simultaneously, we observed a 270% increase in signal amplitude and a new long distance which corresponded to distance between two CheW's bound to CheAΔ289 dimer.

We did not observe any change in the dipolar signal in the presence of unlabeled receptor (Figure 3.9). All the results have been summarized in Table 3.2.

3.2.4 Cross-linking experiments

a) Free CheA

Site-directed disulphide cross-linking is an important tool for determination of proximity between residues in an individual protein fold or at the interface of protein complexes[37]. In the latter case, given a suspected binding surface, the approach involves mutating consecutive residues on the interface in each of the protein components to cysteines, and thereafter monitoring the rate of disulphide formation with ambient or supplied oxidizing agent. For soluble proteins, a redox catalyst (also called an initiator (I)) such as Cu (II) (1, 10 phenanthroline)$_3$ is commonly used to initiate and accelerate the reaction. In the absence of non-specific interactions, only those cysteine pairs on the interface, which have their β centers separated by 4-8Å, readily form disulphide bonds (or cross-link). With a number of cysteine variants of CheAΔ289 in hand, we applied this strategy to confirm if the sub-domain 2 of the P5 domain indeed is exclusively involved in self-association of CheAΔ289.

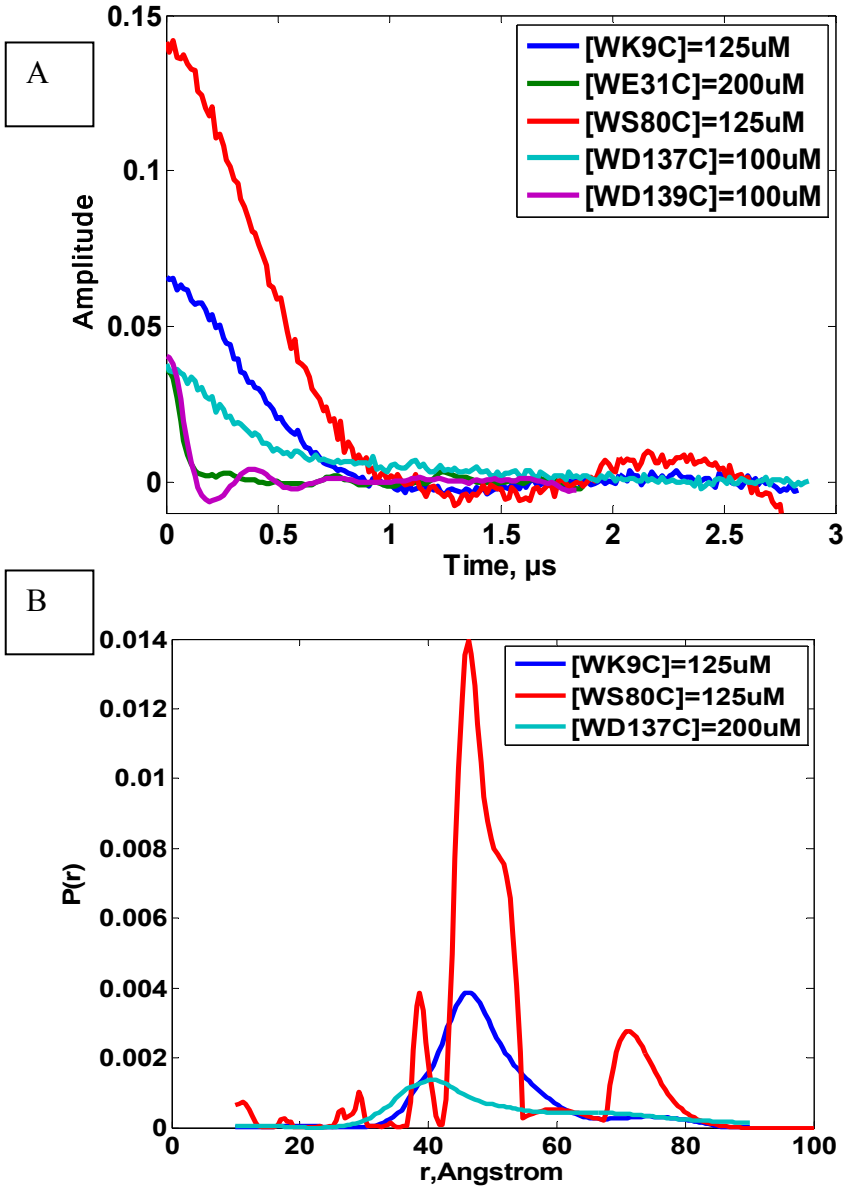

Figure 3.8. Time domain signals and distance distributions from spin labeled CheW. A) Time domain signals from five sites on CheW. B) Distance distributions from sites 9, 80 and 137 on CheW.

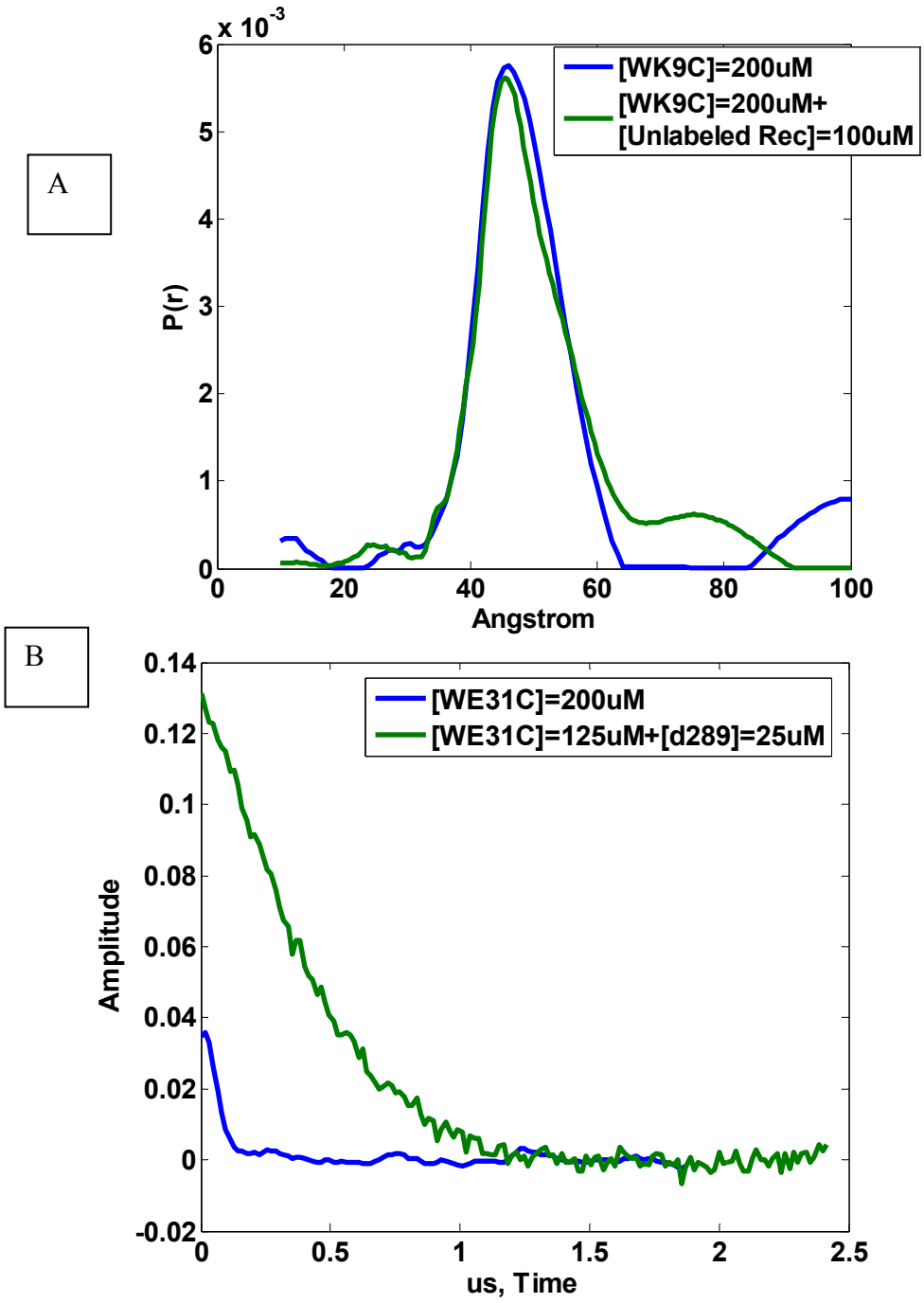

Figure 3.9. Effect of unlabeled receptor and CheAΔ289 on CheW dimers. A) Addition of unlabeled receptor did not change distance distribution from site 9 on CheW. B) Addition of wild type CheAΔ289 disrupts CheW dimers and increases the signal amplitude due to the complex formed by dimeric CheAΔ289 and two molecules of CheW.

Table 3.2 Relative amplitude of dipolar signals from five sites on CheW as a function of protein concentrations. The reported amplitude is the amplitude of DEER signal after the baseline correction and subtracting 1 (signal from a pair of uncorrelated spins for a given pulse sequence)

	Protein Concentration				
CheW	25 μM	100 μM	125 μM	200 μM	125μM + 250μM CheW
K9C			0.06	0.1	
E31C				0.03	
S80C	0.06		0.16		0.1
D137C				0.04	
D139C				0.04	

We tested fourteen variants of CheAΔ289 for their ability to cross-link. The cysteine substitutions were evenly divided between the P4 and P5 domains and were uniformly distributed over the surface of these domains (Figure 3.4). While all the cysteine substitutions on the P4 domain gave negative results, we were able to isolate two: E646C and D579C on the P5 domain which readily formed cross-links (Figure 3.10). An increase in the efficacy of cross-linking with protein concentration,

indicated that both the 646 and 579 disulfide bonds were being formed intermolecularly, i.e. between, not within, CheA dimers.

Effect of CheW and receptor fragments on cross-linking

The autophosphorylation activity of kinase CheA is regulated by CheW and chemoreceptors[38,39].The presence or absence of either CheA, or CheW, results in drastic changes in receptor cluster formation emphasizing their structural inter-dependence[3]. Interestingly the crosslinking at E646C significantly decreased in the presence of CheW, which perhaps reflects the fact that CheW binds to the subdomain 1 of P5, where position 646 resides. In contrast, no reduction of D579C crosslinking was observed when CheW was added. The presence of an unlabeled receptor cytoplasmic signaling domain that is known to inhibit *T.maritima* CheA(Pollard et al, unpublished), did not affect crosslinking from either the 646 or 579 site, irrespective of the presence or absence of CheW.

3.3 DISCUSSION

We have applied Pulsed Dipolar ESR spectroscopy to probe aggregation properties of histidine kinase CheA. Traditionally, this technique has been applied to higher oligomeric states only in the study geometry of polynitroxide radicals[40], clusters formed by biradicals[30], small peptides and only recently, small-size proteins (~15kD)[41]. In all or at least in most of these small systems, aggregation properties could be derived from the magnitude or shape of the dipolar signal rather than monitoring changes in baseline with subsequent addition of unlabeled component, as we have performed in the magnetic dilution studies of CheAΔ289. Here, for the first time, we have applied the application of baseline shape analysis to study aggregation states of high molecular weight molecules (the dimer of CheAΔ289 is ~84kD).

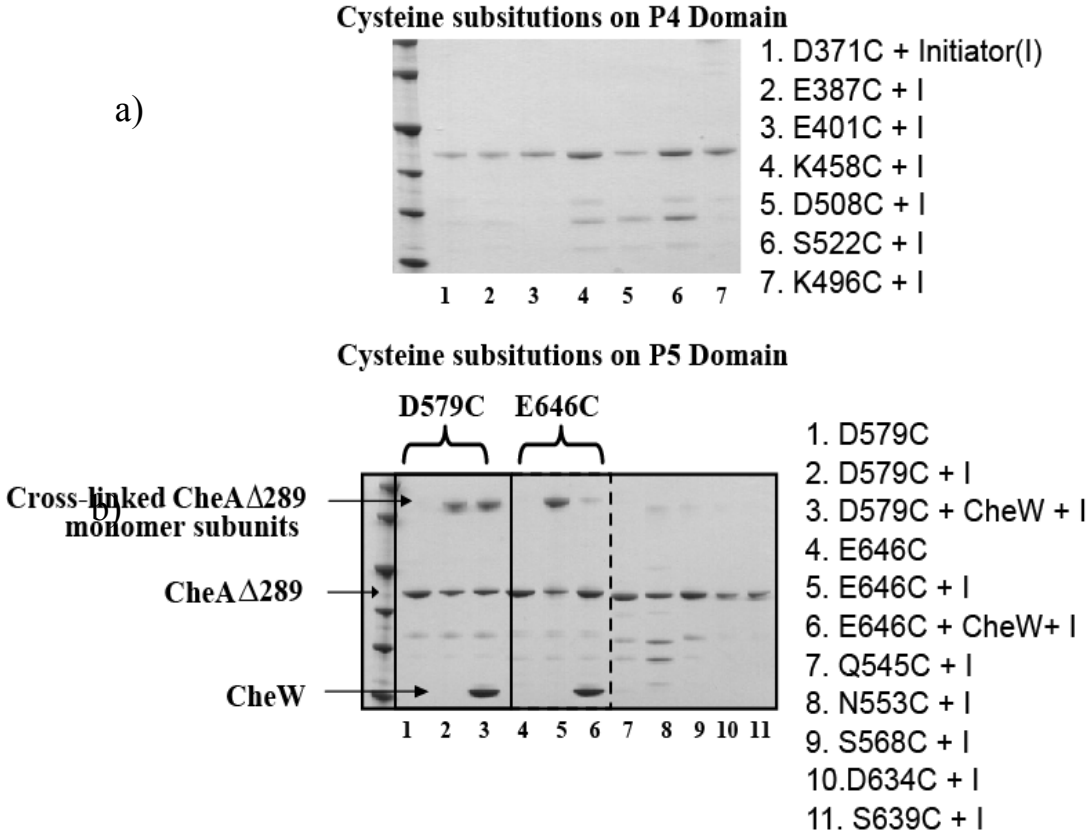

Figure 3.10. Fourteen cysteine substituted variants of CheAΔ289 were tested for their ability to form disulphide bond or crosslink in presence of a cross-linking reagent. a) None of the seven cysteine substitutions on P4 domain successfully cross-linked. b) Out of seven positions on P5 domain, D579C and E646C (lane 2 and 5 respectively) cross-linked. The disulphide formations was severely affected in presence of CheW for E646C (lane 6) while that for D579C was unaffected (lane 3).

As an added advantage, we demonstrate that this method can also specifically determine the protein regions and surfaces that participate in aggregation. In aggregates formed by doubly spin labeled small-size protein, both the inter-molecular and intra-molecular spin distances are within PDS detectable range. Therefore, all of the spin-

label sites on the protein surface will likely have somewhat similar sensitivity to magnetic dilution. But for large-size proteins, sites located close or far away (exceeding the upper detection limit of PDS which is about 75Å[30]) from the aggregation surface will behave differently, and this variation in response can be used to identify interaction surfaces, as we have shown for CheA.

Chemotaxis proteins CheA, CheW and receptors interact closely and form compact clusters at the poles of the cell. Even though several models of the architecture of this assembly have been proposed[8-11,16,24,28,42,43], none of them can be viewed as unique solutions in light of the current experimental evidence. At the molecular level, only the mode of association of CheW with CheA is reliably known. Clearly, clustering can be very crucial for signal processing and amplification as it provides a potential mechanism for the high degree of cooperativity that connects kinase response to ligand binding[5,44-46]. The self-association behavior of receptors has been well demonstrated *in vitro* as well as *in vivo* fluorescence microscopic studies which show that the receptor clusters become more compact in the presence of CheA or CheW. Interestingly, these tight associations may loosen in response to chemoattractant[47]. It is intuitive to propose that CheA and CheW may not just play a role in controlling how the receptors talk to each other, but they also act as a signal propagator within the dense assembly. Self association of CheA or CheW, similar to that observed for the receptor, could well be an important element of the architecture of the signaling particle and may undergo modification during signal propagation. We report here, for the first time, that CheA and CheW indeed have a tendency to self-associate in solution.

CheW is a 17kDalton protein and its structure is made up of two β barrels like domains, called subdomain 1 and 2. In Chemotaxis, CheW is referred to as the adaptor protein which interacts with CheA as well as with Receptors. This suggests that there are multiple protein interaction surfaces concentrated on a relatively small size protein.

Besides the hydrophobic core in sub-domain 1 and 2, the top half of subdomain 2 and the surface between the two sub-domains form hydrophobic patches[25]. These may be potential sites for interacting with other proteins. In the absence of its interacting partner, CheW may associate with itself to bury one of these hydrophobic surfaces. Our observation of CheW dimers in solution is consistent with this idea. It should be noted that the relative population of CheW dimers to monomers in solution is very low, indicating that they have weak binding affinity. Expectedly, these dimers dissociate in presence of a competing stronger interaction partner like CheA. This explains the disappearance of short distance between CheW dimers when wild type CheAΔ289 is added.

Fluorescence microscopy has showed that chemoreceptor clusters become more compact in the presence of CheW, emphasizing that CheW can independently bind to receptors[3]. *In vitro* experiments have calculated the binding affinity (K_d) between the two to be about 10 μM[39]. The presence of CheW dimers have not been reported before. Hence, we were interested to see if these dimers also interact with receptors. In the pulsed dipolar experiments, we did not observe any change in distances between the CheW dimers in the presence of unlabeled receptor. This suggests that CheW dimers do not interact with receptors. Perhaps the receptor interaction surface in CheW dimers is no longer accessible.

Given the qualitative estimate of five set of distances within CheW dimers, these constraints are not sufficient to predict the structure of the dimer. However, initial modeling attempts with these distances do suggest that it is unlikely that CheW's associate symmetrically via the surface at the end of subdomain 1. The P5 domain of CheA binds to CheW through this interface.

Our initial observations of additional peaks or shoulders corresponding to the molecular weight of CheAΔ289 tetramers (dimer of dimers) in the elution profile of gel

filtration chromatography were the first sign of self association. Because native CheAΔ289 has no cysteine residues, it is reasonable to assert that favorable non-covalent interactions must drive the two CheAΔ289 dimers to associate with each other.

DEER experiments with spin-labeled CheAΔ289 molecules further reinforced these findings. The dipolar signal between two coupled spins sits on a baseline that is a contribution from the average local concentration of spins in the sample, which for a homogenous solution is close to the bulk concentration. For some sites on CheAΔ289, this number is considerably greater than that for bulk spin concentration in the sample. In protonated solvents, dipolar signals between spin labels separated by as far as 60 Å[30] can be accurately measured by DEER. Slightly longer distances, till ~75 Å can be determined with relatively less accuracy[30] while those within 70-100 Å only add to the slope of the signal baseline. If these long distances arise due to molecular contacts, such as within large aggregates, the corresponding dipolar signals will disappear if excess unlabeled CheAΔ289 dimers are added to the sample. This is simply because the unlabeled dimers will replace their spin-labeled counterparts within the aggregates and hence decrease the local spin concentration (contributing to the slope of DEER signal). This is likely the case for spin labeled sites D508C and D579C (located on P4 and P5 domain respectively) since the slope of the signals consistently decreased with magnetic dilution Figure 3.5(a), (b)). In the absence of a rigorous theory for dipolar signals from aggregates of large proteins like CheAΔ289, it is difficult to quantitatively derive an aggregation number for this system. But the changes in the baseline just with 3X magnetic dilution definitely points to the presence of low order aggregates.

Importantly, we observed only minor changes in baseline for spin labels at the P3 domain (E301C) or those on the P5 domain that were located very close to the P3 domain (Q545C). This indicates that the intermolecular distances between sites on the P3 domains are outside the ESR detectable range. In other words, association through

the peripheral P4-P5 domains holds the P3 domains relatively far apart in the aggregates. The DEER results emphasize the probable role of P4 and P5 domains in association, thus placing important restrictions on the structure of aggregates.

We reported previously, that the hydrophobic region in the sub-domain 2 of the P5 domain, which is primarily spanned by β10 and β11 strands (Figure 3.1), mediates contacts with the P5 domain of an adjacent symmetry related molecule in the crystal lattice of CheAΔ289 [18]as well as in the complex of CheW with CheAΔ354[16]. If indeed, CheAΔ289 self-associates through this interface in solution, then it should be possible to detect short distances between spin-labeled sites located very close to this interface. Since CheAΔ289 is itself a dimer, it becomes challenging to separate the large intramolecular (within the dimer) from the intermolecular distances (between self-associated dimers) if both of them are comparable. Any unambiguous conclusion can be made only when the two distances are substantially different and can be easily distinguished in the ESR signal. Out of seven cysteine mutations spanning the surface on the P5 regulatory domain, the 579 residue is furthest away from the dimerization domain (P3), which places it in proximity to the hydrophobic surface at one end of P5 domain (Figure 3.1). The intra-dimer distance measured between the C_β coordinates at this residue in the crystal structure of CheAΔ289 dimer is 103 Å, while the inter-dimer distance calculated by generating the symmetry-related molecules is only 8 Å. Thus, if the association between dimers is reasonably populated, the two signals can be distinctly observed in DEER. It should be noted that distances <20 Å are not readily measurable by DEER[30], but the additional length and flexibility of protein backbone at that site, or motion of the spin label, might make the separations between the nitroxides longer, and hence fall within the detectable range. With residue 579, we successfully observed a weak (low population in the sample) but distinct dipolar signal corresponding to a short

distance (centered about 20 Å) along with the expected long intra-dimer distance from DEER (Figure 3.7(b)).

It should be noted, that the overall effect of aggregation on the DEER signal is not large, as is evident from the case of D579C, where the short distance accounted for only 15% of the overall signal amplitude. With reasonable baseline correction (estimated to first order polynomial in most cases as discussed in Chapter 1), the intramolecular distances within the CheAΔ289 dimer, which are the major contribution to the signal, can be accurately determined with little interference from the aggregation effects.

Since the dipolar signal originating from short distances between spin labels at D579C were rather weak, we decided to use cross-linking studies to independently identify specific regions of P4 and P5 domains that could participate in non-covalent interactions. The advantage of cross-linking studies is that they accumulate product. The sites selected for substitutions with cysteine residues are distributed uniformly over the surface of these domains. The failure of seven sites (E387C, E401C, D371C, K458C, K496C, D508C and S522C) on P4 domains to cross-link probably eliminates the role of this domain in aggregation. In contrast, we isolated two sites, E646C and D579C on the P5 domain that cross-link readily. In the crystal structure of CheAΔ289 dimer, the two P5 domains are widely separated in space by the dimerization domain. This, along with the concentration dependence of the crosslinking makes it highly unlikely that in solution, the P5 domains would move close enough to form intra-molecular disulphide bonds. Also, when mapped onto the structure of the P5 domain, the residues 646 and 579 are sufficiently far apart and belong to two distinct hydrophobic regions, one of which has been shown to bind strongly to CheW[16,21,22,24,25]. The accessibility and mobility of this region of P5 should be significantly affected by CheW, which was indeed manifested as an apparent decrease

in the cross-linking of E646C in the presence of CheW, while no such effect was observed with D579C. One interpretation of this data is that the hydrophobic ends of the P5 subdomain 1 and 2 have a strong tendency to associate with a like surface, whether it be found on another P5 domain or CheW. Thus, in the absence of CheW, both ends of P5 can mediate self-association with another P5, but when CheW is present, its high specificity for subdomain 1 blocks access of another P5 domain. As CheW does not appear to interact with P5 subdomain 2, this domain remains free to mediate dimer-to-dimer contacts. In two separate fluorescence microscopy experiments, CheW and the C-terminal P5 domain were found to promote receptor clustering[3]. Given the fact that both of them are structurally similar, the hydrophobic surfaces in each of them could well be involved in self-association and hence instrumental in bringing the receptors together.

The presence of a C-terminal P5 domain in CheA may not be sufficient to promote clustering in all cases. In such instances, it should be noted that the association between P5 domains could be modulated by other CheA domains, CheW (as seen in our cross-linking experiments) or receptors, which would explain how different CheA fragments affect receptor clustering in *cheA:cheW* cells[3]. The $CheA^{short}$ differs from full-length CheA in the removal of 96 amino acids from the N-terminus (i.e. the P1 domain and its linker to P2). Whereas full-length CheA requires CheW to enhance receptor clustering, $CheA^{short}$ will enhance receptor clustering independently. The P1 domain in full-length CheA likely only interacts primarily with the P4 domain, but this interaction could indirectly affect the position of the P5 domains, and perhaps destabilize the interaction between self-associating dimers. CheW binding to P5 domain may then somehow readjust this interaction and facilitate clustering. It is also possible that P5-P5' interaction plays an instrumental role in controlling how small receptor clusters talk to each other. Changes in gluteraldehyde cross-linking

efficieny[47] and theoretical proposals [45,48] suggest that the receptor lattices disrupt to some extent under high attractant concentrations. Thus, the receptor state may also influence CheA self-associations. In fact in *E.coli*, cysteine scanning analysis identified sites very close to the P5-P5' interaction surface where residue substitutions failed to deactivate the kinase[21]. However, three mutants of the P5 domain at the P5-P3 interface isolated as phenotypic suppressors of receptor defects (V606M, G627D, G627C) also failed to deactivate kinase in presence of attractant[22]. In these cases, it is likely the restricted motion of the P5 domain due to introduction of amino acids with larger side-chains at these sites that is probably responsible for deactivation defects. All of these studies point to changes in the positioning and interaction of the P5 domains as being important for kinase regulation. Our work here suggests that the peripheral end of P5 subdomain 2 is a primary site for mediating such contacts. Nonetheless, in contrast to the findings with *E.coli*, the cysteine substituted sites close to the P5-P5' surface of kinase from *S. typhimurium* did not manifest any deactivation defects in the reconstituted signaling complex, when modified with fluorescence labels[24].

We emphasize that the conserved hydrophobic surface at the sub-domain 2 of P5 domain is an attractive binding site for like domains. How these potential linkage sites play out in the various structural states of the signaling particle remains an open question. Furthermore, it is worth noting, that if P5 subdomain 1 binds CheW subdomain 2, and P5 subdomain 2 binds another P5 subdomain 2, there remains an unsatisfied "valency" on the end of CheW subdomain 1, which could also potentially mediate contacts. Although the details remain to be worked out, it does appear that the CheW and P5 domains have the capability to supply important latch points within higher order assembly of the signaling particle.

3.4 MATERIALS AND METHODS

Characterization of protein association/aggregation by Pulsed Dipolar ESR Spectroscopy (PDS)

PDS is a valuable technique used for structural determination of protein complexes[16,49-57]. The method involves measuring magnetic dipolar couplings between two unpaired electrons of nitroxide spin labels attached specifically to genetically engineered cysteine residues on a protein. The dipolar coupling in angular frequency units ($A(\mathbf{r},\theta)$) between spins A and B separated by **r** is given by:

$$A(\mathbf{r},\theta)= \omega_d (1-3\cos^2 \theta) \text{ with } \omega_d = \gamma_e^2 h/(4*\pi^2 *r^3) \quad (1)$$

where γ_e is the gyromagnetic ratio of an electron spin, h is Planck's constant and **r** is the radial vector between the two spins, and θ is the angle between **r** and the direction of the external magnetic field (Figure 1.6). Distance distributions for the interacting spins can be readily reconstructed using several methods[57-60],[61],[49,50,62] of which, the most powerful are based on application of Tikhonov Regularization[59,62,63].

Currently, the two most common methods for distance measurements from dipolar spin-couplings are pulsed double electron-electron resonance (DEER or PELDOR) [16,30,49,64]and double-quantum coherence (DQC)[33,65]. The two methods provide similar information, but DQC is more effective in resolving dipolar couplings over short distances and in dilute samples. We used DEER extensively for our measurements, because the distances that we encountered in spin-labeled chemotaxis proteins were ≥ 20 Å and the proteins could easily be concentrated. Apart from providing distance distributions between spin-labeled sites on the protein components, DEER also provides critical information about the state of homogeneity in the protein sample. The reason for this is that in many cases the amplitude of the dipolar interaction (V(t)) can be factored into a specific "intramolecular" contribution (V_{intra})

that reflects the interaction between a pair of relatively close spins (i.e. on the same molecule), and a non-specific "intermolecular" contribution (V_{inter}) from formally all the spins in the sample but actually those located within a few hundred Å of the pair.[31].

$$V(t) = V_{intra}V_{inter} \quad (2)$$

For the case of a magnetically dilute isotropic sample, the V_{inter} background is known to be a simple exponential decay function, with the exponent proportional to the spin concentration. (Although, it should be noted, V_{inter} can deviate from a simple exponential as t approaches 0. This may be caused by the existence of a minimal spin separation, caused by sterical constraints, or else by spatial correlation of protein distribution, i.e. repulsion or attraction. That is:

$$V_{inter} = \exp(-pkCt) \quad [66] \quad (3)$$

where $k = 2\pi g_A g_B \mu_B^2 \mu_0 / 9\sqrt{3}h$, g_A, and g_B are the g values of two spins, μ_B is the Bohr magneton and p is the fraction of spins flipped by a pump pulse. Note, that C actually is a local concentration of spins that can be estimated to good accuracy from the slope of the logarithmic plot of the signal vs time.

$$\ln(V(t)) = \ln(V_{intra}(t)) + \ln(V_{inter}(t)) \quad (4)$$

$$= \ln(V_{intra}(t)) - kCt \qquad \text{(from Equation 3)} \quad (5)$$

$$\text{Slope} = \ln(V_{intra}(t))/ V(t))/t = kC \quad (6)$$

Pulsed ESR measurements

Double Electron Electron Resonance (DEER) experiments were carried out at 17.5GHz on a home-built 2D-FT ESR spectrometer[16,67]. When measuring signals in protein complexes, the proteins were mixed together and the sample incubated at room temperature for 30-60 mins before freezing them for the ESR experiments. Protein concentrations used for DEER experiments were in the range of 25-50 μM. The intermolecular signal (or the baseline) was approximated by a linear polynomial in most cases. Subsequently, distance distributions were calculated by Tikhonov regularization [63] and further refined by a maximum entropy regularization method (MEM)[62].

Magnetic dilution experiments were performed by keeping the protein spin concentration constant while increasing the concentration of wild type (i.e. unlabeled) CheAΔ289. We added the wild type protein in three (denoted by 3 X, where X is the concentration of spin labeled protein) and five times (5 X) excess of concentration of spin labeled protein (usually 25 μM).

Protein expression and purification

Genes encoding CheAΔ289 (P3-P4-P5 domain, 290-671), CheW (1-151) and thecytoplasmic domain (residues 40-213) of *T.maritima* receptor TM0014 were PCR cloned into the vector pET28a (Novagen), and the proteins expressed with an N-terminal His_6 tag and purified by Ni-NTA affinity chromatography and size-exclusion chromatography as described previously[17,18].

Site directed mutagenesis and spin labeling

In a cysteine-less background of CheAΔ289, seven residues (Q545, N553, S568, D579, E646, D634 and S639) in the P5 domain and an equal number in the P4

domain (D371, E387, E401, K458, K496, D508, and S522) were separately changed to cysteines by Quickchange mutagenesis (Strategene). These proteins were spin labeled with (1-oxyl-2, 2, 5, 5-tetramethylpyrolinly-3-methyl)-methanethiosulfonate (MTSL) with the procedure described previously[16].

Crosslinking experiments

The stock solution of the initiator Cu(II)(1,10 phenanthroline)$_3$ was prepared according to the procedure of Bass and Falke[37]. For each reaction, the final reaction volume was kept constant at 15 µl, which included 5 µl of NuPAGE LDS sample dye. All the proteins were solubilized in gel filtration buffer (50mM TRIS, pH 7.5 and 150mM NaCl). The final concentration of cysteine-substituted CheAΔ289 proteins varied between 1-2µM in the final reaction mixture, whereas the initiator concentration was fixed to 0.1mM in all cases. 10 µl of the reaction mixture was loaded on SDS PAGE gel for analysis by coomassie staining.

REFERENCES

1. Maddock, J. R. & Shapiro, L. (1993). Polar location of the chemoreceptor complex in Escherichia coli cell. *Science* **259**, 1717-1723.
2. Sourjik, V. & Berg, H. C. (2000). Localization of components of the chemotaxis machinery of Escherichia coli using fluorescent protein fusions. *Molecular Microbiology* **37**, 740-751.
3. Kentner, D., Thiem, S., Hildenbeutel, M. & Sourjik, V. (2006). Determinants of chemoreceptor cluster formation in Escherichia coli. *Molecular Microbiology* **61**, 407-417.
4. Zhang, P. J., Khursigara, C. M., Hartnell, L. M. & Subramaniam, S. (2007). Direct visualization of Escherichia coli chemotaxis receptor arrays using cryo-electron microscopy. *Proceedings of the National Academy of Sciences of the United States of America* **104**, 3777-3781.
5. Hazelbauer, G. L., Falke, J. J. & Parkinson, J. S. (2008). Bacterial chemoreceptors: high-performance signaling in networked arrays. *Trends in Biochemical Sciences* **33**, 9-19.
6. Briegel, A., Ding, H. J., Li, Z., Werner, J., Gitai, Z., Dias, D. P., Jensen, R. B. & Jensen, G. J. (2008). Location and architecture of the Caulobacter crescentus chemoreceptor array. *Molecular Microbiology* **69**, 30-41.
7. Khursigara, C. M., Wu, X. W. & Subramaniam, S. (2008). Chemoreceptors in Caulobacter crescentus: Trimers of receptor dimers in a partially ordered hexagonally packed array. *Journal of Bacteriology* **190**, 6805-6810.
8. Kim, K. K., Yokota, H. & Kim, S. H. (1999). Four-helical-bundle structure of the cytoplasmic domain of a serine chemotaxis receptor. *Nature* **400**, 787-792.

9. Studdert, C. A. & Parkinson, J. S. (2004). Crosslinking snapshots of bacterial chemoreceptor squads. *Proceedings of the National Academy of Sciences of the United States of America* **101**, 2117-2122.

10. Studdert, C. A. & Parkinson, J. S. (2005). Insights into the organization and dynamics of bacterial chemoreceptor clusters through in vivo crosslinking studies. *Proceedings of the National Academy of Sciences of the United States of America* **102**, 15623-15628.

11. Ames, P., Studdert, C. A., Reiser, R. H. & Parkinson, J. S. (2002). Collaborative signaling by mixed chemoreceptor teams in Escherichia coli. *Proceedings of the National Academy of Sciences of the United States of America* **99**, 7060-7065.

12. Boldog, T., Grimme, S., Li, M. S., Sligar, S. G. & Hazelbauer, G. L. (2006). Nanodiscs separate chemoreceptor oligomeric states and reveal their signaling properties. *Proceedings of the National Academy of Sciences of the United States of America* **103**, 11509-11514.

13. Lefman, J., Zhang, P. J., Hirai, T., Weis, R. M., Juliani, J., Bliss, D., Kessel, M., Bos, E., Peters, P. J. & Subramaniam, S. (2004). Three-dimensional electron microscopic Imaging of membrane invaginations in Escherichia coli overproducing the chemotaxis receptor Tsr. *Journal of Bacteriology* **186**, 5052-5061.

14. Weis, R. M., Hirai, T., Chalah, A., Kessel, M., Peters, P. J. & Subramaniam, S. (2003). Electron microscopic analysis of membrane assemblies formed by the bacterial chemotaxis receptor Tsr. *Journal of Bacteriology* **185**, 3636-3643.

15. Khursigara, C. M., Wu, X. W., Zhang, P. J., Lefman, J. & Subramaniam, S. (2008). Role of HAMP domains in chemotaxis signaling by bacterial

chemoreceptors. *Proceedings of the National Academy of Sciences of the United States of America* **105**, 16555-16560.

16. Park, S. Y., Borbat, P. P., Gonzalez-Bonet, G., Bhatnagar, J., Pollard, A. M., Freed, J. H., Bilwes, A. M. & Crane, B. R. (2006). Reconstruction of the chemotaxis receptor-kinase assembly. *Nature Structural & Molecular Biology* **13**, 400-407.
17. Pollard, A. M., Bilwes, A. M. & Crane, B. R. (2009). Structure of a soluble chemoreceptor suggests a mechanism for propagating conformational signals. *Biochemistry* **48**, 1936-1944.
18. Bilwes, A. M., Alex, L. A., Crane, B. R. & Simon, M. I. (1999). Structure of CheA, a signal-transducing histidine kinase. *Cell* **96**, 131-141.
19. Morrison, T. B. & Parkinson, J. S. (1994). Liberation of an interaction domain from the phosphotransfer region of cheA, a signaling kinase of Escherichia coli. *Proceedings of the National Academy of Sciences of the United States of America* **91**, 5485-5489.
20. Zhou, H. J., McEvoy, M. M., Lowry, D. F., Swanson, R. V., Simon, M. I. & Dahlquist, F. W. (1996). Phosphotransfer and CheY-binding domains of the histidine autokinase CheA are joined by a flexible linker. *Biochemistry* **35**, 433-443.
21. Zhao, J. S. & Parkinson, J. S. (2006). Cysteine-scanning analysis of the chemoreceptor-coupling domain of the Escherichia coli chemotaxis signaling kinase CheA. *Journal of Bacteriology* **188**, 4321-4330.
22. Zhao, J. H. & Parkinson, J. S. (2006). Mutational analysis of the chemoreceptor-coupling domain of the Escherichia coli chemotaxis signaling kinase CheA. *Journal of Bacteriology* **188**, 3299-3307.

23. Boukhvalova, M., VanBruggen, R. & Stewart, R. C. (2002). CheA kinase and chemoreceptor interaction surfaces on CheW. *Journal of Biological Chemistry* **277**, 23596-23603.

24. Miller, A. S., Kohout, S. C., Gilman, K. A. & Falke, J. J. (2006). CheA kinase of bacterial chemotaxis: Chemical mapping of four essential docking sites. *Biochemistry* **45**, 8699-8711.

25. Griswold, I. J., Zhou, H. J., Matison, M., Swanson, R. V., McIntosh, L. P., Simon, M. I. & Dahlquist, F. W. (2002). The solution structure and interactions of CheW from Thermotoga maritima. *Nature Structural Biology* **9**, 121-125.

26. Liu, J. D. & Parkinson, J. S. (1991). Genetic evidence for interaction between the CheW and Tsr proteins during chemoreceptor signaling by Escherichia coli. *Journal of Bacteriology* **173**, 4941-4951.

27. Boukhvalova, M. S., Dahlquist, F. W. & Stewart, R. C. (2002). CheW binding interactions with CheA and Tar - Importance for chemotaxis signaling in Escherichia coli. *Journal of Biological Chemistry* **277**, 22251-22259.

28. Shimizu, T. S., Le Novere, N., Levin, M. D., Beavil, A. J., Sutton, B. J. & Bray, D. (2000). Molecular model of a lattice of signalling proteins involved in bacterial chemotaxis. *Nature Cell Biology* **2**, 792-796.

29. Hamel, D. J., Zhou, H. J., Starich, M. R., Byrd, R. A. & Dahlquist, F. W. (2006). Chemical-shift-perturbation mapping of the phosphotransfer and catalytic domain interaction in the histidine autokinase CheA from Thermotoga maritima. *Biochemistry* **45**, 9509-9517.

30. Borbat, P. P. & Freed, J. H. (2007). Measuring distances by pulsed dipolar ESR spectroscopy: Spin-labeled histidine kinases. *Two-Component Signaling Systems, Pt B* **423**, 52-+.

31. Jeschke, G. & Polyhach, Y. (2007). Distance measurements on spin-labelled biomacromolecules by pulsed electron paramagnetic resonance. *Physical Chemistry Chemical Physics* **9**, 1895-1910.

32. Schiemann, O. & Prisner, T. F. (2007). Long-range distance determinations in biomacromolecules by EPR spectroscopy. *Quarterly Reviews of Biophysics* **40**, 1-53.

33. Borbat, P. P. & Freed, J. H. (2000). Double-Quantum ESR and Distance Measurements. In *Distance Measurements in Biological Systems by EPR* (Berliner, L. J., Eaton, G. R. & Eaton, S. S., eds.), Vol. 19, pp. 383-459. Kluwer Academic/Plenum Publishers, New York.

34. Gegner, J. A. & Dahlquist, F. W. (1991). Signal transduction in bacteria-CheW forms a reversible complex with the protein kinase CheA. *Proceedings of the National Academy of Sciences of the United States of America* **88**, 750-754.

35. Surette, M. G., Levit, M., Liu, Y., Lukat, G., Ninfa, E. G., Ninfa, A. & Stock, J. B. (1996). Dimerization is required for the activity of the protein histidine kinase CheA that mediates signal transduction in bacterial chemotaxis. *Journal of Biological Chemistry* **271**, 939-945.

36. Park, S. Y., Quezada, C. M., Bilwes, A. M. & Crane, B. R. (2004). Subunit exchange by CheA histidine kinases from the mesophile Escherichia coli and the thermophile Thermotoga maritima. *Biochemistry* **43**, 2228-2240.

37. Bass, R. B., Butler, S. L., Chervitz, S. A., Gloor, S. L. & Falke, J. J. (2007). Use of site-directed cysteine and disulfide chemistry to probe protein structure and dynamics: Applications to soluble and transmembrane receptors of bacterial chemotaxis. *Two-Component Signaling Systems, Pt B* **423**, 25-51.

38. Bourret, R. B., Borkovich, K. A. & Simon, M. I. (1991). Signal transduction pathway involving protein phosphorylation in prokaryotes. *Annual Review of Biochemistry* **60**, 401-441.

39. Gegner, J. A., Graham, D. R., Roth, A. F. & Dahlquist, F. W. (1992). Assembly of an MCP receptor, CheW and kinase CheA complex in the bacterial chemotaxis signal transduction pathway. *Cell* **70**, 975-982.

40. Bode, B. E., Margraf, D., Plackmeyer, J., Durner, G., Prisner, T. F. & Schiemann, O. (2007). Counting the monomers in nanometer-sized oligomers by pulsed electron - Electron double resonance. *Journal of the American Chemical Society* **129**, 6736-6745.

41. Tong, J., Borbat, P. P., Freed, J. H. & Shin, Y. K. (2009). A Scissor Mechanism for Stimulation of SNARE-Mediated Lipid Mixing by Cholesterol. *Proceedings of the National Academy of Sciences of the United States of America* **106,** 5141-5146.

42. Francis, N. R., Wolanin, P. M., Stock, J. B., DeRosier, D. J. & Thomas, D. R. (2004). Three-dimensional structure and organization of a receptor/signaling complex. *Proceedings of the National Academy of Sciences of the United States of America* **101**, 17480-17485.

43. Shimizu, T. S. & Bray, D. (2002). Modelling the bacterial chemotaxis receptor complex. *In Silico Simulation of Biological Processes* **247**, 162-181.

44. Sourjik, V. (2004). Receptor clustering and signal processing in E coli chemotaxis. *Trends in Microbiology* **12**, 569-576.

45. Bray, D., Levin, M. D. & Morton-Firth, C. J. (1998). Receptor clustering as a cellular mechanism to control sensitivity. *Nature* **393**, 85-88.

46. Parkinson, J. S., Ames, P. & Studdert, C. A. (2005). Collaborative signaling by bacterial chemoreceptors. *Current Opinion in Microbiology* **8**, 116-121.

47. Lamanna, A. C., Ordal, G. W. & Kiessling, L. L. (2005). Large increases in attractant concentration disrupt the polar localization of bacterial chemoreceptors. *Molecular Microbiology* **57**, 774-785.

48. Albert, R., Chiu, Y. W. & Othmer, H. G. (2004). Dynamic receptor team formation can explain the high signal transduction gain in Escherichia coli. *Biophysical Journal* **86**, 2650-2659.

49. Milov, A. D., Maryasov, A. G. & Tsvetkov, Y. D. (1998). Pulsed electron double resonance (PELDOR) and its applications in free-radicals research. *Applied Magnetic Resonance* **15**, 107-143.

50. Milov, A. D., Tsvetkov, Y. D., Formaggio, F., Oancea, S., Toniolo, C. & Raap, J. (2003). Aggregation of spin labeled trichogin GA IV dimers: Distance distribution between spin labels in frozen solutions by PELDOR data. *Journal of Physical Chemistry B* **107**, 13719-13727.

51. Milov, A. D., Tsvetkov, Y. D., Formaggio, F., Oancea, S., Toniolo, C. & Raap, J. (2004). Solvent effect on the distance distribution between spin labels in aggregated spin labeled trichogin GA IV dimer peptides as studied by pulsed electron-electron double resonance. *Physical Chemistry Chemical Physics* **6**, 3596-3603.

52. Jeschke, G., Wegener, C., Nietschke, M., Jung, H. & Steinhofft, H. J. (2004). Interresidual distance determination by four-pulse double electron-electron resonance in an integral membrane protein: the Na+/proline transporter PutP of Escherichia coli. *Biophysical Journal* **86**, 2551-2557.

53. Zhou, Z., DeSensi, S. C., Stein, R. A., Brandon, S., Dixit, M., McArdle, E. J., Warren, E. M., Kroh, H. K., Song, L. K., Cobb, C. E., Hustedt, E. J. & Beth, A. H. (2005). Solution structure of the cytoplasmic domain of erythrocyte

membrane band 3 determined by site-directed spin labeling. *Biochemistry* **44**, 15115-15128.

54. Hilger, D., Jung, H., Padan, E., Wegener, C., Vogel, K. P., Steinhoff, H. J. & Jeschke, G. (2005). Assessing oligomerization of membrane proteins by four-pulse DEER: pH-dependent dimerization of NhaA Na+/H+ antiporter of E-coli. *Biophysical Journal* **89**, 1328-1338.

55. Jeschke, G., Abbott, R. J. M., Lea, S. M., Timmel, C. R. & Banham, J. E. (2006). The characterization of weak protein-protein interactions: Evidence from DEER for the trimerization of a von Willebrand factor A domain in solution. *Angewandte Chemie-International Edition* **45**, 1058-1061.

56. Dzikovski, B. G., Borbat, P. P. & Freed, J. H. (2004). Spin-labeled gramicidin A: Channel formation and dissociation. *Biophysical Journal* **87**, 3504-3517.

57. Borbat, P. P., McHaourab, H. S. & Freed, J. H. (2002). Protein structure determination using long-distance constraints from double-quantum coherence ESR: Study of T4 lysozyme. *Journal of the American Chemical Society* **124**, 5304-5314.

58. Jeschke, G., Koch, A., Jonas, U. & Godt, A. (2002). Direct conversion of EPR dipolar time evolution data to distance distributions. *Journal of Magnetic Resonance* **155**, 72-82.

59. Jeschke, G., Panek, G., Godt, A., Bender, A. & Paulsen, H. (2004). Data analysis procedures for pulse ELDOR measurements of broad distance distributions. *Applied Magnetic Resonance* **26**, 223-244.

60. Bowman, M. K., Maryasov, A. G., Kim, N. & DeRose, V. J. (2004). Visualization of distance distribution from pulsed double electron-electron resonance data. *Applied Magnetic Resonance* **26**, 23-39.

61. Raitsimring, A. M. & Salikhov, K. M. (1985). Electron spin echo method as used to analyze the spatial distribution of paramagnetic centers. *Bull. Magn. Reson.* **7**, 184-217.

62. Chiang, Y. W., Borbat, P. P. & Freed, J. H. (2005). Maximum entropy: A complement to Tikhonov regularization for determination of pair distance distributions by pulsed ESR. *Journal of Magnetic Resonance* **177**, 184-196.

63. Chiang, Y. W., Borbat, P. P. & Freed, J. H. (2005). The determination of pair distance distributions by pulsed ESR using Tikhonov regularization. *Journal of Magnetic Resonance* **172**, 279-295.

64. Jeschke, G. (2002). Distance measurements in the nanometer range by pulse EPR. *Chemphyschem* **3**, 927-932.

65. Borbat, P. P. & Freed, J. H. (1999). Multiple-quantum ESR and distance measurements. *Chemical Physics Letters* **313**, 145-154.

66. Jeschke, G., Pannier, M. & Spiess, H. W. (2000). Double Electron-Electron Resonance. In *Distance Measurements in Biolgical Systems by EPR* (Berliner, L. J., Eaton, G. R. & Eaton, S. S., eds.), Vol. 19, pp. 493-512. Kluwer Academic/Plenum Pbulishers, New York.

67. Upadhyay, A. K., Borbat, P. P., Wang, J., Freed, J. H. & Edmondson, D. E. (2008). Determination of the oligomeric states of human and rat monoamine oxidases in the outer mitochondrial membrane and octyl beta-D-glucopyranoside micelles using pulsed dipolar electron spin resonance spectroscopy. *Biochemistry* **47**, 1554-1566.

CHAPTER 4

INTERACTION OF UNLABELED RECEPTOR WITH SPIN LABELED CHEA/CHEW COMPLEX

4.1 INTRODUCTION

The signal transduction pathway of chemotaxis is a two-component system that controls the movement of bacteria in the presence of chemicals. The three central components that control this cascade are the transmembrane chemoreceptors, the auto-kinase CheA and the adaptor protein CheW. These proteins closely interact with each other and form dense clusters at the poles of the cell[1-6]. The architecture of these assemblies is the key to understanding signal processing, amplification and cooperativity in chemotaxis.

Low resolution images from electron tomography of wild type as well as cells over-expressing chemoreceptors showed the existence of partially ordered hexagonal lattice[7,8]. A recent study has reported that a trimer of receptor dimers occupy each vertex of the hexagon, while CheA and CheW only occur beneath alternate vertices[7]. In another study, a continuous density for CheA and CheW has been observed under the hexagonal arrays[8]. However, it is still uncertain how the three proteins assemble at the molecular level. *In vitro* studies have reaffirmed the key signaling unit of receptors to be composed of a trimer of dimers[9-12]. One of the initial models of this assembly predicted the trimer-of-dimers to sit at the corners of vertices of the hexagon, separated from each other by a CheA dimer[13]. The predicted geometry of the model agreed with that observed in cells, but the lattice spacing was found to be inconsistent with the hexagonal pattern in cells. Based on the arrangement of *T.maritima* receptor TM1143 in the crystal lattice, another model of the lattice based on a “hedgerow of

dimers" of receptors has been suggested[14]. This model emphasized the association between P5 domains from different CheA dimers as being crucial in propagating the signal in the lattice. The receptor dimers were then thought to fit into the cleft formed between two CheW's. However, the size of the cleft is clearly not large enough to accommodate a trimer-of-dimers of receptors. A study based on protein-interactions-by cysteine modification identified a large receptor interaction surface on CheA[15]. This surface is defined by a rather few number of sites and is interspaced with sites whose modification have minimal effects on the assembly and function of the core ternary complex.

In this work, we have used long-range distance restraints from Pulsed Dipolar ESR spectroscopy (PDS)[16 17-19] to study the structure of the CheA/CheW complex in the presence of receptor. We systematically measured dipolar distances between symmetrical sites on a CheA dimer or CheW's bound to the CheA dimer. The changes in the motion of CheA domains and CheW in the absence and presence of receptor are directly reflected in the average distances and the distance distributions between spin labeled sites. The set of average distances were used to perform rigid body refinement and predict the conformation of CheA/CheW in the presence of receptor. Compared to the model of CheA/CheW based on crystal structures[14], in the new structure , the receptor-interaction surface on CheW[20,21] is more accessible. We did not observe any significant change in the distances between P4 domains with unlabeled receptor. In the crystal structure of CheAΔ289, the two subunits had different orientations. Our results suggest that in the presence of receptor, this asymmetry is even more reinforced.

4.2 RESULTS

The interaction of unlabeled receptor with CheAΔ289 and CheW is expected to result in changes in domain orientations. In order to understand these changes, we

measured distances between sites symmetrically located on CheAΔ289 dimer and on CheW's bound to this dimer, in the absence and presence of unlabeled receptor. The change in the distances before and after receptor interaction directly reflects the change in orientations of domains on receptor binding.

4.2.1 Interaction between P1's in full length CheA

CheA is composed of five domains, from P1 to P5 and each has a different function. The P1 domain contains the conserved histidine which undergoes phosphorylation when the kinase is activated. The P1 domain is connected to the P2 domain (which docks response regulator CheY for phosphate transfer) via a linker of about 40 residues. The aim of these experiments was to study the interactions between the P1 domains in CheA by measuring distances between symmetrical sites on P1 domain in the CheA dimer.

Our previous pulsed ESR measurements from sites 12 and 14 on P1 domain produced long (more than 60 Å) and broadly distributed distances[14]. Full length CheA has two native cysteine residues: C63 and C208 which are found on P1 and P2 domains respectively. The dipolar signal from CheA spin-labeled at site 63 (with the background of C208S), did give broad distance distributions as before (Full Width at Half Maximum is 30 Å but with R_{avg} of about 42 Å). This contradicts our previous measurements from sites 12 and 14 on helix A (Figure 4.1) which gave substantially longer distances. However, it is possible that the distance distributions from these sites report on the local flexibility of this helix in addition to the overall flexibility of the domain. In order to investigate further, we introduced three new cysteine substitutions: D83C, T53C and S76C in a cysteine-less background of CheA. The positions of all the sites are depicted in Figure 4.1.DEER experiments with corresponding spin-labeled proteins produced very long, broadly distributed distances which were not possible to

measure with accuracy (Figure 4.2). These results are more consistent with our previous results from sites 12 and 14 on P1 domain. We have assigned the results from site 63 as an anomaly which may arise due to unusual orientations of spin label in the protein or due to oligomerization of the tethered domains induced by the spin label at this position. Overall, our results indicate that P1 domains are indeed widely separated and sample many orientations.

Addition of unlabeled receptor produced no significant change in the dipolar signals from site 63 on P1 domain. With site 76, the R_{max} increased by 4 Å on addition of receptor which indicates that P1 domains move further apart. However, this result should be confirmed by spin labeling other sites on the P1 domain.

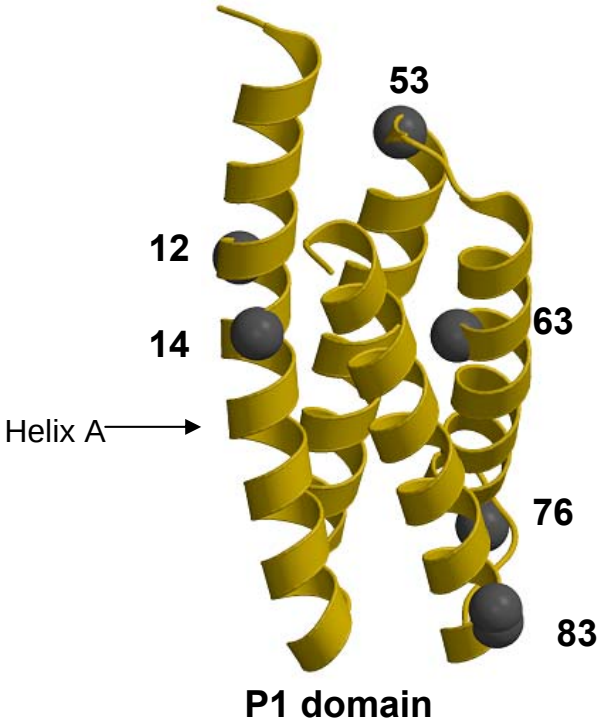

Figure 4.1 Position of spin label sites on P1 domain.

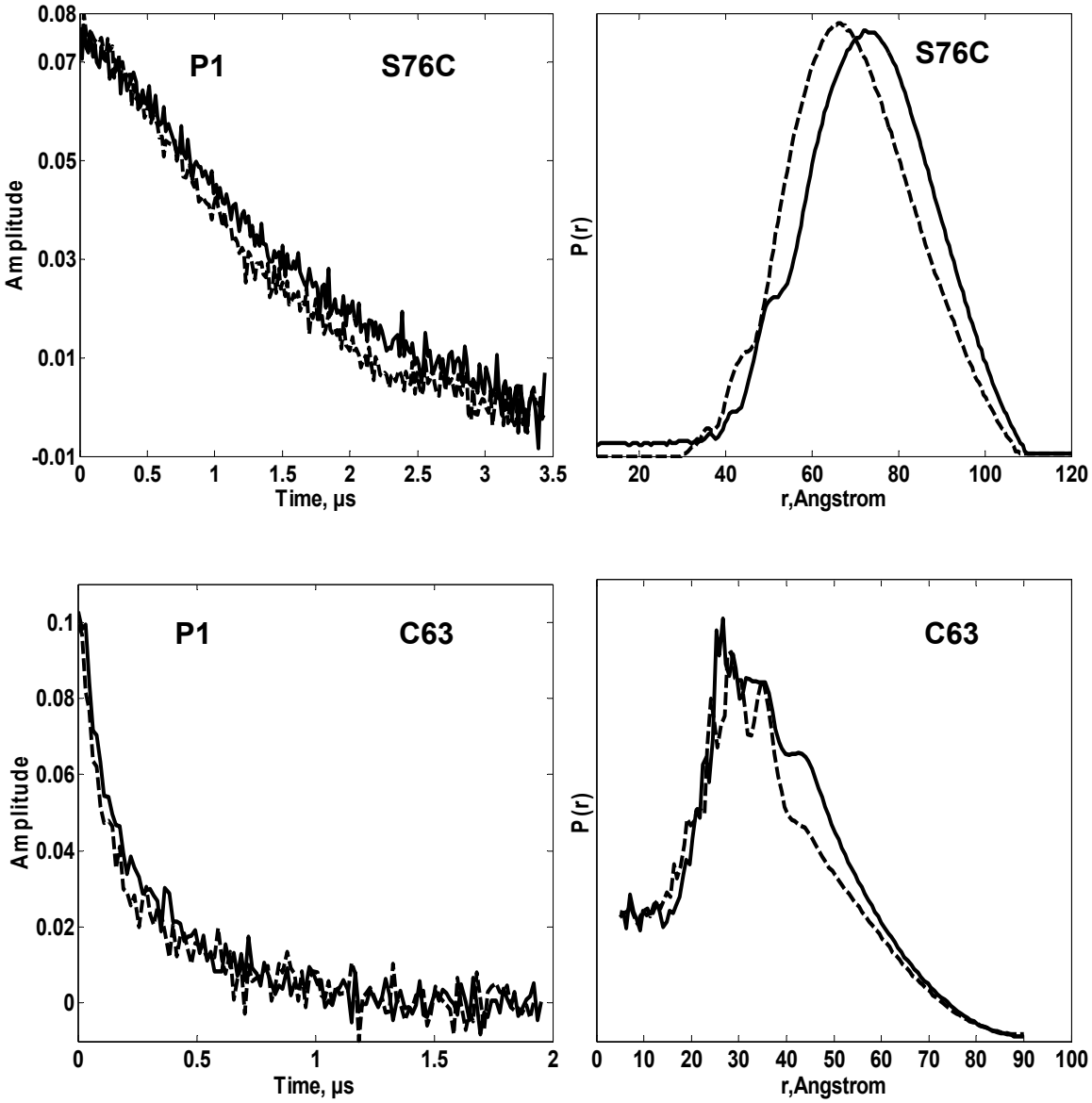

Figure 4.2. Time domain signals and corresponding distance distributions from sites 76 and 63 on P1 domain. Line curves in absence of unlabeled receptor (– –) are compared with those in the presence of unlabeled receptor (——). The concentrations of CheA, CheW were 25 µM, 125 µM in both cases. The concentration of unlabeled receptor was 225 µM and 300 µM for CheAS76C and CheA 63 respectively. All time domain signals and distance distributions are scaled to a common value for ease in comparison.

4.2.2 Interaction between P2's in full length CheA

In a cysteine-free background, the dipolar signals from sites 208 and 178 on the P2 domain (Figure 4.3) gave similar widely distributed distance distributions in the range 20-60 Å (Figure 4.4). Mapped onto the structure of the P2 domain, the two sites belong to the same region of the protein. We did not notice any change in the distance distributions from either sites in presence of unlabeled receptor. The addition of CheY produced only minor changes in the dipolar signals.

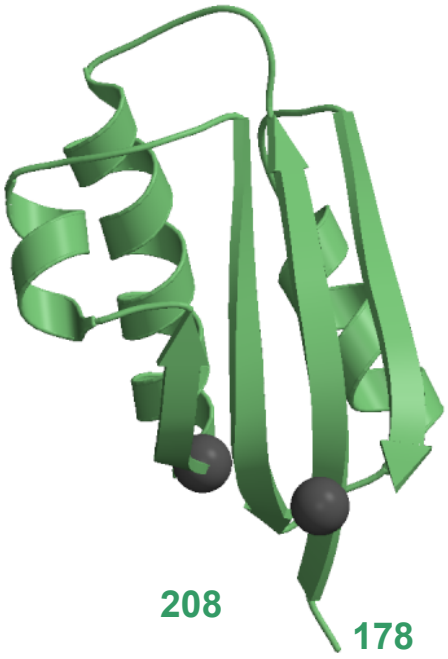

Figure 4.3 Position of spin label sites 178 and 208 on P2 domain.

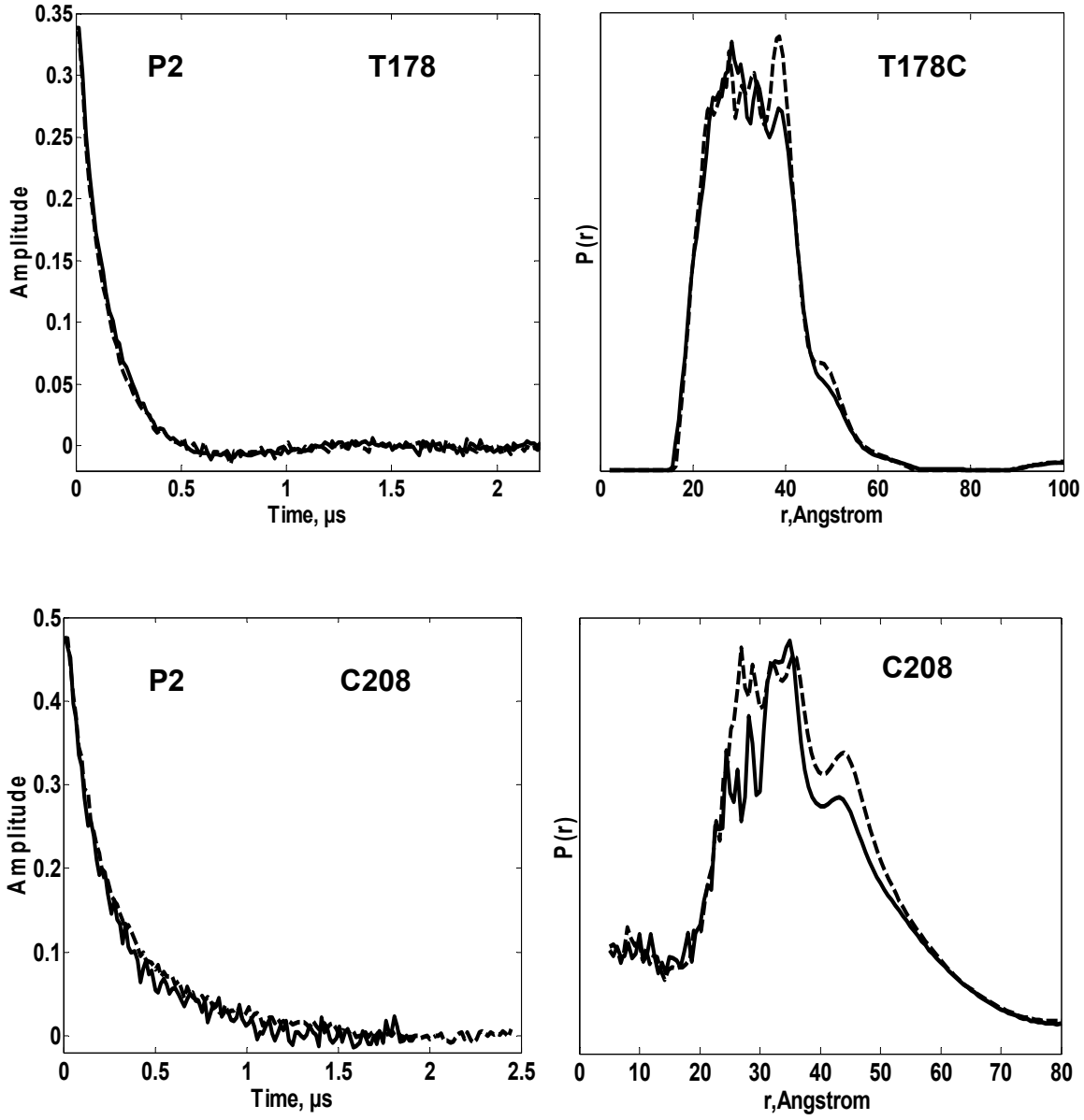

Figure 4.4. Time domain signals and corresponding distance distributions from sites 178 and 208 on P2 domain. Line curves in absence of unlabeled receptor (– –) are compared with those in the presence of unlabeled receptor (___). The concentrations of CheA, CheW and unlabeled receptor were 25 μM, 125 μM and 300 μM in both cases. All time domain signals and distance distributions are scaled to a common value for ease in comparison.

4.2.3 Interaction of unlabeled receptor with CheAΔ289 (domain P3-P4-P5 together)

P3 domains

We did not see any change in dipolar signals on addition of unlabeled receptor from sites 301, 318 and 331 (Figure 4.5). The dimerization domain remained rigid in the presence of receptor.

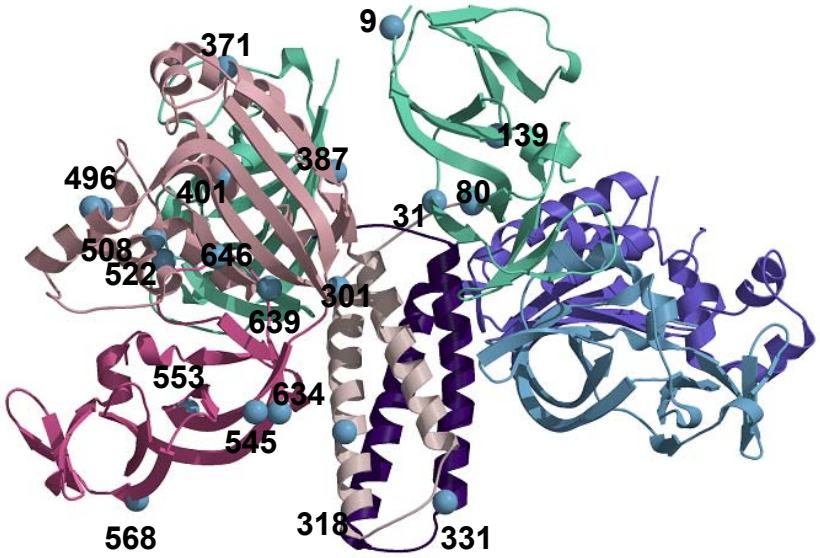

Figure 4.5. Position of spin label sites on CheAΔ289/CheW complex. All positions have symmetry equivalent labeling sites on the adjacent subunit of the dimer (blue) that are omitted for clarity.

P4 domains

In our previous work[14], we reported that P4 domains sample a range of orientations based on our observation of broad distance distributions between P4-P4 or between P4-P3 and P4-P5 domains. Our conclusions at that stage were limited by a

rather small number of spin label sites on P4, namely 387, 496 and 508. For a thorough investigation, we introduced four new cysteine substitutions at 371, 401, 458 and 522 which uniformly covered the surface of domain. Out of a total of seven sites, 496, 458 and 522 produced weak dipolar signals with only 40% of the expected full amplitude. We removed these sites from further study. It is possible that these sites are separated by a distance which exceeds the maximum limit of distance detection by DEER, (at least using protonated solvents).

Dipolar signals from sites 371, 401, 387 and 508 did not change significantly in the presence of receptor (Figure 4.6 and 4.7). The average distances increased or decreased only of the order of 2 Å (Table 4.1) and no major change in distance distributions was observed.

Effect of ATP in dipolar signals from P4 domain

Autophosphorylation of CheA requires the transfer of phosphate group from P4 to P1 domain. In CheAΔ289, we tested if the binding of ATP to P4 domain resulted in a change in distance of separation between the P4 domains. We noticed only minor changes in the lineshape of time domain dipolar signals in the presence of ATP from sites 401 and 508 (Figure 4.8). However, a significant change was observed in dipolar signals from site 496 (Figure 4.9) which resides on the ATP loop. In the presence of ATP, the average distance between these sites on the two CheAΔ289 subunits decreased. Since we did not observe this effect from sites 401 and 508, we believe that this change in distance distribution is attributed to the flexibility of the ATP loop after ATP binding rather than flexibility of the P4 domain as a whole.

The addition of ATP led to 20% decrease in dipolar amplitude from site 401 on P4 domain. We did not observe a similar effect from other sites, hence this observation may be due to the uncertainty in the baseline correction.

Table 4.1 Comparison of ESR averages in the absence and presence of unlabeled receptor. All measurements are in units of Å.

Average distance measurements between symmetric sites on CheAΔ289/CheW		
	Free CheAΔ289/CheW complex	CheAΔ289/CheW/Receptor complex
CheW		
K9C	53 (28)	51(20)
E31C	50 (22)	49(14)
S80C	56 (6)	56(6)
D139C	63(19)	67(24)
P4 domain		
D371C	50(23)	50(23)
E387C	50(18)	48(20)
E401C	50(25)	51(29)
D508C	60(20)	62(21)
P5 domain		
Q545C	44(23)	40(8)
N553C	63(25)	58(32)
S568C	62(22)	63(17)
D634C	42(15)	38(13)
S639C	45(13)	45(13)
E646C	58(14)	61(23)

Full width at half maxima for each distance distribution is reported in parenthesis.

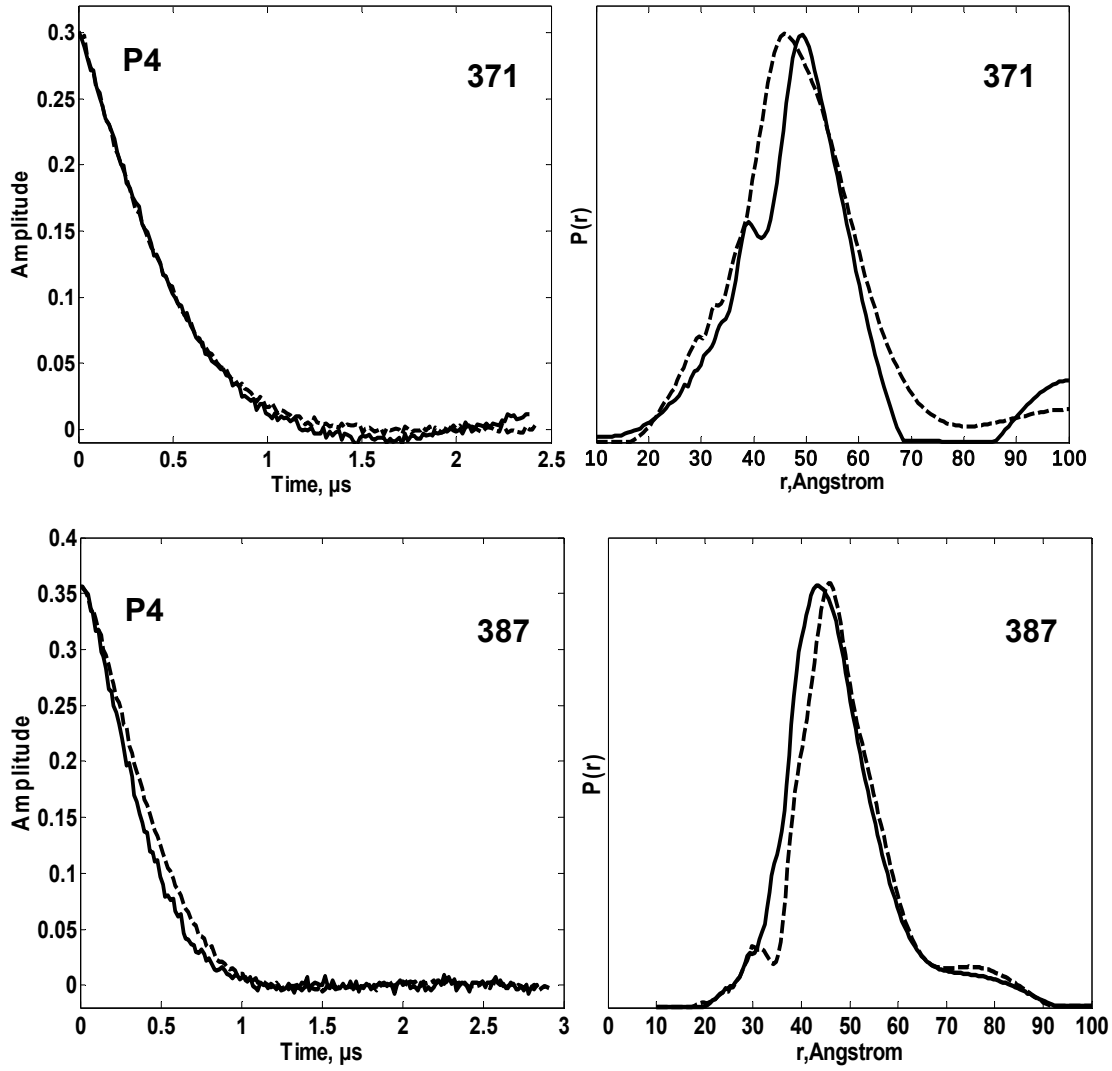

Figure 4.6. Time domain signals and corresponding distance distributions from sites 371 and 387 on P4 domain of CheAΔ289. Line curves in absence of unlabeled receptor(– –) are compared with those in the presence of unlabeled receptor (——). Unlabeled receptor of concentration 200 μM was added to constant concentration of 50 μM CheAΔ289E371C and 100 μM CheW. On the other hand, unlabeled receptor of concentration 300 μM was added to constant concentration of 25 μM CheAΔ289E387C and 125 μM CheW. All time domain signals and distance distributions are scaled to a common value for ease in comparison.

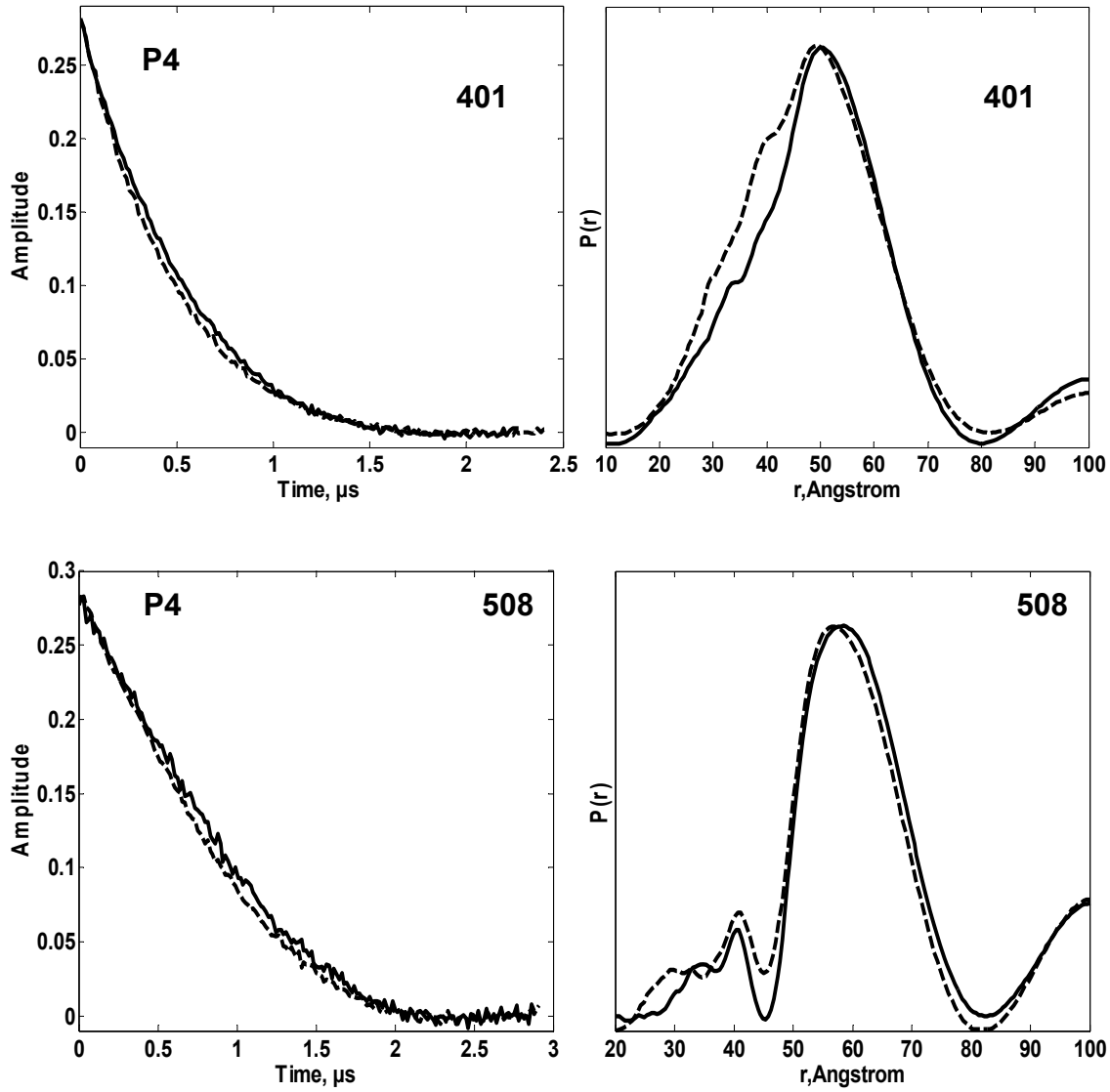

Figure 4.7. Time domain signals and corresponding distance distributions from sites 401 and 508 on P4 domain of CheAΔ289. Line curves in absence of unlabeled receptor (– –) are compared with those in the presence of unlabeled receptor (——). Unlabeled receptor of concentration 350 μM was added to constant concentration of 50 μM CheAΔ289E401C and 100 μM CheW. On the other hand, unlabeled receptor of concentration 400 μM was added to constant concentration of 50 μM CheAΔ289D508C and 100 μM CheW. All time domain signals and distance distributions are scaled to a common value for ease in comparison.

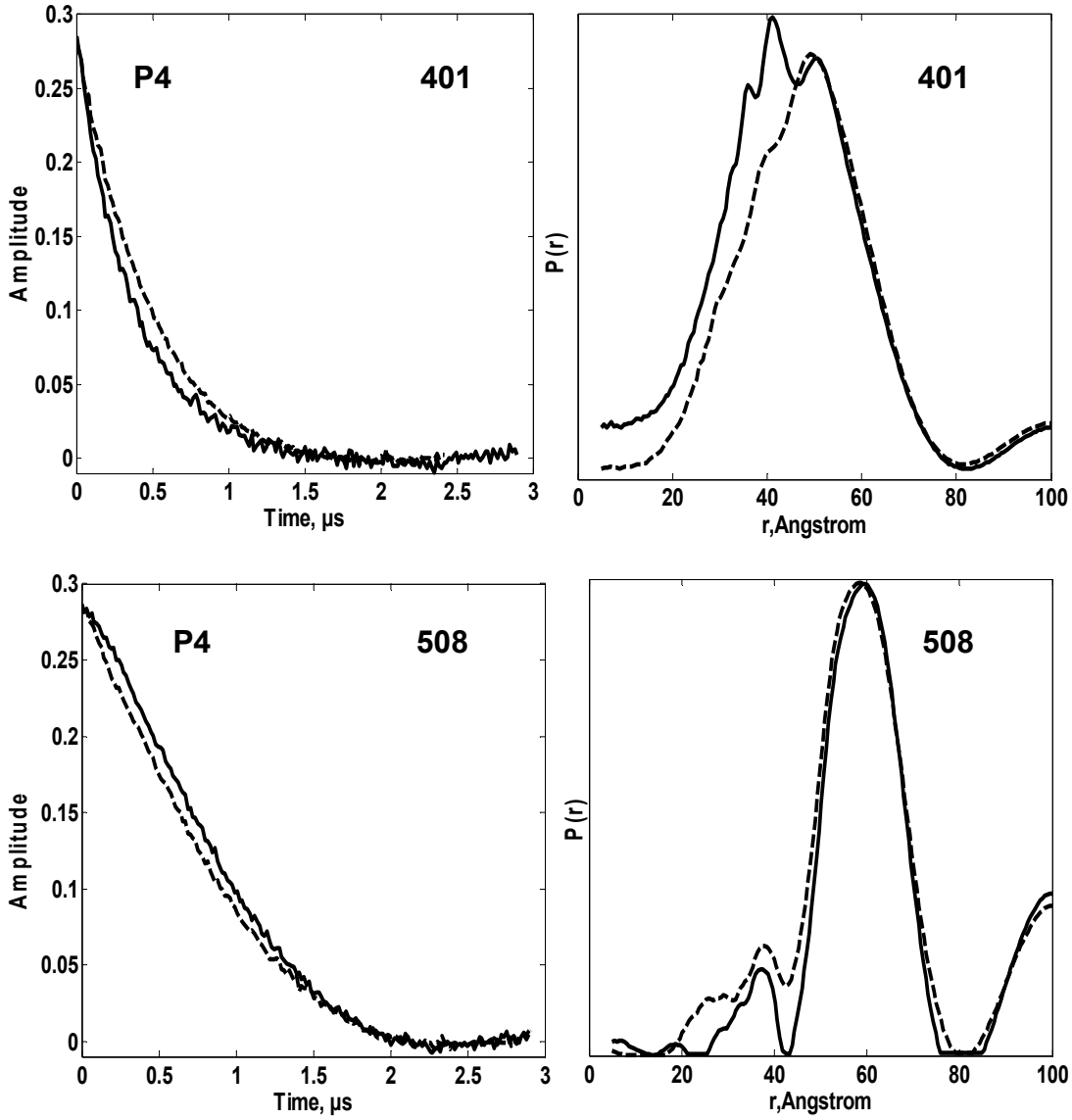

Figure 4.8. Effect of ATP on time domain signals and corresponding distance distributions from sites 401 and 508 on P4 domain of CheAΔ289. Line curves in absence of ATP (– –) are compared with those in the presence of ATP (——). Concentrations of spin labeled CheAΔ289, wild type CheW and ATP were 50 μM, 100 μM and 500 μM respectively. $MgCl_2$ (500 μM) was added to samples containing ATP. All time domain signals and distance distributions are scaled to a common value for ease in comparison.

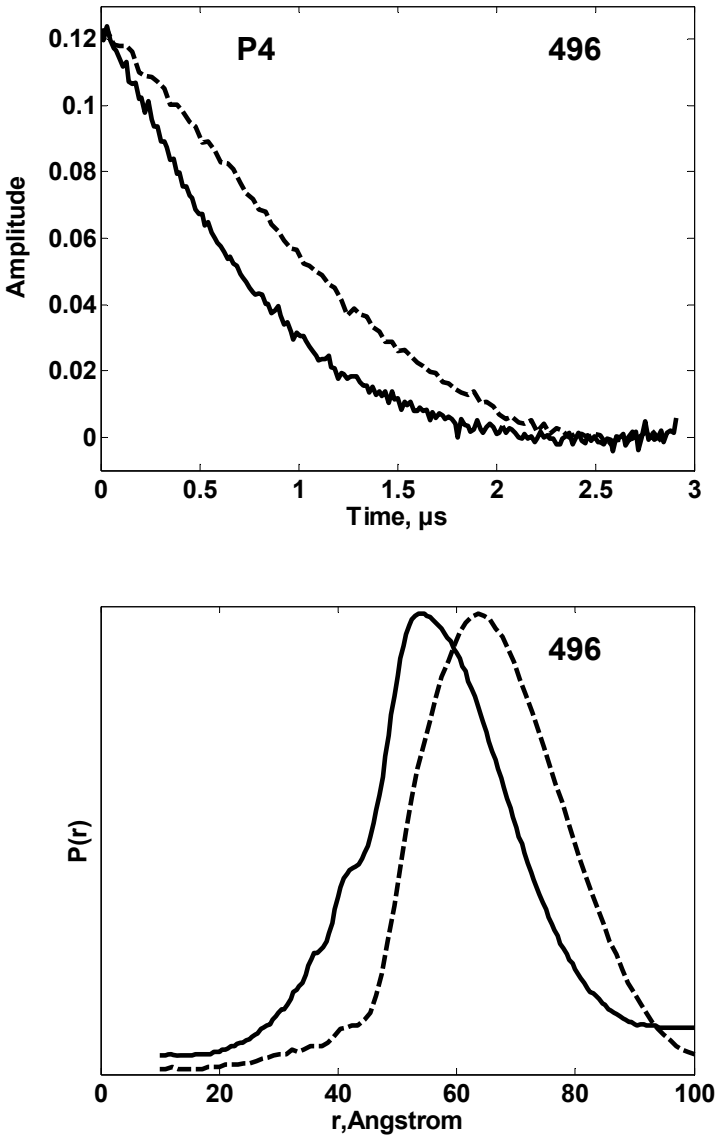

Figure 4.9. Effect of ATP on time domain signals and corresponding distance distributions from sites 496 on P4 domain of CheAΔ289. Line curves in absence of ATP (‾ ‾) are compared with those in the presence of ATP (——). Concentrations of spin labeled CheAΔ289, wild type CheW and ATP were 50 µM, 100 µM and 500 µM respectively. $MgCl_2$ (500 µM) was added to samples containing ATP. All time domain signals and distance distributions are scaled to a common value for ease in comparison.

P5 domains

Distance distributions from six spin labeled sites (545, 553, 568, 634, 639 and 646) on the P5 domain reported moderate to significant changes in distance distributions between receptor bound/unbound CheA/CheW complexes. Three of the six sites (545, 634 and 553) reported a decrease in the average separation on addition of receptor (Table 4.1). The effect of unlabeled receptor on the dipolar signals was particularly striking for site Q545C (on the β7 strand) which is located very close to the dimerization domain (Figure 4.5). In the absence of receptor, the P(r) is widely distributed but it becomes much more rigid and R_{avg} decreases from 44 to 40 Å in presence of receptor. Another site, 634 (on the β14 strand) which is spatially close to 545 expectedly responded in a similar manner to the presence of receptor (Figure 4.10). Specifically, the contribution of the long distance component at 50 Å decreases which reduced the R_{avg} from 40.2 Å to 37.9 Å. The consistent shortening of inter-domain distances from sites 545 and 634 confirm that P5 domains indeed are closer to each other in presence of receptor and form a better defined structure (see half widths of the P(r) in table 4.1)

The third site 553 is on the loop connecting β7 and β8 and the average inter-domain separation of 63 Å (peak maxima at 57 Å) agrees well with C_β separations of 64 Å in crystal structure. The addition of receptor results the appearance of a new peak at 42 Å whose amplitude increases with the receptor concentration (Figure 4.11). This is a clear manifestation of a receptor binding event leading to the formation of a ternary complex. We observed similar effect with 545 as well where the distance distribution becomes much more rigid in the presence of receptor with two narrow peaks at 32 and 37 Å. The narrow bimodal peaks probably correspond to two slightly different orientations of spin labels. In the ternary complex, the sites 646 are have

moved apart by 5 Å compared to their separation in the unbound CheA/CheW complex.

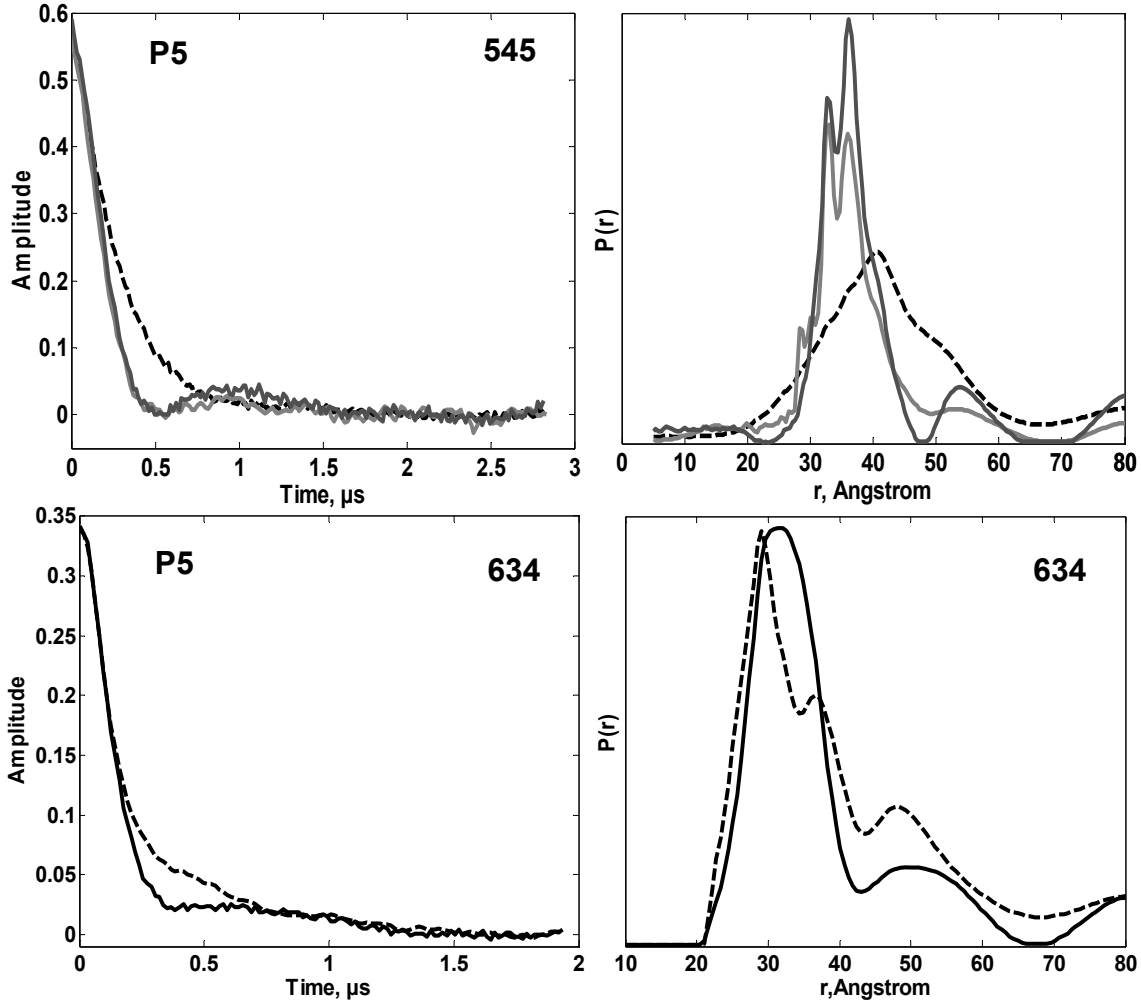

Figure 4.10. Time domain signals and corresponding distance distributions from sites 545 and 634 on P5 domain of CheAΔ289. Line curves in absence of unlabeled receptor (– –) are compared with those in the presence of increasing concentration of unlabeled receptor from 150 µM (——) to 300 µM (——). The concentrations of spin labeled CheAΔ289 and wild type CheW was constant at 25 µM and 125 µM respectively. All time domain signals and distance distributions are scaled to a common value for ease in comparison.

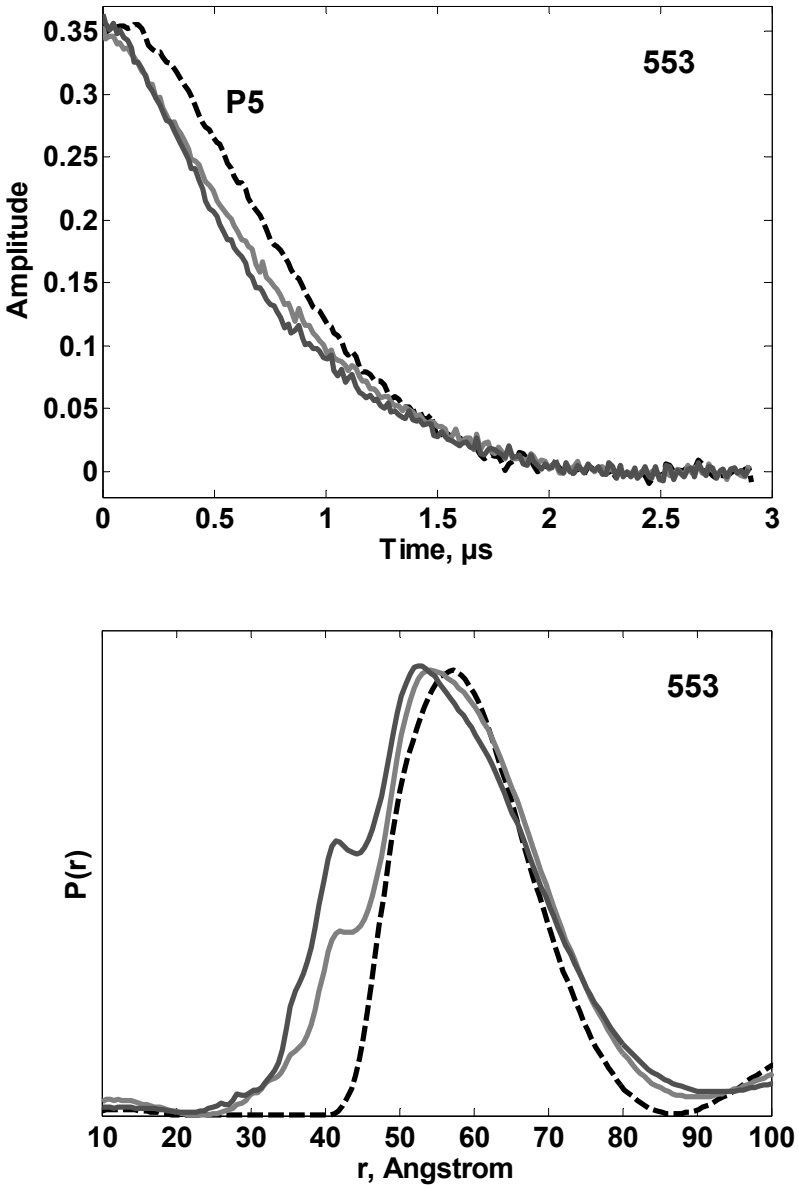

Figure 4.11. Time domain signals and corresponding distance distributions from sites 553 on P5 domain of CheAΔ289. Line curves in absence of unlabeled receptor (– –) are compared with those in the presence of increasing concentration of unlabeled receptor from 75 µM (—) to 225 µM (———). The concentrations of spin labeled CheAΔ289 and wild type CheW was constant at 25 µM and 125 µM respectively. All time domain signals and distance distributions are scaled to a common value for ease in comparison.

The binding interaction between CheW and the P5 domain results in conformational stability across the interface for both the proteins. We recorded dipolar signals from two sites 639 and 646 which belong to the sub-domain 1 of P5 on the surface that interacts with CheW. In both cases, expectedly, we observed relatively localized distance distributions (full width at half maximum is within 12-14 Å). Addition of receptor did not result in further shortening of distances for 639 but resulted in broadening of the distance distribution as well as an increase in average separations by 3 Å for site 646 (Figure 4.12). Apart from the major peak at 55 Å for 646, there are minor peaks at short distances between 20-40 Å as well. Given the weak amplitude of these signals, we chose to ignore these peaks in our analysis, as they may arise due to noise in the signal. The site 568 reported only minor a change in dipolar signals in the presence of receptor.

4.2.4 Interaction of unlabeled receptor with CheW

DEER experiments with spin labeled CheW at sites 15, 72, 80 and 139 on (in complex with wild type CheA) produced long distances, most of them within 60-70 Å[14]. Since the accuracy of distance measurement in DEER in protonated solvents is limited to about 65 Å[16], we searched for new sites on CheW that would produce shorter CheW-CheW separations. We selected sites 9, 28, 31, 35, 101, 102 and 137 on CheW, all of which lie on the surface of CheW that faces inside the cleft formed by the two CheW's in the model of the CheAΔ289/CheW complex. The C_β separations at these sites between the two CheW's are within 45 Å. However, within the subset of sites mentioned above, we were able to record and analyze dipolar signals only from sites 9 and 31. Site 28 was difficult to work with as the spin label spontaneously oxidized, detached and accelerated the formation of disulphide linked CheW dimers. Cysteine substitution and subsequent spin-labeling at site 35 caused oligomerization of

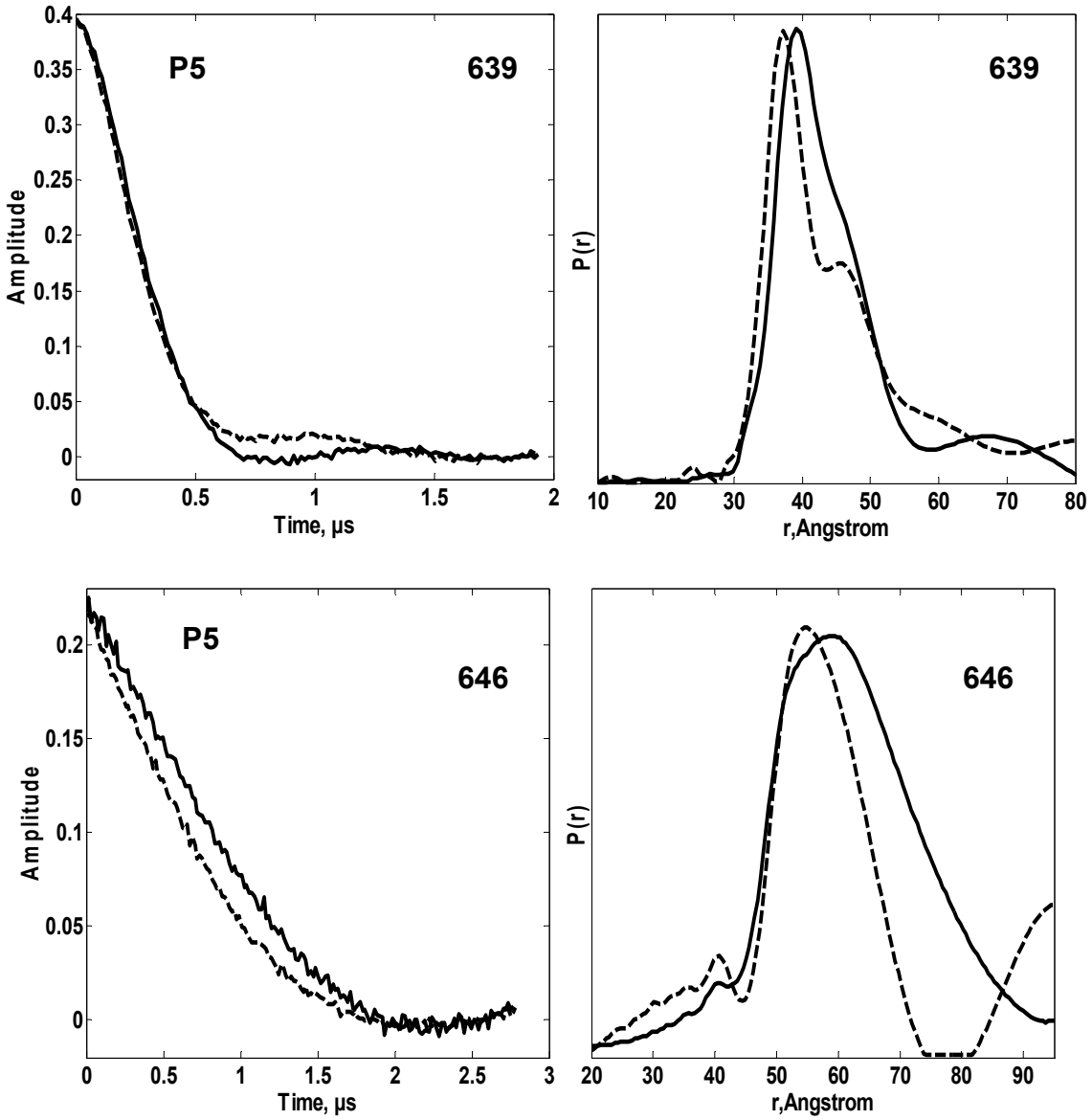

Figure 4.12. Time domain signals and corresponding distance distributions from sites 639 and 646 on P5 domain of CheAΔ289. Line curves in absence of unlabeled receptor (– –) are compared with those in the presence of unlabeled receptor (———). Unlabeled receptor of concentration 350 µM was added to constant concentration of 25 µM CheAΔ289S639C and 125 µM CheW. On the other hand, unlabeled receptor of concentration 400 µM was added to constant concentration of 25 µM CheAΔ289E646C and 50 µM CheW. All time domain signals and distance distributions are scaled to a common value for ease in comparison.

the protein. CheW proteins spin labeled at 101, 102 and 137 suffered from poor spin-labeling possibly due to partial burial of the site.

In the first set of experiments we recorded signals from spin labeled CheW (sites 9, 31, 80 and 139) bound to wild type CheAΔ289 and compared with those obtained on adding unlabeled receptor. Interestingly, in the absence of receptor, the P(r) from spin labeled CheWK9C showed a distinct bimodal distribution which is indicative of two distinct conformations of either CheW or the spin label itself (Figure 4.13). The unusual broad distance distribution at this site (Full width at half maximum is 28 Å) is accounted for by the flexible nature of N-termini of CheW as seen in NMR experiments[20]. The interaction with the receptor results in a narrowing of the distance distribution by 8 Å and a reduction in R_{avg} from 53 to 51 Å. We repeated the experiment with full length CheA incomplex with CheWK9C and found a similar effect of the receptor on the CheW-CheW separation (data not shown). A reduction in distribution width was also seen for site 31, even though the average separation remained the same (Figure 4.13).

Site 139 is located at the C-terminal helix of CheW. The CheW-CheW separations at this site are longer in the ternary complex with the receptor than in the complex with only CheA. Dipolar signals from site 80 did not change on addition of receptor (Figure 4.14).

Unlike most of the dipolar signals from CheAΔ289, the spin labeled sites on CheW consistently produced signals which were relatively weak in amplitude (only 50% of the expected full signal amplitude). The possibility that a part of the population of CheAΔ289 binds to only one CheW contradicts the results from Isothermal Calorimetric experiments which clearly showed the binding of two molecules of CheW to single CheAΔ289 dimer[22]with nanomolar affinity.

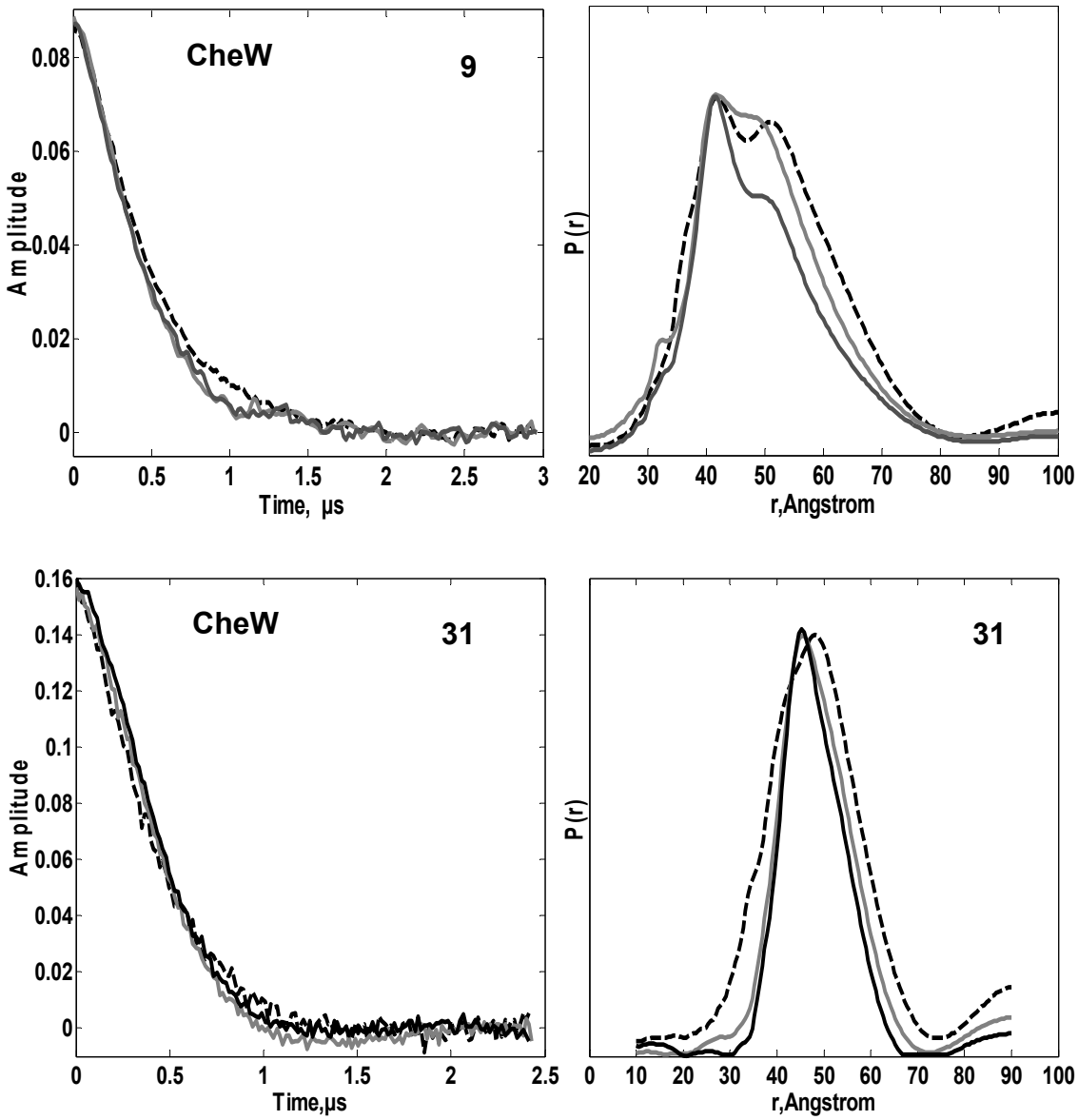

Figure 4.13. Time domain signals and corresponding distance distributions from sites 9 and 31 on CheW. Line curves in absence of unlabeled receptor (– –) are compared with those in the presence of increasing concentration of unlabeled receptor from 150 µM (——) to 300 µM (——). The concentrations of wild type CheAΔ289 and spin labeled CheW was constant at 25 µM and 125 µM respectively. All time domain signals and distance distributions are scaled to a common value for ease in comparison.

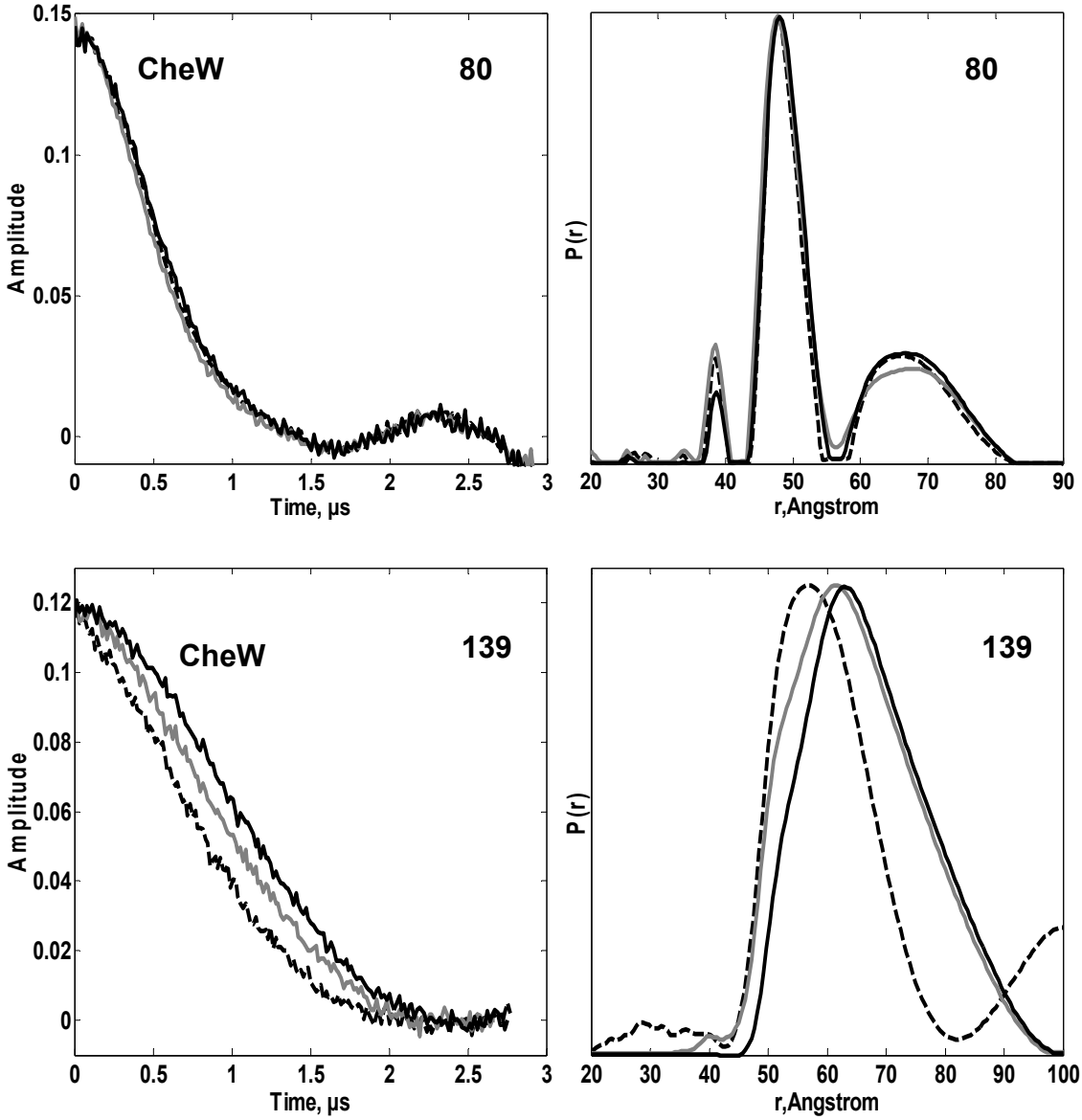

Figure 4.14. Time domain signals and corresponding distance distributions from sites 80 and 139 on CheW. Line curves in absence of unlabeled receptor (– –) were recorded for both sites at protein concentrations of 25 µM /125 µM and 50 µM /100 µM for CheAΔ289/CheWS80C and CheAΔ289/CheWD139C respectively. The concentration of unlabeled receptor was increased from 150 µM (—) to 300 µM (——) in the former case and from 100 µM (—) to 200 µM (——). All time domain signals and distance distributions are scaled to a common value for ease in comparison

We believe that the two CheW's, while still bound to the P5 domain, sample certain orientations that result in large separations between them which fall outside the maximum distance detected with DEER in protonated systems. In the future, we plan to measure DEER signals on dueterated spin-labeled CheW proteins which will allow us to measure distances up to 130 Å[16].

4.2.5 Rigid body refinement with distance restraints in presence of unlabeled receptor

The differential effect of receptor on distances from the CheA/CheW complex should be understood in terms of rearrangements of individual domains, and hence the overall structure of the complex. Previously, we developed a method that performs rigid body refinement based on long-range distance restraints and predicts the minimized final structure(also chapter 2 of this thesis)[23]. We utilize the same method here and use the set of measured distances in presence of receptor to predict the conformation of CheA/CheW in the presence of receptor. For the starting conformation of the complex, we used the model of CheA/CheW developed from combining the coordinates from the crystal structures of CheAΔ289 and CheW in complex with CheAΔ354. For each measurement, we assigned the uncertainty to be d_{minus}=5Å and d_{plus}=1Å. In our refinement procedure, we assumed that in each subunit, the P4 domains and CheW and P5 together move as a rigid body. In the final refined structure, the change in conformation of domains is evaluated by comparing with the initial structure. This is done by superimposing the final structure of CheA/CheW complex on the initial structure by aligning along the P3 domains (Figure 4.15).

We noticed several interesting changes in conformation of different domains upon refinement. The most striking effect is on the orientations of the CheW's from both of the subunits. The CheW's seem to undergo a rotation as well as a translation

motion such that the surface on CheW that initially faced inside the cleft, is now oriented away and is more exposed. The P5 domains come slightly closer to each other and there is no significant change in positions of P4 domains.

4.3 DISCUSSION

4.3.1 Mobility of P1 and P2 domains in full length CheA and interaction with unlabeled receptor

In full length CheA from *T.maritima*, the P1 and P2 domains are linked to each other and to the CheAΔ289 via long linkers of length 42 and 25 amino acid residues respectively. The NMR study on a CheA fragment containing only domains P1 and P2 showed that the two domains reorient independently in solution[24]. Our ESR experiments were aimed at understanding how the P1 and P2 domains of one CheA subunit interact with corresponding domains of the other subunit within the CheA dimer. We also wanted to investigate the effect of unlabeled receptor on the dipolar signals.

P1 domains

We tested five spin-labeled sites on P1 domain, and found that five of the sites (12, 14, 53, 76 and 83) produced dipolar signals which were consistent with the idea of P1 domains being far apart from each other. In some cases, our inability to investigate the effects of unlabeled receptor on dipolar signals were due to the weak amplitude of dipolar signals. Overall, our results suggest that the two P1 domains are widely separated from each other in the absence or presence of receptor.

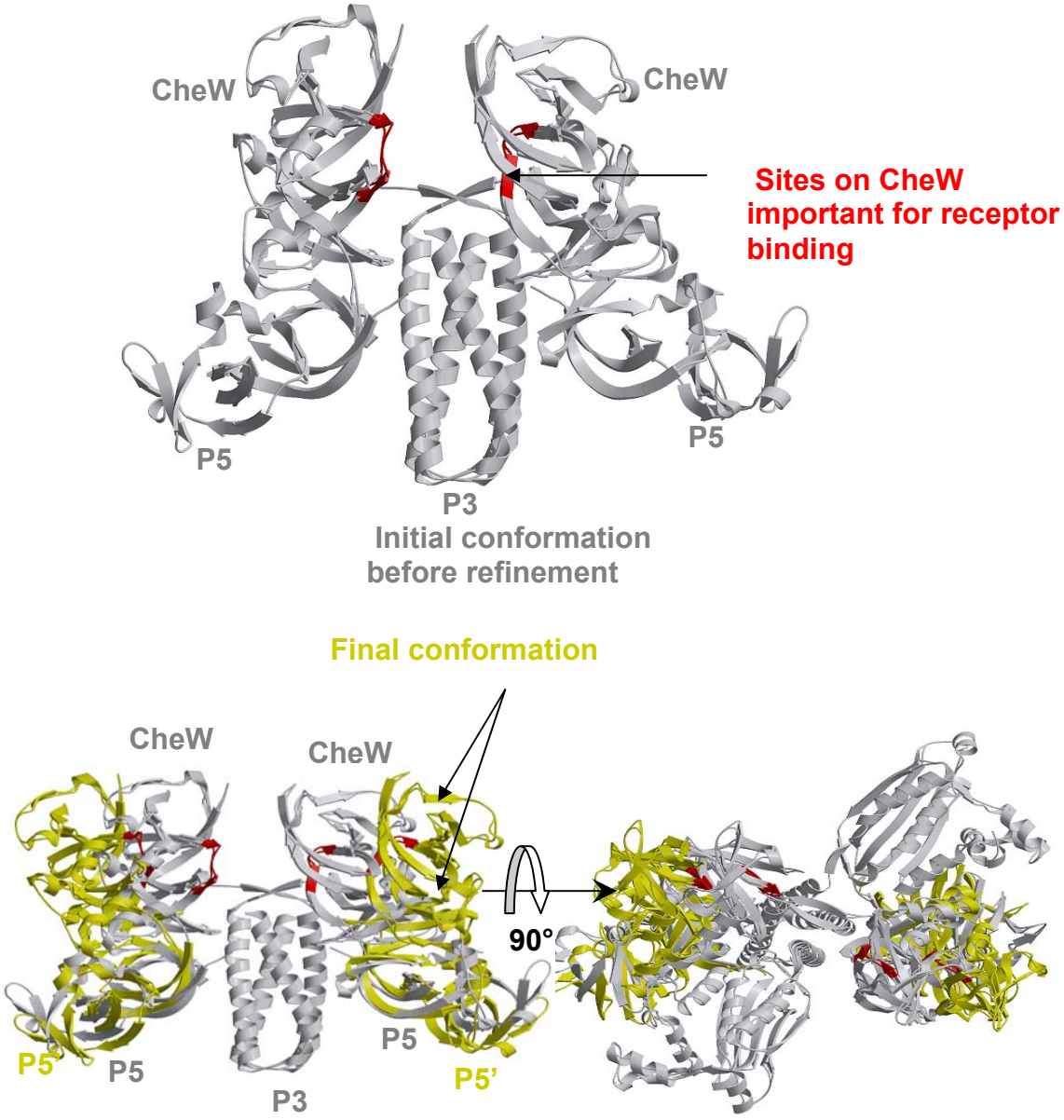

Figure 4.15. Comparison of final and initial structures of CheAΔ289/CheW complex after refinement with rigid body refinement. P4 domains are omitted from the structures for clarity. The final conformation of the complex after refinement (in yellow) is superimposed on the initial structure (in grey) for comparison.

P2 domains

Compared to observations from the P1 domains, our experiments with spin label sites on P2 domain lead to a different conclusion. The two sites 178 and 208 produced similar broad distance distributions with R_{avg} between 34-40 Å. In the completely extended form, when measured along the bond lengths, the length of the linker joining P2 domain to CheAΔ289 can be as long as 106 Å. This suggests that if the two P2 domains are oriented completely away from each other in opposite directions, distances between any two symmetrical sites on these domains would be too long to detect with DEER. Our current results with inter-domain distances within 20-60 Å argue against this scenario. The unusually wide width of the distribution does implicate substantial inter-domain flexibility. In the context of full length CheA from *E.coli*, the flexible nature of P2 domain has been previously determined by NMR [25]which led to the conclusion that P2 domains share no stable interactions with the rest of the protein. However, crystallographic evidence from structures of CheY in complex with the P2 domain show tight interactions between the P2 domains belonging to two symmetry related [26]and non-crystallographic symmetry related molecules in the asymmetric unit[27].No such interaction has been found in crystal structures from *T.maritima* proteins[14]. While there is no direct evidence of interaction between P2 domains in solution, it is possible that the two linkers connecting the domains to the rather rigid structure of the P3-P4-P5 domains are inter-twined to some extent, which restricts the two domains from moving away very far from each other. To verify this hypothesis, more DEER experiments with spin labeled sites on the linker region need to be performed.

In our study the two sites 178 and 208 are not widely separated in the structure of the P2 domain. But, there are wide distance distributions from both sites, so it is

reasonable to conclude that the P2 domains sample different orientations relative to each other.

The receiver domain CheY docks the P2 domain for the transfer of phosphate group from the P1 domain. In the presence of CheY, we noticed only minor changes in the dipolar signals from P2 spin-labeled sites. A possible explanation is that the sites C208 and T178C are away from the interaction surface between CheY and P2 and hence are not ideal reporter sites to sense changes on binding of CheY.

4.3.2 Interaction of unlabeled receptor with CheAΔ289 and CheW

The autophosphorylation of CheA is regulated by Chemoreceptors and the coupling protein CheW. The C-terminal domain of CheA is essential for coupling the kinase activity to the chemoreceptor. All of these functions probably require CheA domains to move and reorient in order to favorably couple with CheW and receptor. The five domains in CheA possess varying degree of freedom. CheAΔ289 is composed of P3, P4 and P5 domains and form a somewhat rigid construct which probably facilitated the crystallographic structure determination[28]. In this structure, the two subunits are oriented asymmetrically within the CheAΔ289 dimer. They differ only in the slightly different orientation of P4 and P5 domains, presumably originating from the rotation of these domains about the hinges connecting them to each other. Hence, it is reasonable to expect that in solution these domains can sample multiple conformations. Interaction with Chemoreceptors and CheW can result in changes in domain motions and bring overall stability to the CheA structure. In-line with this hypothesis, in our previous work, we successfully recorded changes in dipolar signals from sites on CheAΔ289 on binding with CheW. In this work, we have extended this study to investigate how the binding of receptor influences the overall structure of CheA/CheW complex. The effect of this interaction was monitored by recording

dipolar signals from spin label sites distributed uniformly on CheA and CheW, and then comparing with the signals in presence of unlabeled receptor. In all cases, for ease in visualization, the PDS time domain data was processed to give distance distributions which were used for analysis. We placed spin labels on each of the domains of CheAΔ289: 301, 318, 331 on P3; 371, 387, 401, 458, 496, 508, 522 on P4; 545, 634, 639, 646, 568, 553 on P5 (Figure 4.5). The inter-subunit separation between symmetrical sites on CheAΔ289 dimer was recorded in the absence and presence of unlabeled receptor. The changes in distances are a direct measure of conformational adjustments in CheA as it binds to the receptor. It should be noted that the receptor binding can cause the domains in the two subunits to move in a manner that does not change the separation between the spin label sites. In the following subsections, we discuss our results from spin label sites in each domain.

In Chapter 3, we reported self-association behavior of CheAΔ289. However, the nature of interaction between CheAΔ289 molecules is weak given that the amplitude of the intermolecular signal accounted for only 10% of the maximum amplitude. The intramolecular dipolar signals in the CheAΔ289 on the other hand are of almost full amplitude, hence we can safely ignore any effects on the signals due to aggregation of CheA.

P3 domain

The dimerization domain P3 is a rigid four helical bundle which retains its structure in the presence of receptor. This observation is not surprising since the dissociation of the CheA subunit is not energetically favorable[28].

P4 domain

The changes in dipolar signals due to receptor binding from sites on the P4 domain were more subtle as compared to our observations with the P5 domain. Three of the sites: 496, 458 and 522 produced weak dipolar signals, possibly due to the fact that their separations are too large to fit in the current detection window of DEER (using protonated solvents). On the structure of the P4 domain, all these sites cluster near the ATP binding region of the P4 domain. This suggests that the P4 domains are positioned in a way that their catalytic centers face away from each other. This arrangement agrees with the orientations of domains as found in the crystal structure of CheAΔ289. The dipolar signals from rest of the four sites: 371, 387, 401 and 508 did not change significantly with receptor. We reported before that P4 domains sample a wide range of orientations in solution[14]. It is possible that interaction with receptor restricts this sampling to some extent. Even though we did not measure directly the effect of receptor on distances between sites on the P3-P4 domain, our inability to observe a significant change in P4-P4 distances probably rules out any stabilization effect of receptor. It is possible that P4 domains do not interact directly with receptor in the inhibitory state of the ternary complex (unpublished Pollard et al). In the active state then, receptor may cause the P4 domain to orient favorably for phosphate transfer to P1 domain.

Effect of ATP on motion of P4 domains

We tested the effect of ATP on the dipolar signals from sites on P4 domain. The binding of ATP at the catalytic site may result in changes in protein conformation or flexibility. We did not observe any significant change in signals from two sites 401 and 508, which suggests that changes induced by ATP binding may be local to the catalytic site. We observed a significant effect of ATP on dipolar signals from site 496

which sits on the ATP loop. Change in conformations of ATP lid on nucleotide binding has been previously observed in the crystal structures[29] and hence is consistent with our result.

P5 domain and CheW

Selected sites on the P5 domain and CheW produced consistent changes in distance distribution as the concentration of unlabeled receptor was increased. The effects of receptor binding varied from a gradual narrowing of the distance distribution to the formation of new peaks which were directly correlated with the formation of a ternary complex. We were unable to do experiments with higher concentration of protein components due to instability of proteins at these concentrations. The fact that we did not observe a monotonous increase or decrease in average distances from evenly distributed sites on P5 domain and CheW, a mere translational motion of these domains away or towards each other is ruled out. We believe that the receptor causes a rotational motion instead which simultaneously satisfies all the distance changes. CheW is structurally similar to the P5 domain of CheA and is composed of two β barrel like sub-domains. At the interface of these sub-domains lies a highly hydrophobic surface which is proposed to interact with receptor[30]. Sites on CheW identified as suppressor mutations of receptor mutants also localize in the same region[31]. Several biochemical studies[15,32,33], direct crystallographic and spectroscopic evidence [14]have established that CheW binds tightly to the P5 domain of CheA. In the context of the CheAΔ289 dimer, this places two CheW molecules on top of P5 domains, with the proposed region of interaction with receptor facing inside the cleft formed by the two CheW's. The presence of receptor should cause CheW to change its orientation in a manner that would make the proposed region of interaction accessible to it. Since the binding constant between CheW and CheA is tens of nanomolar, we

propose that CheW and the P5 domain likely move together in a coordinated manner. The rotational motion of CheW can bring the proposed receptor binding surface to face away from the cleft formed by two CheW's. This orientation would allow CheW to interact with receptor if it is positioned adjacent to the P3 domain, with its helical axis either parallel or antiparallel to that of the P3 domain.

4.3.3 Final conformation of CheA/CheW complex after rigid body refinement

Rigid body refinement with distance restraints in the presence of unlabeled receptor produces a structure that has several remarkable features. When compared with the model of CheAΔ289/CheW complex (which was based on crystal structures of CheAΔ289[28] and CheAΔ354/CheW[14]), the most pronounced change occurs in the position and orientation of the CheW's. The residues important for receptor binding cluster on the interface region of two subdomains in CheW [21,31] (Figure 4.15). In the initial conformation, the surface mapped out by these residues on both the CheW's faces inside the cleft. This orientation of CheW's led us to propose that a single receptor dimer sits inside this cleft. However, the space is clearly not wide enough to accommodate a trimer of dimers, which has been established to be the key signaling team of receptors.

The final structure of CheAΔ289/CheW suggests a new mode of interaction with the receptor. In this structure, because of the rotation of CheW's, the proposed receptor surface now faces outwards instead of facing inside the cleft. In this orientation, the surface on CheW is more exposed and CheW is optimally oriented to interact with receptors if they are modeled to be located along the P3 domain. The space on ether side of the P3 domain is large enough to accommodate a receptor dimer (Figure 4.16), as well as a trimer of dimers.

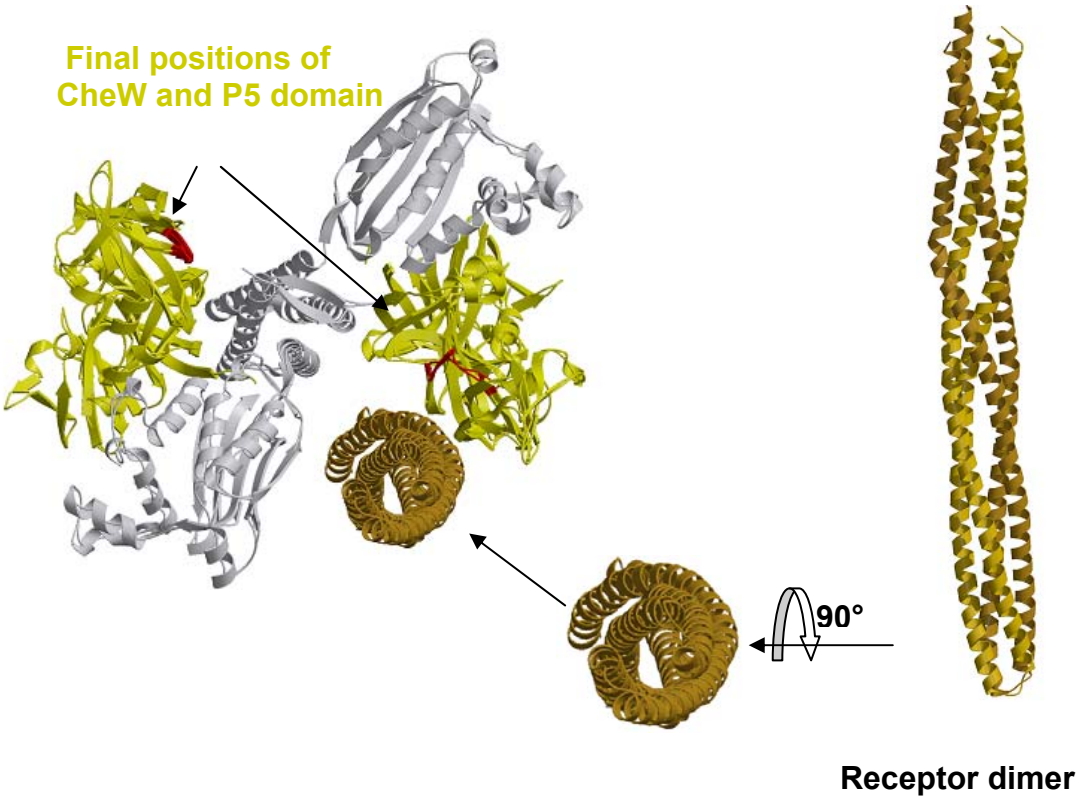

Figure 4.16. Modeling of receptor dimer in the final structure of CheAΔ289/CheW complex.

We did not notice a significant change in the positions of the P4 and P5 domains after refinement. Closer inspection reveals that the P5 domains do come closer to each other in the final structure. This indicates that binding of receptor leads to asymmetry in the CheAΔ289/CheW complex.

Thus, the proposed structure of CheAΔ289/CheW in the presence of receptor suggests new mode of binding with the receptor.

4.4 MATERIALS AND METHOD

Cloning, mutagenesis and spin labeling of proteins

Gene encoding *T.maritima* proteins CheAΔ289 (290-671), CheW(1-151) and fragment of TM14 receptor (40-213) were cloned and purified as described in Chapter 2. In a cysteine-less background of CheAΔ289, six residues in P5 domains: Q545, N553, S568, E646, D634 and S639, and seven in P4 domain: D371, E387, E401, K458, K496, D508, and S522 and three in P3 domain: E301, E318 and E331 were separately changed to cysteines by Quickchange mutagenesis (Strategene). Full length CheA has two native cysteines at site 63 and 208 which are in P1 and P2 domain respectively. Cysteine-less CheA was prepared by selectively substituting each of these cysteines to serine residues. This template was used for introducing cysteine substitutions at sites 53, 83 on P1 domain and 178 on P2 domain. The proteins were spin labeled for ESR experiments as described in Chapter 2.

Pulsed ESR measurements

The procedure has been described in Chapter 3.

Rigid body refinement

This program has been described in Chapter 2. For the refinement, the initial structure of CheAΔ289 and CheW was from the crystal structures of CheAΔ289[28] and CheW in complex with CheAΔ354[14].The average ESR distances in the presence of receptor(Table 4.1) were used with d_{min} and d_{plus} of 5 Å and 1Å respectively.

REFERENCES

1. Maddock, J. R. & Shapiro, L. (1993). Polar location of the chemoreceptor complex in the Escherichia coli cell. *Science* **259**, 1717-1723.
2. Sourjik, V. & Berg, H. C. (2000). Localization of components of the chemotaxis machinery of Escherichia coli using fluorescent protein fusions. *Molecular Microbiology* **37**, 740-751.
3. Kentner, D. & Sourjik, V. (2006). Spatial organization of the bacterial chemotaxis system. *Current Opinion in Microbiology* **9**, 619-624.
4. Kentner, D., Thiem, S., Hildenbeutel, M. & Sourjik, V. (2006). Determinants of chemoreceptor cluster formation in Escherichia coli. *Molecular Microbiology* **61**, 407-417.
5. Zhang, P. J., Khursigara, C. M., Hartnell, L. M. & Subramaniam, S. (2007). Direct visualization of Escherichia coli chemotaxis receptor arrays using cryo-electron microscopy. *Proceedings of the National Academy of Sciences of the United States of America* **104**, 3777-3781.
6. Zhang, P. J., Khursigara, C., Hartnell, L. & Subramaniam, S. (2007). Molecular architecture of receptor arrays in intact E.coli cells determined using cryo electron tomography. *Microscopy and Microanalysis* **13**, 36-37.
7. Khursigara, C. M., Wu, X. W. & Subramaniam, S. (2008). Chemoreceptors in Caulobacter crescentus: Trimers of receptor dimers in a partially ordered hexagonally packed array. *Journal of Bacteriology* **190**, 6805-6810.
8. Briegel, A., Ding, H. J., Li, Z., Werner, J., Gitai, Z., Dias, D. P., Jensen, R. B. & Jensen, G. J. (2008). Location and architecture of the Caulobacter crescentus chemoreceptor array. *Molecular Microbiology* **69**, 30-41.

9. Kim, K. K., Yokota, H. & Kim, S. H. (1999). Four-helical-bundle structure of the cytoplasmic domain of a serine chemotaxis receptor. *Nature* **400**, 787-792.

10. Studdert, C. A. & Parkinson, J. S. (2004). Crosslinking snapshots of bacterial chemoreceptor squads. *Proceedings of the National Academy of Sciences of the United States of America* **101**, 2117-2122.

11. Studdert, C. A. & Parkinson, J. S. (2005). Insights into the organization and dynamics of bacterial chemoreceptor clusters through in vivo crosslinking studies. *Proceedings of the National Academy of Sciences of the United States of America* **102**, 15623-15628.

12. Boldog, T., Grimme, S., Li, M. S., Sligar, S. G. & Hazelbauer, G. L. (2006). Nanodiscs separate chemoreceptor oligomeric states and reveal their signaling properties. *Proceedings of the National Academy of Sciences of the United States of America* **103**, 11509-11514.

13. Shimizu, T. S., Le Novere, N., Levin, M. D., Beavil, A. J., Sutton, B. J. & Bray, D. (2000). Molecular model of a lattice of signalling proteins involved in bacterial chemotaxis. *Nature Cell Biology* **2**, 792-796.

14. Park, S. Y., Borbat, P. P., Gonzalez-Bonet, G., Bhatnagar, J., Pollard, A. M., Freed, J. H., Bilwes, A. M. & Crane, B. R. (2006). Reconstruction of the chemotaxis receptor-kinase assembly. *Nature Structural & Molecular Biology* **13**, 400-407.

15. Miller, A. S., Kohout, S. C., Gilman, K. A. & Falke, J. J. (2006). CheA kinase of bacterial chemotaxis: Chemical mapping of four essential docking sites. *Biochemistry* **45**, 8699-8711.

16. Borbat, P. P. & Freed, J. H. (2007). Measuring distances by pulsed dipolar ESR spectroscopy: Spin-labeled histidine kinases. *Two-Component Signaling Systems, Pt B* **423**, 52-+.

17. Jeschke, G. & Polyhach, Y. (2007). Distance measurements on spin-labelled biomacromolecules by pulsed electron paramagnetic resonance. *Physical Chemistry Chemical Physics* **9**, 1895-1910.

18. Schiemann, O. & Prisner, T. F. (2007). Long-range distance determinations in biomacromolecules by EPR spectroscopy. *Quarterly Reviews of Biophysics* **40**, 1-53.

19. Borbat, P. P. & Freed, J. H. (2000). Double-Quantum ESR and Distance Measurements. In *Distance Measurements in Biological Systems by EPR* (Berliner, L. J., Eaton, G. R. & Eaton, S. S., eds.), Vol. 19, pp. 383-459. Kluwer Academic/Plenum Publishers, New York.

20. Griswold, I. J., Zhou, H. J., Matison, M., Swanson, R. V., McIntosh, L. P., Simon, M. I. & Dahlquist, F. W. (2002). The solution structure and interactions of CheW from Thermotoga maritima. *Nature Structural Biology* **9**, 121-125.

21. Boukhvalova, M. S., Dahlquist, F. W. & Stewart, R. C. (2002). CheW binding interactions with CheA and Tar - Importance for chemotaxis signaling in Escherichia coli. *Journal of Biological Chemistry* **277**, 22251-22259.

22. Park, S. Y., Quezada, C. M., Bilwes, A. M. & Crane, B. R. (2004). Subunit exchange by CheA histidine kinases from the mesophile Escherichia coli and the thermophile Thermotoga maritima. *Biochemistry* **43**, 2228-2240.

23. Bhatnagar, J., Freed, J. H. & Crane, B. R. (2007). Rigid body refinement of protein complexes with long-range distance restraints from pulsed dipolar ESR. *Two-Component Signaling Systems, Pt B* **423**, 117-+.

24. Zhou, H. J., McEvoy, M. M., Lowry, D. F., Swanson, R. V., Simon, M. I. & Dahlquist, F. W. (1996). Phosphotransfer and CheY-binding domains of the

histidine autokinase CheA are joined by a flexible linker. *Biochemistry* **35**, 433-443.

25. McEvoy, M. M., delaCruz, A. F. A. & Dahlquist, F. W. (1997). Large modular proteins by NMR. *Nature Structural Biology* **4**, 9-9.

26. Gouet, P., Chinardet, N., Welch, M., Guillet, V., Cabantous, S., Birck, C., Mourey, L. & Samama, J. P. (2001). Further insights into the mechanism of function of the response regulator CheY from crystallographic studies of the CheY-CheA(124-257) complex. *Acta Crystallographica Section D-Biological Crystallography* **57**, 44-51.

27. Welch, M., Chinardet, N., Mourey, L., Birck, C. & Samama, J. P. (1998). Structure of the CheY-binding domain of histidine kinase CheA in complex with CheY. *Nature Structural Biology* **5**, 25-29.

28. Bilwes, A. M., Alex, L. A., Crane, B. R. & Simon, M. I. (1999). Structure of CheA, a signal-transducing histidine kinase. *Cell* **96**, 131-141.

29. Bilwes, A. M., Quezada, C. M., Croal, L. R., Crane, B. R. & Simon, M. I. (2001). Nucleotide binding by the histidine kinase CheA. *Nature Structural Biology* **8**, 353-360.

30. Griswold, I. J. & Dahlquist, F. W. (2002). The dynamic behavior of CheW from Thermotoga maritima in solution, as determined by nuclear magnetic resonance: implications for potential protein-protein interaction sites. *Biophysical Chemistry* **101**, 359-373.

31. Liu, J. D. & Parkinson, J. S. (1991). Genetic evidence for interaction between the CheW and Tsr proteins during chemoreceptor signaling by Escherichia coli. *Journal of Bacteriology* **173**, 4941-4951.

32. Boukhvalova, M., VanBruggen, R. & Stewart, R. C. (2002). CheA kinase and chemoreceptor interaction surfaces on CheW. *Journal of Biological Chemistry* **277**, 23596-23603.

33. Zhao, J. S. & Parkinson, J. S. (2006). Cysteine-scanning analysis of the chemoreceptor-coupling domain of the Escherichia coli chemotaxis signaling kinase CheA. *Journal of Bacteriology* **188**, 4321-4330.

CHAPTER 5

INTERACTION OF SPIN LABELED RECEPTOR WITH CHEA/CHEW COMPLEX

5.1 INTRODUCTION

In chapter 4, we reported changes in the conformations of CheA and CheW in the presence of unlabeled receptor. In this work, we propose two models of the ternary complex based on direct dipolar distances between receptor and CheA/CheW and constraints from disulphide crosslinking. The two models, referred as A and B, are closely related and share general features but differ in the tilt of the receptor axis. Overall, the models suggest that the tip of the receptor is in close proximity to the N-terminus of CheW, and the receptor sits on the side of the P3 domain rather than above the N-terminal end of P3 as we predicted before[1]. In model A, the receptor axis is completely anti-parallel to P3 helical axis, while in model B, it makes an angle of 20° with it. Our data qualitatively agrees with both the models.

5.2 RESULTS

5.2.1 Spin labeled TM14 receptor form dimers in solution

Methyl-accepting chemotaxis proteins (MCP) or chemoreceptors spontaneously form dimers composed of four-helix bundles with a coiled-coil domain structure. Soluble fragments of chemoreceptors belonging to organisms *E.coli* and *T.maritima* crystallized as trimers of dimers [2]and hedgerows of dimers [1,3]respectively. We used the soluble fragment of TM14 receptor exclusively for our experiments, since it interacts more strongly with CheA and CheW than TM1143. DEER experiments

with TM14 receptor spin labeled at site 125 produced predominantly a strong dimer distance (R_{max} at 28 Å) (Figure 5.1). We did not observe any higher order oligomers.

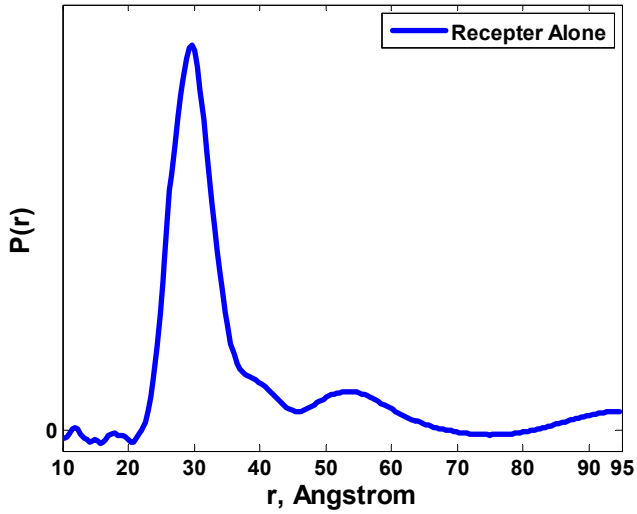

Figure 5.1 Distance distribution from a spin labeled receptor dimer at site 125 in presence of wild type CheAΔ289 and CheW.

5.2.2 Measurement of intermolecular distances between Receptor and CheA/CheW complex

Preparation of spin labeled single chain receptors

Dipolar distances between spin-labeled receptor and CheAΔ289 or CheW would provide restraints on how the three proteins are arranged in the complex. These inter-molecular distances that we aimed to measure are accompanied by the intra-molecular distances within homodimers of CheAΔ289 and receptors which complicates data analysis. In order to address this problem, we cloned single chain receptors where the C-terminus of a receptor monomer was linked to the N-terminus

of the other via a linker of 4-5 amino acid residues (Figure 5.2). With site directed mutagenesis, we introduced specific single cysteine substitutions on the receptor dimer and subsequently prepared spin-labeled proteins. In order to test if the single chain construct has the same properties as the receptor homodimer, we studied its effect on distance distribution from spin labeled CheAQ545C and wild type CheW. We found that the distance distribution became rigid (data not shown) as was observed on addition of receptor homo-dimer (Chapter 4). Thus, we conclude that the single chain receptor construct retain the same affinity and specificity in its interaction with CheA as the wild type protein.

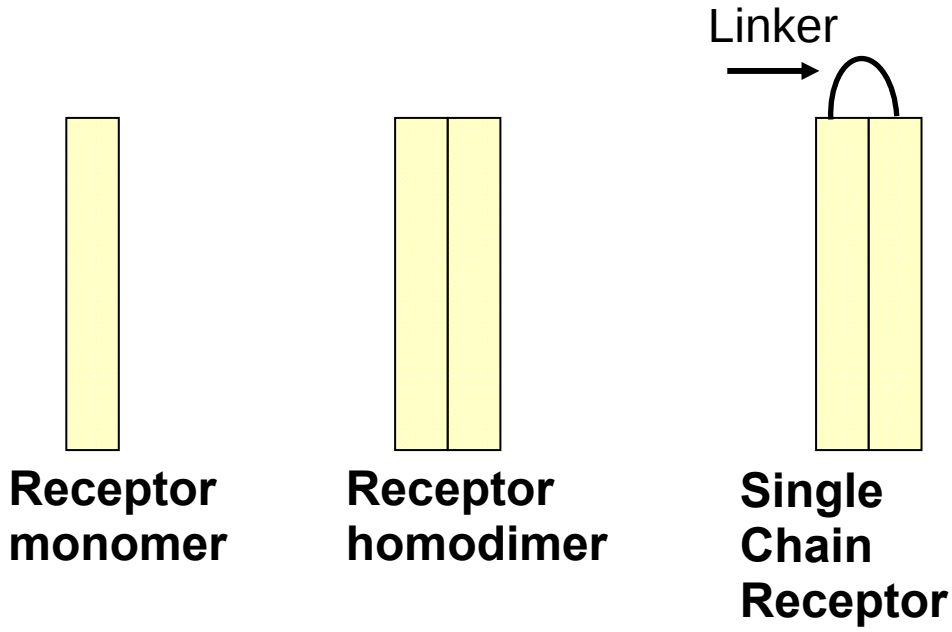

Figure 5.2. Schematic diagram for comparison between structure of receptor monomer with homodimer and single chain receptor.

On the single chain receptor construct, we introduced spin labels at five sites (100, 111, 149, 160 and 167). All of the cysteine substitutions belong to the same

receptor subunit. Site 100 is 75 Å away from the tip, site 149 is right at the tip and the rest of the sites span the region in between these two sites (Figure 5.3).

All the spin labeled proteins used in our experiments were divided into small aliquots and stored at -80°C for future use. However, we observed that some of the proteins lost a significant amount (roughly 30%) of spin label over a period of 2-3 months. The loss in spin label is reflected in reduction in amplitude of the primary echo. In order to be consistent in our analysis, each distance measurement experiment between spin labeled receptor and CheA/CheW was preceded by two control experiments: 1) spin labeled receptor with wild type CheAΔ289/CheW and 2) unlabeled receptor with spin labeled CheAΔ289/CheW. Receptor dimers with a single spin label in complex with wild type CheAΔ289/CheW produced weak dipolar signals amounting to only 10% of the total amplitude. Freshly prepared receptor proteins with wild type CheAΔ289/CheW showed almost no dipolar signals. We believe that over time, receptors associates non-specifically to some extent.

Detection and analysis of intermolecular dipolar signals in the ternary complex

In the context of the ternary complex, the addition of spin labeled single chain receptor dimer to spin labeled CheA/CheW results in a total of three spin label sites: two on the CheA dimer, or on two CheW molecules bound to CheA, and one on the receptor dimer. In other words, at all times, the intermolecular signal is accompanied by an intra-dimer CheA or CheW-CheW distance which complicates the data analysis. This gives a total of five distances in the ternary complex (Figure 5.4). In some cases, when the intermolecular distance lies outside the range of intramolecular distance, it can be distinctly detected as a change in the PDS time domain lineshape. For instance,

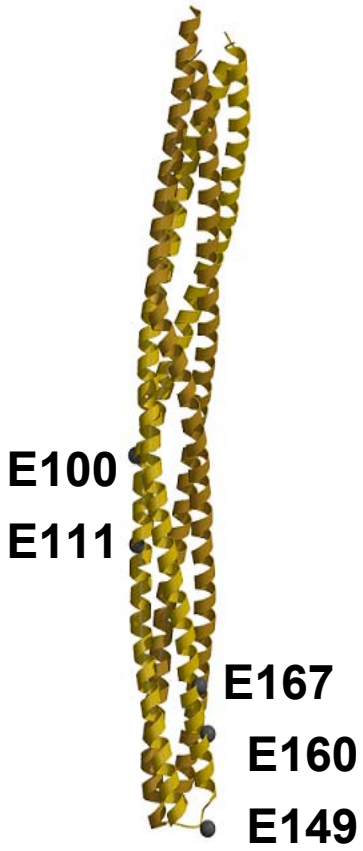

Figure 5.3. Position of spin label sites on single chain receptor.

If the receptor binds to CheA/CheW with both of its symmetric surfaces, it will produce two distances separated by the width of the receptor dimer (about 30 Å). However, due to the flexibility of the spin label, most of the intermolecular distances had a width of 10-30 Å. We measured thirty intermolecular distances between receptor (five sites: 100, 111, 160, 167 and 149) and the CheA/CheW complex (545, 634, 639, 568 and 646 on P5; 371 and 387 on P4; 301, 318 and 331 on P3; 9, 80 and 139 on CheW) summarized in Table 5.1. The positions of sites on CheA and CheW are showed in figure 5.5. In order to identify the sites on the receptor, CheAΔ289 and CheW, the residue numbers are prefixed with R', A' and W' respectively. Out of these, we found that in eleven measurements (highlighted in table), the intermolecular distances were distinct and did not overlap with intra-molecular distances. We used this set of distances in refining our model of CheA/CheW/Receptor complex.

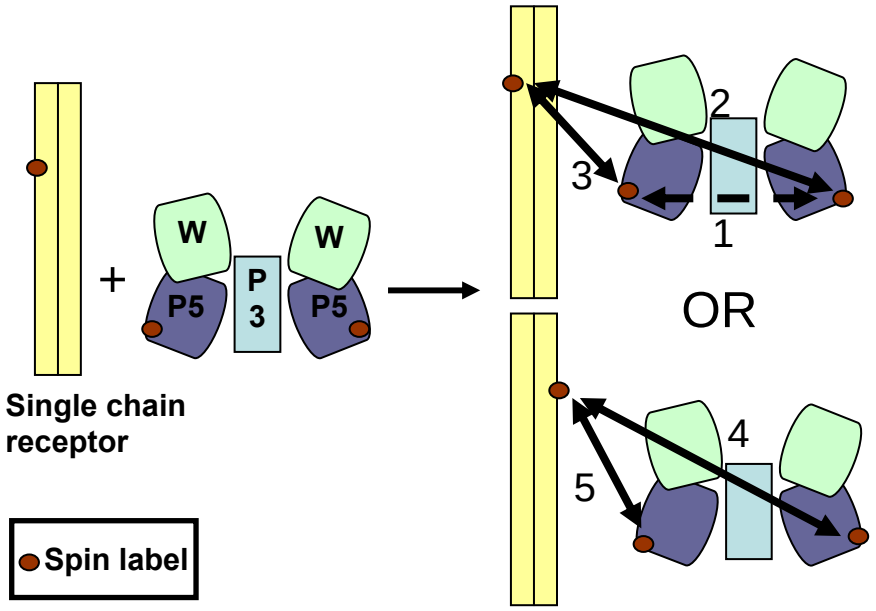

Figure 5.4. Schematic diagram for dipolar distances in a sample containing spin labeled CheAΔ289 dimer and single chain receptor. In CheAΔ289, P4 domains are not shown for clarity. Intermolecular and intramolecular distances are represented by solid and dashed double headed arrow respectively.

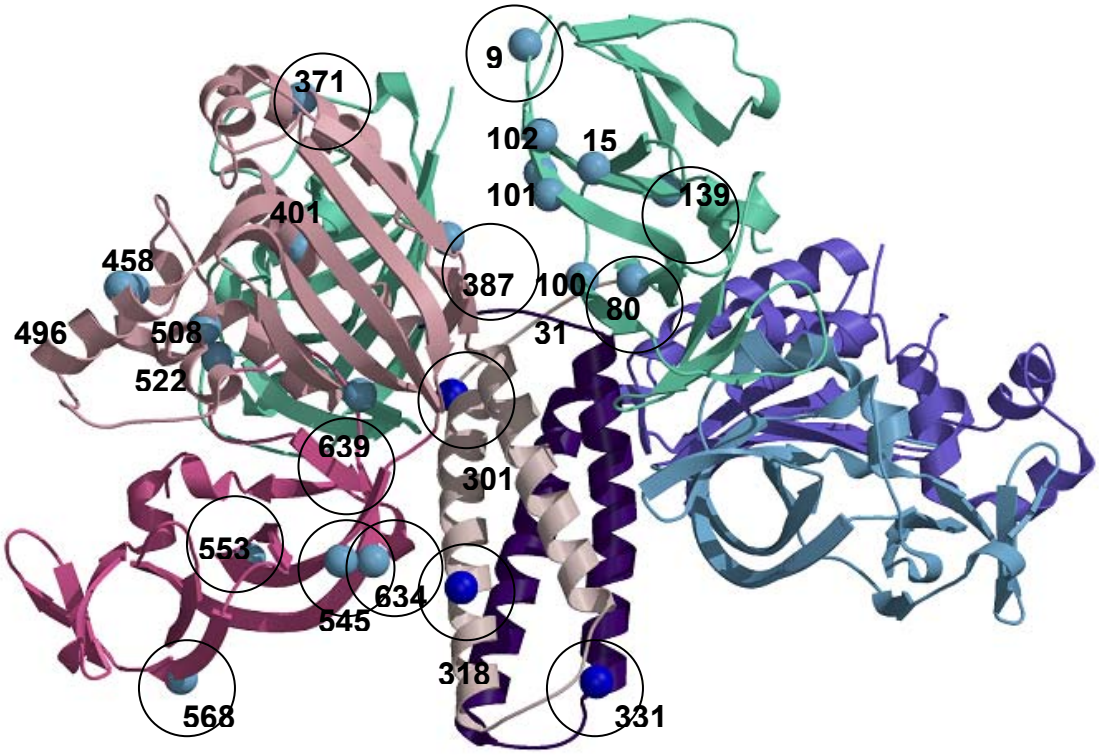

Figure 5.5 Model of CheAΔ289 and CheW complex showing positions of sites tested for ESR and disulphide crosslinking experiments. Sites represented by light blue spheres were testes for crosslinking while those in dark blue and circled in black were tested for ESR experiments.

Table 5.1. Set of intermolecular distances between receptor and CheA/CheW complex

Spin label sites on single chain TM14 receptor

	100	111	149	160	167
CheW					
9	NA	NA	***20-30 Å***	* 20-35Å	Inconclusive
31	NA	* 50-60 Å	NA	NA	Inconclusive
80	Inconclusive	NA	* 20-30 Å And 50-60 Å	NA	***20-30 Å***
137	NA	NA	NA	* 35-45 Å And 50-70 Å	NA
139	NA	NA	#20-30 Å	Inconclusive	NA
P5					
545	***45-75 Å***	***45-60 Å***	NA	Inconclusive	Inconclusive
568	Inconclusive	NA	NA	NA	NA
634	***50-80 Å***	***40-70 Å***	NA	NA	NA
639	X	* 20-30 Å And **40-75 Å**	NA	NA	NA
646	Inconclusive	NA	NA	NA	NA
P4					
371	Inconclusive	NA	Inconclusive	Inconclusive	NA
387	NA	NA	Inconclusive	* 45-65 Å	Inconclusive

(Table 5.1 continued)

P3

301	* >60 Å	Inconclusive	Inconclusive	NA	Inconclusive
318	***45-70 Å***	***45-65 Å***	NA	NA	NA
331	***35-70 Å***	***35-70 Å***	Inconclusive	NA	NA

***** Distance estimated qualitatively from observing the change in lineshape of dipolar signal on addition of spin labeled receptor when compared to dipolar signals measured in presence of unlabeled receptor. It is necessary to perform simulations for rigorous analysis.

Detection of distinct but weak amplitude intermolecular signal. They may arise from oligomerization of single chain receptor itself. It is necessary to perform simulations for rigorous analysis.

Inconclusive: No evidence of intermolecular distances. It is possible that they fall within the same range as intramolecular distances hence are difficult to resolve.

Distances between P3 domains and receptor

Previous experiments with unlabeled receptor confirmed that P3 domains maintain their helical structure in the ternary complex. Due to the rigid structure of this domain in the CheAΔ289 dimer, any spin label site on the P3 domain would produce a constant distance of about 30 Å across the helical bundle. If the intermolecular distance between receptor and P3 domain is greater than this, it can be easily detected. We put spin labels on three different sites on the P3 domain: sites 301 and 331 are at the N-terminus end and hairpin tip of the P3 domain respectively, while site 318 is situated in between these two. We hoped that a consistent change in intermolecular distances from the three sites and a single site on the receptor or vice-versa would reveal the orientation of receptor with respect to the P3 domain axis.

In spite of the considerable width of the distance distributions, we noticed a trend in the intermolecular distances on moving along the length of P3 domain. Site 111 is 58.5 Å way from the tip of the receptor and site 100 is further away by 16.5 Å. From site 318, the R_{max} of the intermolecular distance distributions increased from 48 to 55 Å on moving up the receptor tip from site 111 to 100 (Figure 5.6). This means that site 318 is closer to 111 than is 100 on receptor. However, the distinction between intermolecular distances from site 331 on P3 and sites 100, 111 and 125 is not that apparent (Figure 5.6). In this case, all the distances fall within the range of 35-70 Å. This suggests that the P3 and receptor axis are positioned at an angle to each other.

It should be noted that the presence of intermolecular distances in the range 45-70 Å does not agree with our previous model[1] where the receptor tip sits on the N-terminal end of P3 domain. In the latter case, one would expect considerably longer distances which we did not observe.

We did not observe any distances longer than 30 Å between sites A'301 on P3 and R'167 and R'149. It is possible that the intermolecular distances overlap with the distances within the P3 dimer and hence are not detected.

Distances between P4 and receptor

The interaction with spin labeled receptors resulted in a change in the width of distance distributions between P4-P4 from sites 371 and 387. However, we did not observe any distinct intermolecular distances, hence the position of the receptor with respect to the P4 domains is still uncertain.

Distances between P5 domains and receptor

Similar to the distances across the P3 domain, sites on P5 (545, 634 and 639) located very close to the P3 domain (Figure 5.5) also produce localized distance distributions probably due to restricted freedom of movement in this region. Also, the R_{max} in the intra-domain distances are < 39 Å, which makes any longer intermolecular distances easy to detect. We successfully detected four distinct intermolecular distances between sites 545 and 634 and two sites 100 and 111 on the receptor (Figure 5.7). All were within the 40-70 Å range as we also observed from the P3 domain. Hence, this data further reaffirms that the P3 domain and the receptor axis are not aligned parallel to each other as we suggested before[1]. Simultaneously, the distances suggest that the receptor sits on the side of the P3 domain. Distances from site 639 to R'111 were in two ranges: 20-30 Å and 40-70 Å (Figure 5.8). This suggests that the receptor is closer to one of the P5 subunits than the other.

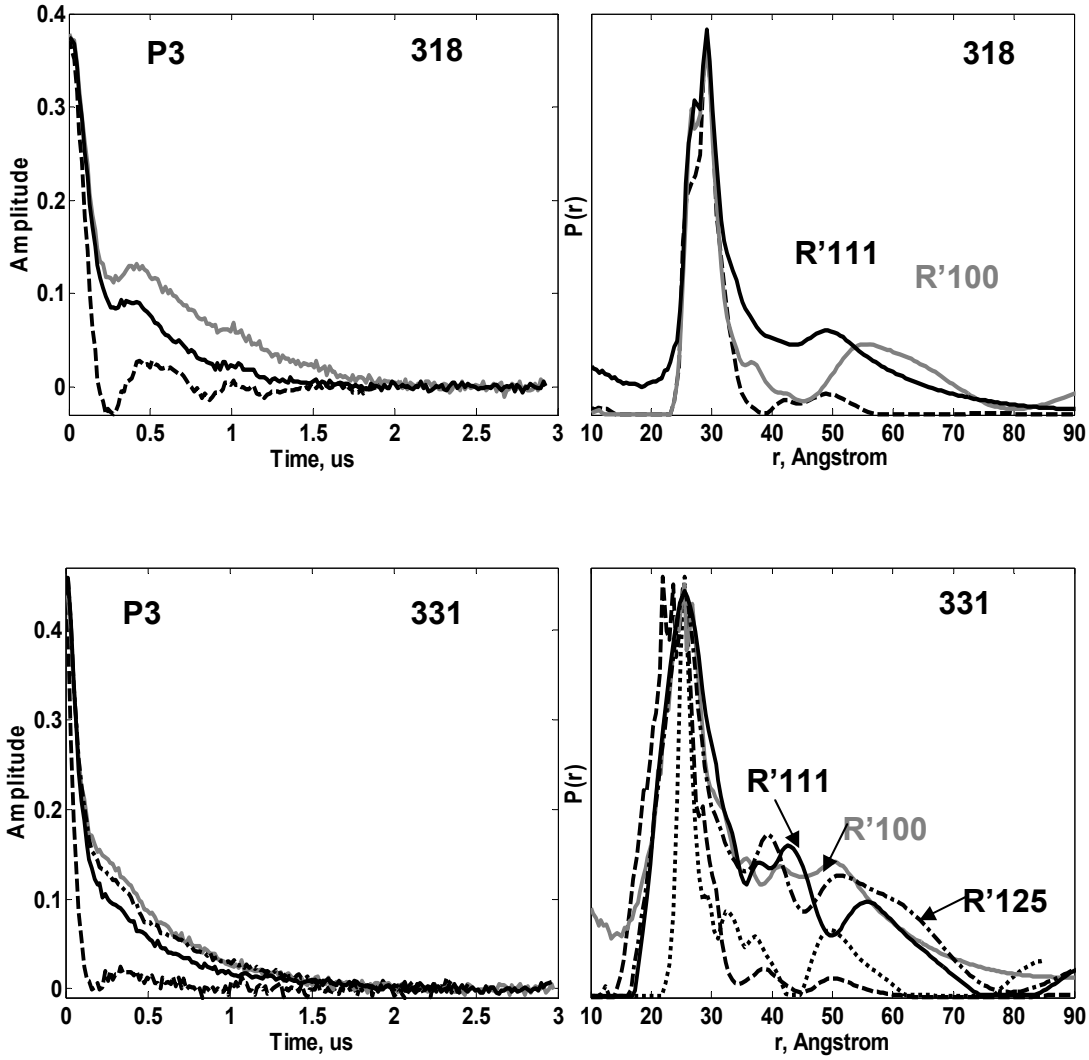

Figure 5.6. Time domain signals and distance distributions from sites 318 and 331 on P3 domain to different spin label receptors. In order to easily detect intermolecular signals, all the signals in time domain and distance distributions were scaled to a common value. The dipolar signals in presence of spin labeled receptors at site 100 (—), 111 (—), 125 (.....) are compared with in presence of unlabeled receptor (– –). Receptor concentrations were 300 μM and CheAΔ289/CheW were at 25 μM and 125 μM respectively.

Sites 545 and 634 are in close proximity, hence, expectedly, the intermolecular distances from these sites to a fixed site on the receptor (for instance site 100) are very similar. This observation is reaffirmed by a similar distance distribution from site 318, which is also very close to 545.

Also, a comparison of distances from site 111 and 100 on the receptor reveals that the former is relatively closer to either of the sites 545 or 634 on the P5 domain.

Distances between CheW and receptor

Intermolecular distances between CheW and receptor were difficult to detect since, to start with, CheW-CheW dipolar signals were just 50% of the maximum expected amplitude. Contrary to sites on P3 and some of the P5 sites, separations between CheW's were greater than 30 Å and distance distributions were broad. Accordingly, we successfully detected two intermolecular distances within 20-40 Å between CheW and receptor (Figure 5.9) (W'9- R'149 and W'80 and R'167). While 149 is at the tip of the receptor and 167 is well within the signaling domain region. This suggests that the signaling domain region of the receptor is close to at least one molecule of CheW. This proximity restraint is a crucial guideline in aligning the receptor in the CheA/CheW complex. The presence of multiple dipolar signals prevented us from predicting the position of the second CheW with certainty.

The magnitude of the intermolecular PDS signal between receptor and CheW directly reflects the amount of ternary complex in the solution. We believe that receptor, CheA and CheW form a complex and that the weak amplitude of intermolecular signal reflects weak binding between receptor and the CheA/CheW complex. In this case, we would expect that the population of ternary complex molecules to increase with concentration of either one of the components. Indeed, we

observed that on doubling the receptor concentration, the dipolar signal between W'80 and R'167 increased by the same magnitude.

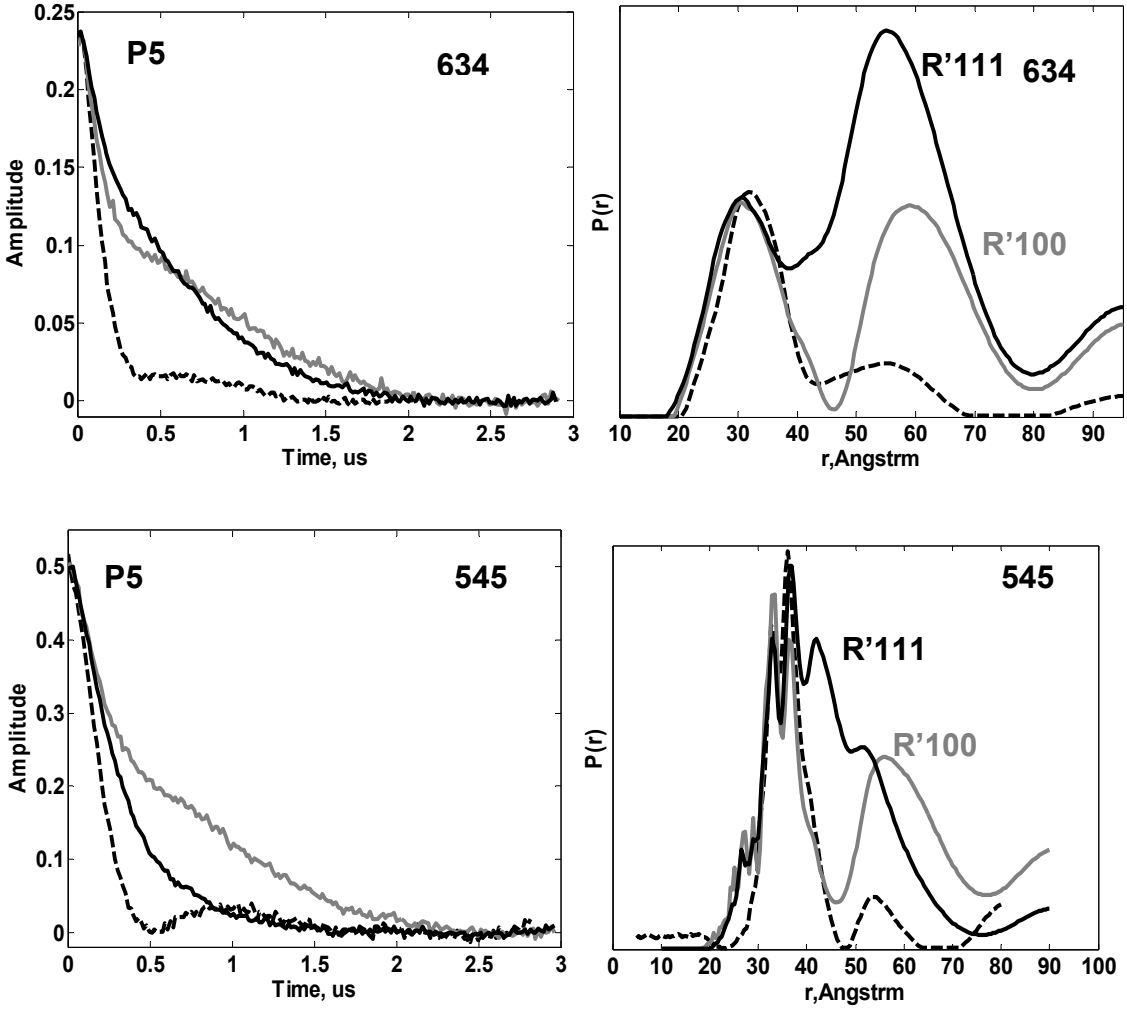

Figure 5.7. Time domain signals and distance distributions from sites 545 and 634 on P3 domain to different spin label receptors. In order to easily detect intermolecular signals, all the signals in time domain and distance distributions were scaled to a common value. The dipolar signals in presence of spin labeled receptors at site 100 ( ) and 111 ( ) are compared with in presence of unlabeled receptor ( ). Receptor concentrations were 300 μM and CheAΔ289/CheW were at 25 μM and 125 μM respectively.

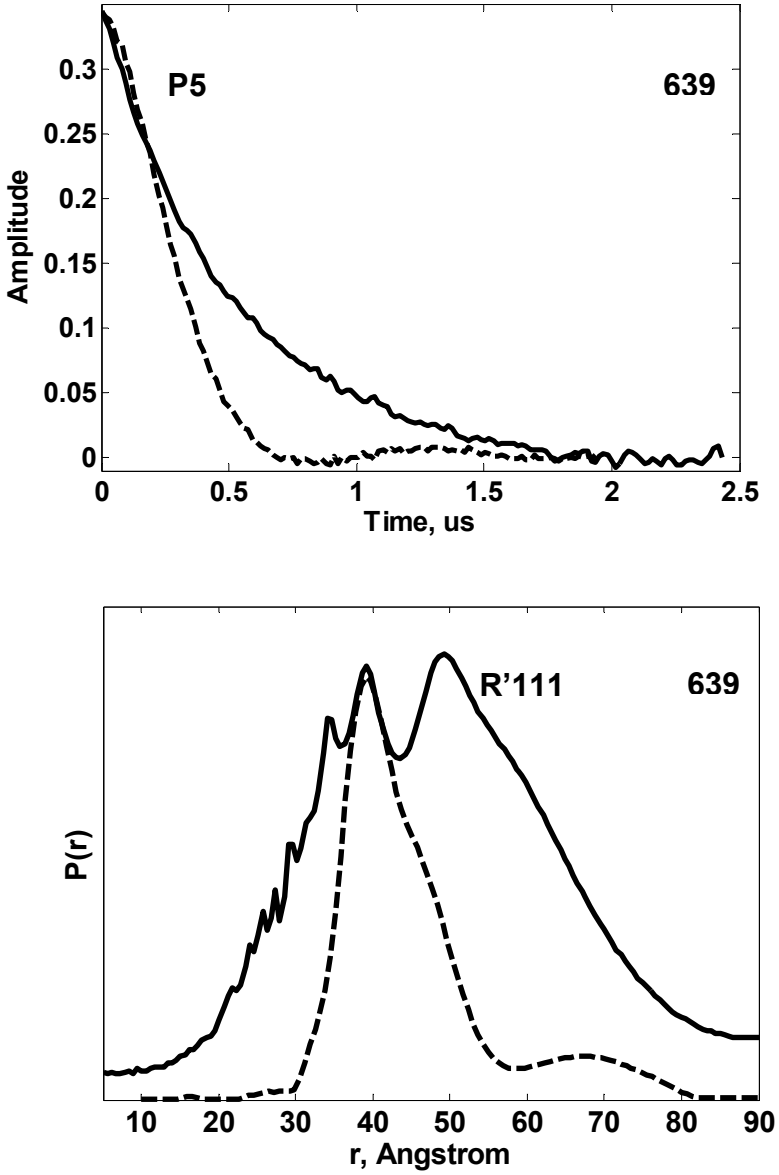

Figure 5.8. Time domain signals and distance distributions from sites 639 on P5 domain to spin label receptors at site 111. In order to easily detect intermolecular signals, all the signals in time domain and distance distributions were scaled to a common value. The dipolar signals in presence of spin labeled receptors at site 111 (———) are compared with in presence of unlabeled receptor (– –). Receptor concentrations were 300 μM and CheAΔ289/CheW were at 25 μM and 125 μM respectively.

5.2.3 Distance measurements with hetero dimers of CheAΔ289

The detection of intermolecular distances is limited by the ability to clearly distinguish them from intramolecular distances. In order to overcome this problem, we prepared heterodimers of CheAΔ289[1] which have a single spin label on them. For this purpose, we selected two sites: 301 and 331 on the P3 domain (Figure 5.2). However, the results of distance measurements between these sites and spin labeled single chain receptor were inconclusive since the dipolar signals had very weak amplitude. Apart from the reason of weak binding of receptor with CheA/CheW complex, a major reason for this observation is the low population of spin labeled heterodimers in solution.

This is primarily due to the fact that the procedure for preparing heterodimers of CheAΔ289 produces wild type CheAΔ289 which cannot be separated from spin labeled heterodimers. Hence, the main limitations of our experiments with heterodimers of CheAΔ289 were the low concentrations of spin labeled components.

5.2.4 Restraints from disulphide crosslinking

In order to confirm the conformation of receptor in the ternary complex, we tested the proximity of cysteine residues between receptor and CheA/CheW complex by performing disulphide crosslinking experiments. All the single cysteine mutations were engineered one at a time in a background of cysteine-less CheA, CheW and receptor. We conducted sixty-three crosslinking experiments with eight, thirteen and six cysteine substituted CheW's, CheAΔ289 and receptors respectively. In receptor, all the cysteine substitutions were on a single chain construct except for site 125. Each experiment involved cysteine substituted receptor with either CheAΔ289 or CheW. In some cases, we tested the ability of crosslinking between two partners in the presence of a third wild type protein component (Table 5.2).

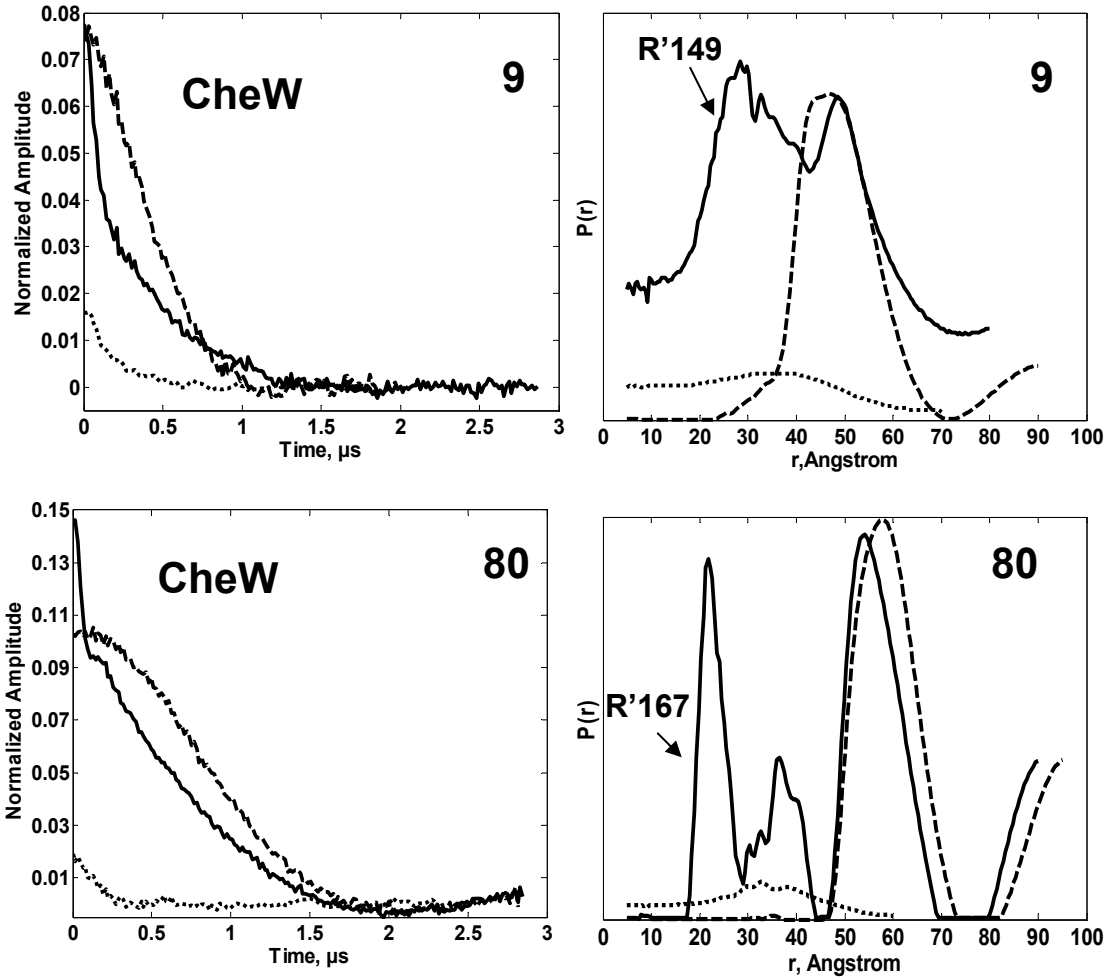

Figure 5.9. Time domain signals and distance distributions from sites on CheW and spin label receptors. In order to easily detect intermolecular signals, all the signals in time domain and distance distributions were scaled to a common value. The dipolar signals between site 9 on CheW and E149 on receptor and site 80 on CheW and E167 on receptor are shown in the first and second panel respectively. The curves in the presence of spin labeled receptor (———) are compared to in the presence of unlabeled receptor (– –) and spin labeled receptor in the presence of wild type CheAΔ289/CheW (·····). CheAΔ289/ spin labeled CheW were at 50 µM and 100 µM respectively while receptor E149C and E167C were are concentrations 300 µM and 400 µM respectively.

Cu(phenanthroline)$_3$ was used as the cross-linking agent. Site E149C at the tip of the single chain receptor selectively crosslinked with the N-terminal residue K9C of CheW (Figure 5.10). This crosslinked pair confirms our previous result from ESR where we obtained short distances between these spin-labeled sites. The cross-linking efficiency increased in the presence of wild type CheAΔ289.

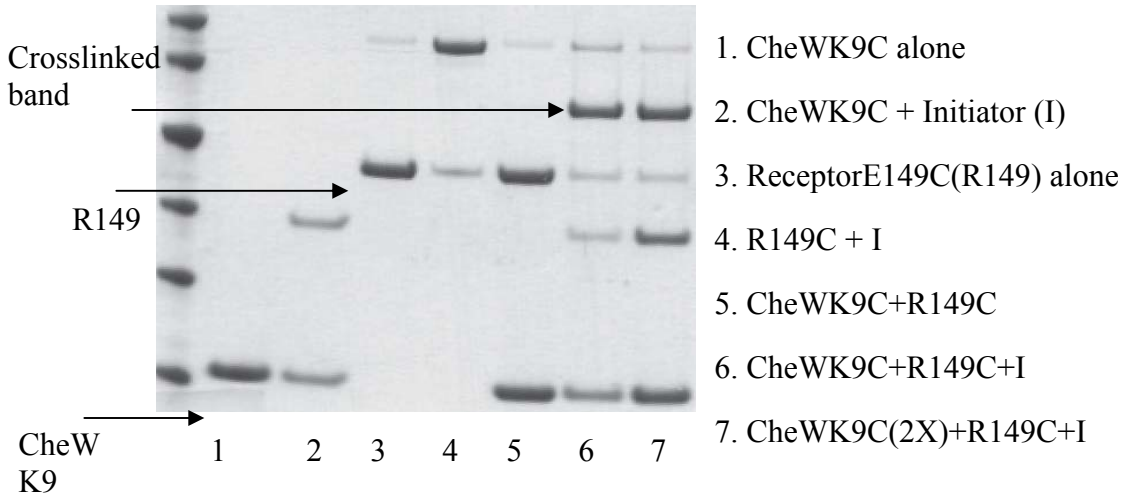

Figure 5.10. Gel showing crosslinking between site K9 on CheW and E149 on single chain receptor. All protein concentrations were about 2μM and Cu(phenanthroline)$_3$ was used as the crosslinking agent.

Our search for other crosslinking partners revealed another pair: K496C on the P4 domain and N125C on the receptor homodimer (Figure 5.11). On the SDS gel, the cross-linked product runs at a higher molecular weight on the gel (75 kDalton) than the expected weight of 68KDalton presumably due to the disulphide bond. The presence or absence of wild type CheW did not effect cross-linking. Distance measurements with DEER were not effective in confirming the proximity of these two sites since the dipolar signal is already dominated by a short distance of ~30 Å corresponding to the width of the receptor homodimer.

Table 5.2 Cysteine substituted sites on receptor and CheW, P4 and P5 domain of CheAΔ289 tested for their ability to cross-link.

Cysteine mutations on TM14 receptor. All are single chain receptors except site 125.

	100	111	125 (homodimer)	149	160	167
CheW						
9	X	X	X	strong*	-	X
15	X	X	X	X	-	X
31	X	X	X	X	X	X
80	-	-	-	X	-	X
100	-	-	-	-	X*	X*
101	weak	X	X	X	X*	X*
102	X	X	X	X	X*	-
139	-	-	-	X	-	X
P5						
545	X	X	-	-	-	X
553	X	X	X	-	-	-
568	-	-	-	-	-	
634	-	-	-	-	-	X
639	X	X	X	-	-	-
646	X	X	X	-	-	-
P4						
371	X	X	X	X	X	-
387	-	-	X	-	X	-

(Table 5.2 continued.)

401	-	-	X	-	-	-
458	-	-	X	-	-	-
496	X	X	strong *#	-	X	X
508	-	-	X	-	-	-
522	-	-	X	-	-	-

X : Negative cross-linking

* : Cysteine substituted sites CheW or CheAΔ289 tested for crosslinking in presence of wild type CheAΔ289 and CheW respectively

: Site 496 on CheAΔ289 did not cross-link with 125 site on single chain receptor

The presence or absence of wild type CheW did not effect cross-linking. Distance measurements with DEER were not effective in confirming the proximity of these two sites since the dipolar signal is already dominated by a short distance of ~30 Å corresponding to the width of the receptor homodimer.

5.2.5 Models of the ternary complex

Distance restraints provided by ESR and crosslinking experiments were used to orient the receptor with respect to the CheA/CheW complex. For our modeling purposes, we used the conformations of receptor and CheA/CheW complex from the crystal structure [3]and that determined by rigid body refinement with distance restraints in the presence of unlabeled receptor. While keeping the conformation of the CheA/CheW complex fixed, we moved the receptor dimer such that the intermolecular constraints are satisfied.

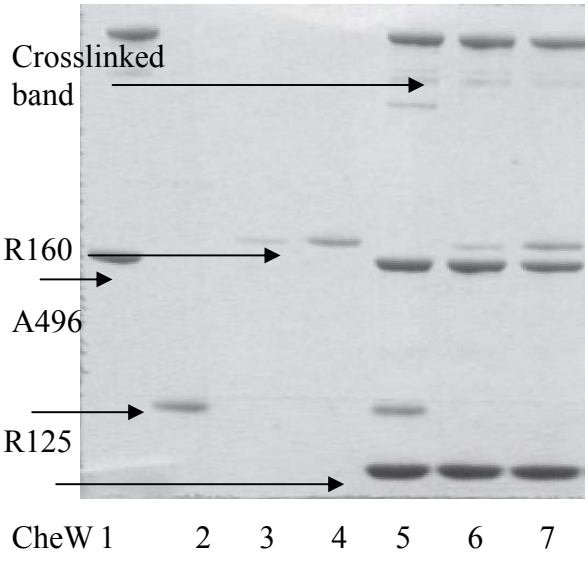

1. CheΔ289K496C (A496) + I
2. Receptor N125C (R125) + I
3. Receptor E160C (R160) + I
4. Receptor E167C (R167) + I
5. A496 + R125 + CheW + I
6. A496 + R160 + CheW + I
7. A496 + R167 + CheW + I

Figure 5.11. Gel showing crosslinking between receptor homodimer N125C and CheΔ289K496C. All protein concentrations were about 2μM and $Cu(phenanthroline)_3$ was used as the crosslinking agent.

Previously, we proposed a model of the ternary complex where the receptor fits into the cleft formed by two CheW's and the tip of the receptor sits on the N-terminal end of the P3 domain [1] (Figure 5.12). We found that the intermolecular distances from the P3 and P5 domains to the receptor completely disagree with the C_β separations of the corresponding sites in that model (Table 5.3). Instead, the 40-70 Å range of distances suggest that the receptor axis sits on the side of the P3 domain axis. The next step is to determine how the two helical axis are aligned with respect to each other.

At this stage of modeling, we are guided by the relatively short distances (20-40 Å) between CheW and receptor which suggest that the signaling domain of the receptor is tightly restrained to be close to CheW. Moreover, the disulphide crosslink between tip of the receptor and the N-termini of CheW provide a further constraint on the proximity between the two sites. Broadly, this condition is satisfied if the long axis of the receptor, (while still being at the side of the P3 domain) is aligned anti-parallel to the P3 long axis and the height of the receptor is adjusted such that the tip region lies close to N-terminus end of CheW. Interestingly, this orientation places the signaling domain of the receptor directly facing the proposed receptor-interaction-region on CheW[4,5].

We noted that the distances between receptor and CheW are not as widely distributed (10-20 Å) as those between receptor and P5/P3 domains. Hence, the signaling domain of the receptor is still positioned close to CheW, however, the orientation with respect to P3 and P5 domains can be determined with less certainty. In order to resolve this issue, we investigated possible orientations of receptor while keeping the position of the signaling domain somewhat fixed. Overall, the search involved changing the angle between the P3 and receptor axis. We found that all possible orientations would fit between two positions of receptor: first, when the

receptor axis is completely antiparallel to P3, and second, when it makes an angle of 20° with it. We refer to these orientations as Model A (Figure 5.13)and Model B (Figure 5.14)respectively and we further tested to see which agrees the best with the experimental data.

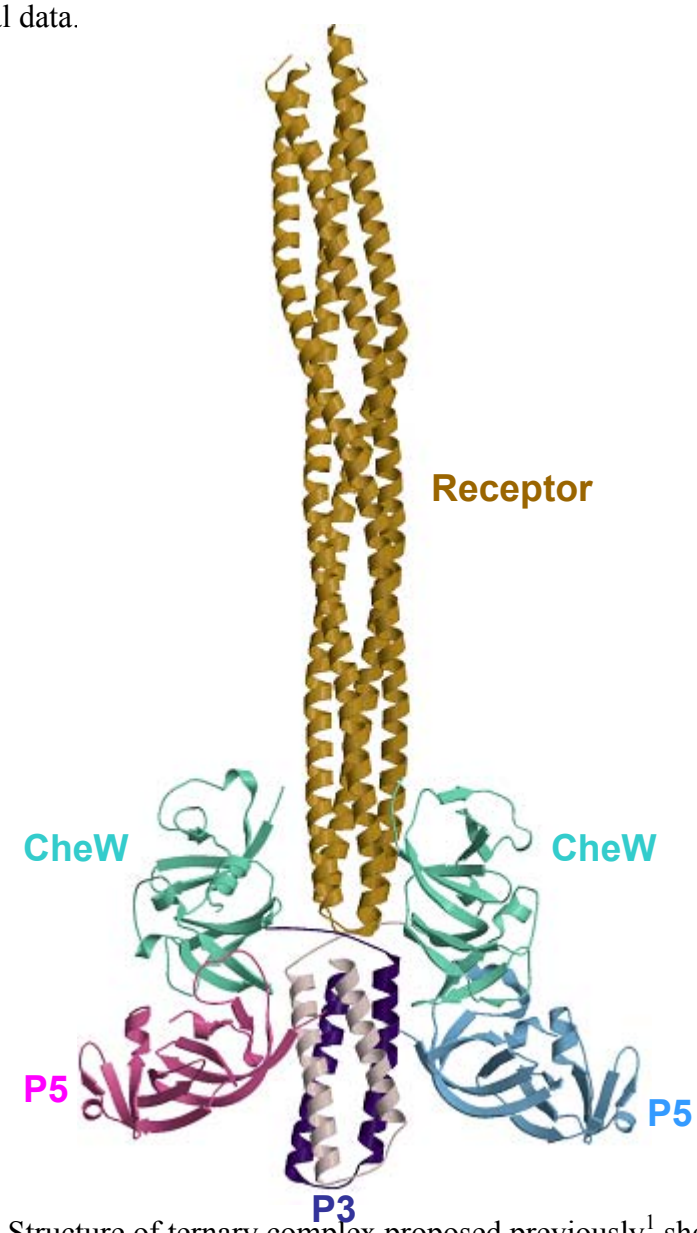

Figure 5.12. Structure of ternary complex proposed previously[1] showing the position of receptor dimer on top of P3 domain and in between the two CheW's. The P4 domains have been omitted for clarity. (The figure is adapted from Figure 4 in reference[1])

Criteria for testing validity of models

We tested the validity of each model by comparing the range of intermolecular distances with the C_β separations from the corresponding sites (Table 5.3). In each case, there are four set of distances: two between sites on the CheAΔ289 dimer, a single site on receptor dimer, and two more if the receptor binds with the other symmetric surface. We developed the following criteria for identifying if model distances agree with the ESR distances: Due to the length of the spin label, ESR distances are typically longer than C_β separations. To account for this, we considered the model distance to agree with the ESR data if it is less than 13 Å than the R_{max} or the lower limit of the ESR range. On the other hand, we put the upper limit on model distances as 5Å. All the distances that do not match this criterion are marked in Italics in Table 5.3. It should be noted that the reason for not using rigid body refinement program to refine the position of receptor with respect to CheA/CheW complex is due to large width of distance distribution. In order to get meaningful refinement, it is necessary to restrict d_{min} and d_{plus} in rigid body refinement program[7] to about 5 Å. The marked distances in the table should not be regarded as disagreeing with the model. We believe that they are still present, but we cannot detect them distinctly since they overlap strongly with the intramolecular distances.

Model A vs Model B

The two models A and B differ in the angle that the receptor axis makes with the P3 domain axis. In model A, the receptor is completely anti-parallel while it is tilted in model B. We found that at least qualitatively, the model distances agree with ESR distances in both of the models. To elaborate, we looked for a relative trend in distances from a fixed site on P3 or P5 to two or more sites on receptor.

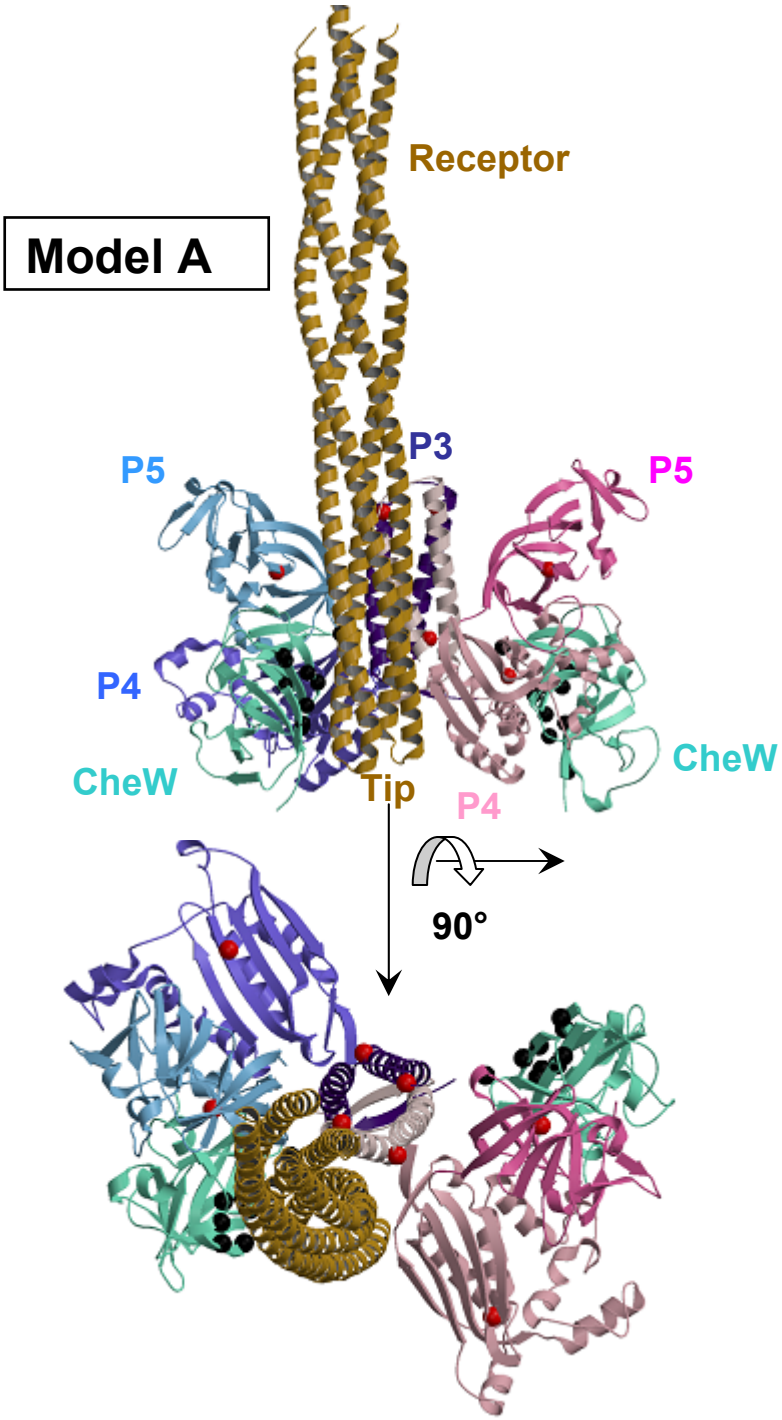

Figure 5.13. Structure of model A. The receptor sits on side of P3 domain and is antiparallel to it. The tip of the receptor is close to N-termini of CheW. Sites on CheW important for binding with receptor are in black spheres[4,5], and those on CheW predicted from protection studies [6]are in red spheres.

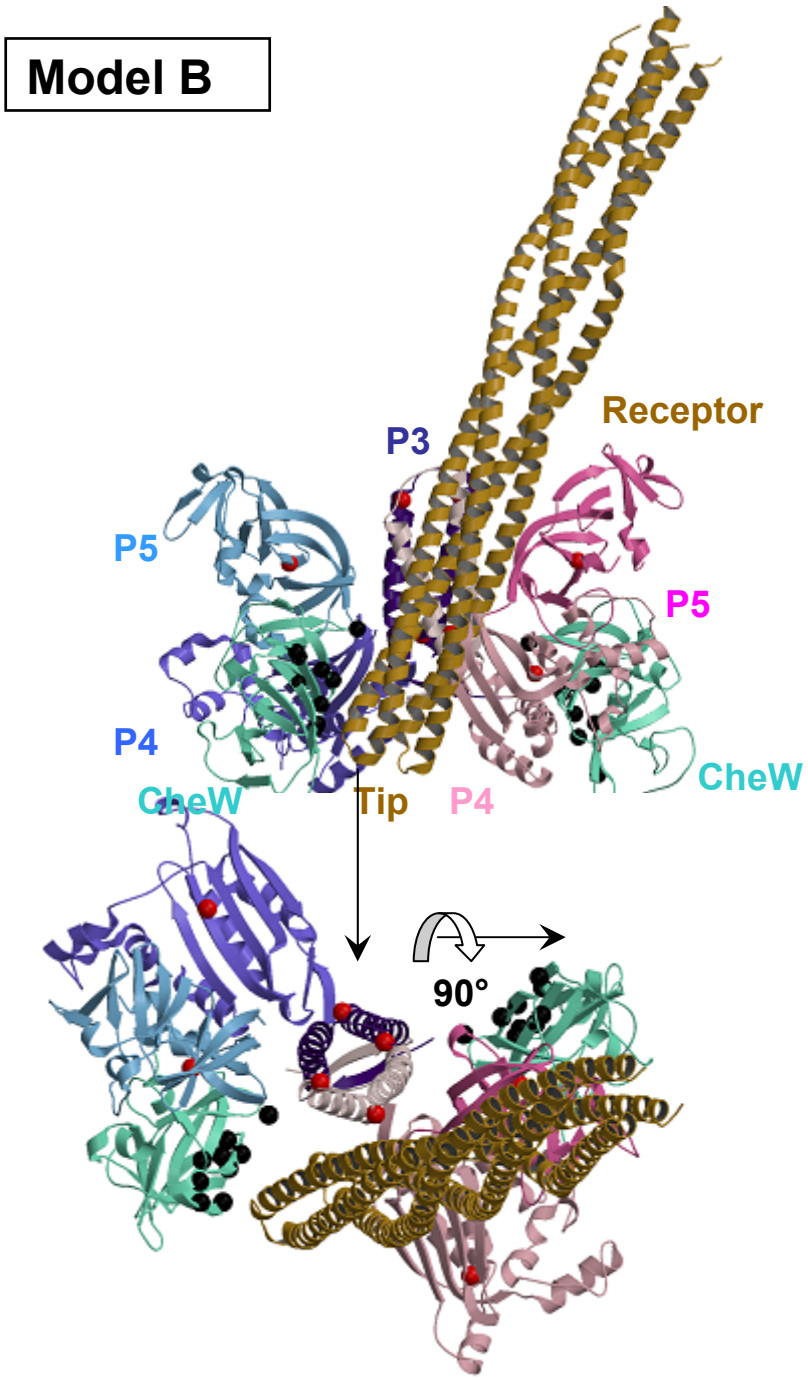

Figure 5.14. Structure of model B. The receptor sits on side of P3 domain and makes an angle of 20° with it. The tip of the receptor is close to N-termini of CheW. Sites on CheW important for binding with receptor are in black spheres[4,5], and those on CheW predicted from protection studies [6]are in red spheres.

Table 5.3. Comparison of intermolecular ESR distances with C_β separations in three different models. All distances are in Å.

	Previous Model[1]	ESR range	Model A	Model B
CheW-R				
W9-R149	31, 28, 24, 34	R_{max} 28, 20-40	22, 40, 20, *55*	18, 44, 19, *59*
W80-R167	44, 35, 34, 43	R_{max} 21;W 6 R_{max} 31;W 6	24, *47*, 17, *62*	30, *42*, 25, *58*
P5-R				
A545-R100	102, 102, 101, 102	R_{max} 56; W 16	47, 47, *36, 34*	55, *33*, 49, *21*
A545-R111	85, 86, 85, 86	R_{max} 42, 40-65	40, 37, *28*, *25*	47, *24*, 39, *8*
A634-R100	101, 100, 100, 100	R_{max} 59; W 17	46, 49, *35*, *35*	51, *38*, 45, *25*
A634-R111	84, 83, 83, 83	R_{max} 55; W 16	*36*, *38*, *24*, *25*	42, *28*, *35*, *13*
A639-R111	66, 66, 66, 67	20-35, R_{max} 39	*45*, *49*, 37, 41	*51*, 38, *46*, **27**
P3-R				
A318-R100	103, 102 100, 102	45-70	46, 42, 32, *29*	48, 34, 40, *24*
A318-R111	86, 85, 84, 86	45-65	37, *31*, *22*, *18*	40, *24*, *30*, *11*
A331-R100	113, 113 112, 113	35-70	44, 31, 25, *17*	36, 35, *21*, 31
A331-R111	96, 96, 95, 97	35-70	39, 27, 22, *11*	33, 31, *18*, 25

(Table 5.3 continued)

W: full width at half maximum

Distances marked in Italics meet either of the following criteria:

1. Distances more than 5 Å of R_{max} or lower limit of ESR range. 2. Distances less than 13 Å of R_{max} or lower limit of ESR range.

For instance, site 111 on receptor is closer to 545 on P5 than site 100. The corresponding distances in both the models also show a similar trend.

However, we did observe that the experimental data agrees a bit more with Model B because of two reasons: First, none of the four model distances from A'634 and R'111 satisfied the previously defined criteria for agreeing with ESR distances. Secondly, in model A, none of the four distances from A'639 and R'100 satisfied the short distance component (20-30 Å) of observed ESR distance. In comparison, one out of four distances in model B did meet this criterion (underlined in Table 5.3).

Our data does not favor model B very strongly over model A. Hence, we believe that in solution either of these receptor orientations may be present. For better understanding, in the following section we discuss the structural differences and similarities between the two models.

Structural comparison of Model A and Model B

The interaction of receptor with CheW is identical in both the models. However, the slightly different tilt of the receptor axis, determines the presence or absence of interaction of receptor with the P3 and P5 domains. In model A, the receptor interacts strongly with the antiparallel P3 domain and only to some extent with the hinge region near the hairpin loop region of P3.

In model B, the tilt of the receptor allows the receptor to interact with the P5 domain of the opposite subunit. This orientation suggests a possible mode of communication between the two subunits as significant interaction surface falls in the hinge region near the hairpin loop of P3 domain. Interactions in this region are critical in controlling the domain motions.

Protection studies[6] have identified four sites on the surface of CheA that are involved in receptor binding. Two of the sites are on the P3 domain and one on each

of the P4 and P5 domain. The orientation of receptor in model A allows the receptor to interact with both the sites on the P3 domain, but only one on model B. However, the site on the P4 domain is much closer to receptor in model B. The site on the P5 domain is rather buried in the structure, hence unlikely to interact with receptor.

It should be noted that the proximity restraint between A'496 and R'125 due to disulphide crosslinking is not satisfied in either of the two models. The C_β separations between these two residues from either of the CheAΔ289 subunits are between 40-50 Å. However, site 496 resides on the ATP lid on P4, hence the region is expected to be mobile. We believe that due to the flexible nature, this region samples certain conformations that brings it close to N125C on the receptor.

Comparison with trimers of dimers of receptor

Numerous *in vitro*, *in vivo* and genetic studies as well as electron microscopy have established that receptors associate together as trimers of dimers[8]. However, we detected only dimers for receptors from *T.maritima*. Our search for the position of receptor in the ternary complex led us to two models which differ from each other only with respect to tilt of the receptor axis. In order to compare these two orientations of receptor with arrangement of dimers in the trimers, we superimposed the receptor dimer from model A on one of the dimers in the trimers model. We found that the receptor orientation in model B aligns significantly with the adjacent dimer in the trimer (Figure 5.15).

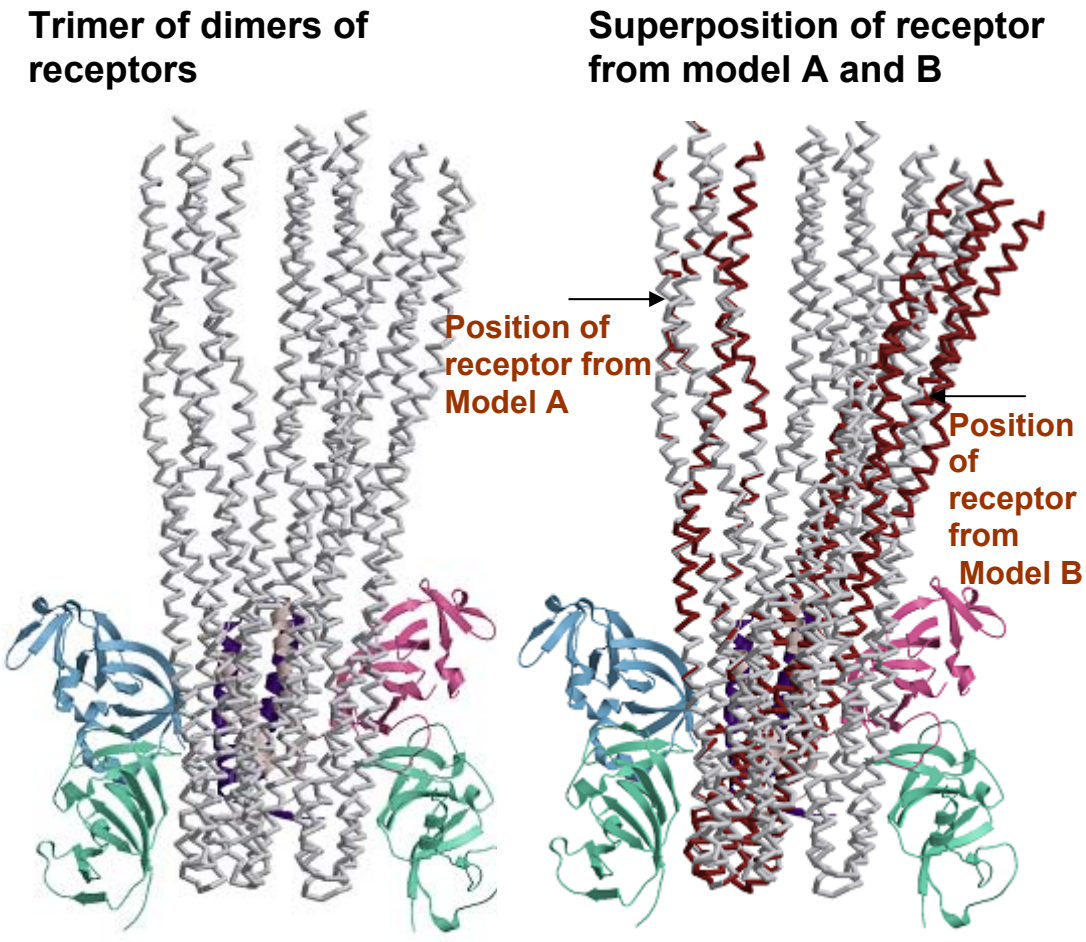

Figure 5.15. Comparison of receptors orientations from model A and B with the arrangement of receptor dimers in a trimer. The receptors from model A and B are colored in brown while receptors in the trimer are in grey. If receptor from model A is superimposed on a single dimer in the trimer, the receptor from model B overlaps with the position and orientation of adjacent dimer in the trimer.

5.3 DISCUSSION

Large assemblies of chemoreceptors, CheA and CheW, localized at the poles of the cell are responsible for controlling the motion of bacteria in presence of chemicals[9-12]. Electron microscopy has determined that inside these clusters, the receptors form a partially ordered hexagonal lattice[12-15]. In solution, CheA, CheW and receptors from *E.coli* associate to form active complexes which vary in their composition[16-18]. Single particle analysis and electron microscopy have provided low resolution envelops of these complexes. Since many of the regions on CheA, CheW and receptors are highly conserved, *in vitro* structural analysis of ternary complexes can in principle provide crucial insight into the association of these proteins in cells. In this work, we have studied the structure of the ternary complex formed by proteins from *T.maritima*. The ternary complex is composed of a cytoplasmic fragment of TM14 receptor, CheAΔ289 and CheW. The activity of this complex has been studied and it's found to be inhibitory (Pollard et al unpublished).

The structural determination is based on long-range distance restraints from Pulsed Dipolar ESR spectroscopy (PDS). The method relies on the detection of dipolar coupling between a pair of electron spins which allows for measurement of the distance between the two. In a binary complex of proteins, if a single spin is introduced on each of the components, the PDS would then reveal the separation between these sites in the complex. A set of distances can be obtained if more spin labeling sites are selected on the components. These restraints are then used to model the structure of the complex. In the ternary complex, this gets translated into obtaining pair-wise intermolecular distances in the complex. In our case, the dimeric nature of receptor and CheA complicates data analysis, since intermolecular distances are accompanied by intramoleular separations. We partly solved this problem by preparing single chain receptors, where the receptor subunits are covalently linked and

a single label can be put on the receptor dimer. However, since the receptor dimer is symmetric, it can still bind to CheA/CheW in two ways, hence will produce two intermolecular distances between receptor and a single site on CheA or CheW. On the other hand, intra-molecular distances within the CheA dimer were always present. The conformation of the CheA/CheW complex in the presence of unlabeled receptor was determined in Chapter 4. Here, we used the intermolecular distances between receptor and CheA/CheW complex to model the structure of the ternary complex. From a set of thirty distances, we were able to separate eleven measurements where the intermolecular and intramolecular separations did not overlap. Disulphide crosslinking studies further provided controls on the spatial proximity of sites within the complex.

5.3.1 *T.maritima* receptors form dimers in solution

Our first set of experiments were directed towards investigating the oligomeric state of TM14 receptor dimers. We found that these receptors predominantly form dimers in solution. We did not observe any significant longer distances which may relate to higher order association of receptors. This observation is consistent with the arrangement of TM14 as well as another *T.maritima* receptor 1143 in the crystal lattice[1,3]. However, the receptors from *E.coli* associate to form trimer of dimers in solution as well as in the crystal lattice[2].

5.3.2 Model of ternary complex

Our search for orientation of receptor that would satisfy all the ESR as well as disulphide crosslinking restraints led us to suggest two models (model A and B ;Figure 5.13, 5.14) which differ from each other only in the tilt of the receptor axis. Overall, the position of the receptor in both the models is very different than we suggested in our previous work where the receptor long axis is parallel and continuous

with P3 long axis [1] (Figure 5.12). We measured short distances between spin label sites on CheW and receptor and the disulphide crosslink between the tip of the receptor and N-terminus of CheW clearly restricted the signaling domain of the receptor to be close to at least one CheW. In our previous model, the tip is right above the N-terminal end of the P3 domain, hence the crosslink condition cannot be satisfied. The presence of distances from P3 or P5 domains to the receptor in the range 40-70 Å also completely disagreed with the previous model, and instead suggested that the receptor is positioned on the side of the P3 domain. This orientation was also suggested in the two other models of ternary complexes which were determined by protection studies[6]. However, in the model with receptor dimer, the data was not sufficient to resolve the parallel or the anti-parallel orientations of long axis of P3 and receptor. On the other hand, our experimental restraints strongly suggest that the receptor is not only aligned to be at the side of P3 domain but is anti-parallel to it, since the tip of receptor is required to be close to the N-terminus of CheW.

Relatively short distances between CheW and receptor restrict the flexibility of the region close to the tip of the receptor. On moving further up the receptor, is the surface that interacts with domains of CheA. The distances measured between receptor and the P3 or P5 domain are widely distributed hence there is uncertainty in the position of receptor with respect to these domains. In other words, if we keep the tip region of the receptor fixed, the receptor can still rotate about the tip and sample different orientations in the space marked by the two P5 domains. From many possible orientations, we considered two limiting orientations of receptor. In the first case, the receptor is closest to the P5 domain which binds to CheW which interacts with it. In this orientation the receptor axis is completely anti-parallel to the P3 helical axis. In the second case, the receptor tilts and makes contact with the P5 domain in the

opposite subunit. We refer to the first and second orientations of receptor as model A and B respectively.

We developed a criterion for evaluating the agreement between model distances, represented by C_β separations and ESR distances. We found that even though our data does lean a bit more towards model B, due to width of distance distributions, both the models qualitatively agree with the ESR distances very well.

The nature of receptor interactions with CheA is different in the two models. In model A, the anti-parallel stacking arrangement of four helical bundles of P3 and receptor brings in symmetry but restricts the receptor interaction with only the P3 domain of CheA. In contrast, the surface on CheA that interacts with receptor in model B is broader and covers partly P3 and P5. Interestingly, on the opposite subunit, the receptor also interacts with the hinges that join P3-P4 and P4-P5 domains. The different orientations of two subunits in the structure of CheAΔ289 suggested motion of domains about the hinges[19]. Interactions in this region of CheA are important because the regulation of kinase activity by receptors probably involves controlling movement of CheA domains. This hypothesis is reinforced by the fact that the residues in the hinge region are highly conserved[6]. Also, in model B, the receptor is held together between the two subunits with CheW and the P5 domain from opposite subunits. CheW and P5 domain share significant structural similarity. Remarkably, the receptor interacts at the same symmetric surface on them.

Protections studies have identified the receptor interaction surface on CheA that covers P3, P4 and P5 domains[6]. However, this surface is not well defined as it is marked by only four sites. Moreover, the site on the P5 domain is buried and unlikely to interact with receptor unless significant conformational change within the domain forces this site to get exposed. Out of the remaining three sites, the receptor surface on CheA in model A and B covers all and two out of three sites respectively. In both the

models, the site on P4 domain resides on the face of P4 that directly faces the receptor and hence agrees with the orientation of P4 domains in the model. However, the tilt of the receptor in model B brings the receptor much closer to P4 than in model A. On the other hand, both sites on the P3 domain interact with the receptor in model A while model B allows interaction with only one.

Our two models highlight different but important interactions with CheA. In model A, the perfect stacking together of the P3 domain and receptor is appealing, but at the same time, the broader receptor interaction surface on CheA in model B has important implications for a way of regulating kinase activity. Since our data doesn't favor one model over the other very strongly, hence we do not know for certain which orientation the receptor samples in solution. However, it is possible that the surface on CheA covered together by both these models is required for receptor binding. We found that this surface is simultaneously covered if receptors were to associate as a trimer of dimers, which is the arrangement observed in *E.coli* and *Caulobacter*[8,20,21]. Moreover, if we superimpose model A on one of the dimers in the trimer, then model B overlaps with the position and orientation of the adjacent dimer (Figure 5.15). This is strong evidence in support of the fact that both the orientations of the receptor dimer mimic the two adjacent dimers in the trimer of receptors. Hence, indirectly, our models also suggest the receptor trimer interaction surface on CheA/CheW complex.

The final model of the ternary complex with receptor trimer does agree in a general sense with the model suggested by protection studies[6]. In the latter case, the domains were optimally oriented so as to satisfy the four main sites which interact with receptor. In contrast, in our modeling, we were guided with many more experimental restraints and the relative orientations of CheA and CheW were determined by performing rigid body refinement with ESR distances.

REFERENCES

1. Park, S. Y., Borbat, P. P., Gonzalez-Bonet, G., Bhatnagar, J., Pollard, A. M., Freed, J. H., Bilwes, A. M. & Crane, B. R. (2006). Reconstruction of the chemotaxis receptor-kinase assembly. *Nature Structural & Molecular Biology* **13**, 400-407.
2. Kim, K. K., Yokota, H. & Kim, S. H. (1999). Four-helical-bundle structure of the cytoplasmic domain of a serine chemotaxis receptor. *Nature* **400**, 787-792.
3. Pollard, A. M., Bilwes, A. M. & Crane, B. R. (2009). Structure of a soluble chemoreceptor suggests a mechanism for propagating conformational signals. *Biochemistry* **48**, 1936-1944.
4. Liu, J. D. & Parkinson, J. S. (1991). Genetic evidence for interaction between the CheW and Tsr proteins during chemoreceptor signaling by Escherichia coli. *Journal of Bacteriology* **173**, 4941-4951.
5. Boukhvalova, M. S., Dahlquist, F. W. & Stewart, R. C. (2002). CheW binding interactions with CheA and Tar - Importance for chemotaxis signaling in Escherichia coli. *Journal of Biological Chemistry* **277**, 22251-22259.
6. Miller, A. S., Kohout, S. C., Gilman, K. A. & Falke, J. J. (2006). CheA kinase of bacterial chemotaxis: Chemical mapping of four essential docking sites. *Biochemistry* **45**, 8699-8711.
7. Bhatnagar, J., Freed, J. H. & Crane, B. R. (2007). Rigid body refinement of protein complexes with long-range distance restraints from pulsed dipolar ESR. *Two-Component Signaling Systems, Pt B* **423**, 117-+.
8. Hazelbauer, G. L., Falke, J. J. & Parkinson, J. S. (2008). Bacterial chemoreceptors: high-performance signaling in networked arrays. *Trends in Biochemical Sciences* **33**, 9-19.

9. Maddock, J. R. & Shapiro, L. (1993). Polar location of the chemoreceptor complex in the Escherichia coli cell. *Science* **259**, 1717-1723.

10. Kentner, D., Thiem, S., Hildenbeutel, M. & Sourjik, V. (2006). Determinants of chemoreceptor cluster formation in Escherichia coli. *Molecular Microbiology* **61**, 407-417.

11. Sourjik, V. & Berg, H. C. (2000). Localization of components of the chemotaxis machinery of Escherichia coli using fluorescent protein fusions. *Molecular Microbiology* **37**, 740-751.

12. Zhang, P. J., Khursigara, C. M., Hartnell, L. M. & Subramaniam, S. (2007). Direct visualization of Escherichia coli chemotaxis receptor arrays using cryo-electron microscopy. *Proceedings of the National Academy of Sciences of the United States of America* **104**, 3777-3781.

13. Weis, R. M., Hirai, T., Chalah, A., Kessel, M., Peters, P. J. & Subramaniam, S. (2003). Electron microscopic analysis of membrane assemblies formed by the bacterial chemotaxis receptor Tsr. *Journal of Bacteriology* **185**, 3636-3643.

14. Lefman, J., Zhang, P. J., Hirai, T., Weis, R. M., Juliani, J., Bliss, D., Kessel, M., Bos, E., Peters, P. J. & Subramaniam, S. (2004). Three-dimensional electron microscopic Imaging of membrane invaginations in Escherichia coli overproducing the chemotaxis receptor Tsr. *Journal of Bacteriology* **186**, 5052-5061.

15. Khursigara, C. M., Zhang, P. J., Lefinan, J., Hartnell, L. M. & Subramaniam, S. (2007). Cryo-electron tomography of E.coli: structure and functional analysis of chemotaxis receptor assemblies. *Biophysical Journal*, 11A-11A.

16. Francis, N. R., Wolanin, P. M., Stock, J. B., DeRosier, D. J. & Thomas, D. R. (2004). Three-dimensional structure and organization of a receptor/signaling

complex. *Proceedings of the National Academy of Sciences of the United States of America* **101**, 17480-17485.

17. Gegner, J. A., Graham, D. R., Roth, A. F. & Dahlquist, F. W. (1992). Assembly of an MCP receptor, CheW and kinase CheA complex in the bacterial chemotaxis signal transduction pathway. *Cell* **70**, 975-982.
18. Wolanin, P. M., Baker, M. D., Francis, N. R., Thomas, D. R., DeRosier, D. J. & Stock, J. B. (2006). Self-assembly of receptor/signaling complexes in bacterial chemotaxis. *Proceedings of the National Academy of Sciences of the United States of America* **103**, 14313-14318.
19. Bilwes, A. M., Alex, L. A., Crane, B. R. & Simon, M. I. (1999). Structure of CheA, a signal-transducing histidine kinase. *Cell* **96**, 131-141.
20. Khursigara, C. M., Wu, X. W. & Subramaniam, S. (2008). Chemoreceptors in Caulobacter crescentus: Trimers of receptor dimers in a partially ordered hexagonally packed array. *Journal of Bacteriology* **190**, 6805-6810.
21. Briegel, A., Ding, H. J., Li, Z., Werner, J., Gitai, Z., Dias, D. P., Jensen, R. B. & Jensen, G. J. (2008). Location and architecture of the Caulobacter crescentus chemoreceptor array. *Molecular Microbiology* **69**, 30-41.

CHAPTER 6

MODELING CHEMOTAXIS PROTEINS IN THE HEXAGONAL LATTICE OF CHEMORECEPTOR ARRAYS

6.1 INTRODUCTION

Chemotaxis proteins are localized at the poles of the cell[1-4]. Recent cryo-electron tomography studies on wild type *Caulobacter crescentus* cells have revealed regular hexagonal arrays, which form a plate-like base that runs parallel to the inner membrane of the cell and is separated from it by distance of about 300 Å[5,6]. The order of this network rapidly deteriorates as the distance between the basal plate and the inner membrane decreases. The extended wall-like continuous density was found to agree well with the length of the receptor. Moreover, the electron density at the vertex of each hexagon can comfortably accommodate a trimer of receptor dimers. The observed geometry, or the lattice spacing in the hexagonal network, is inconsistent with previous models based on a "hedgerow of receptor dimers"[7] and a hexagonal array of CheA/CheW predicted by using plastic models [8]respectively. However, *in vivo* cross-linking studies[9], genetic studies[10]and kinase activation studies with receptors incorporated in nanodiscs[11]have supported a trimer of dimers as being the core signaling unit. The next set of complexity in understanding the architecture of this assembly is investigating the mode of association of CheA and CheW with trimeric receptors arranged into hexagonal arrays. Cryo-electron tomography detected low resolution density for CheA and CheW in the chemoreceptor arrays. Surprisingly, instead of being uniformly distributed over the hexagon, it appeared only beneath every other vertex of the hexagon[5]. However, another study reported it to be a continuous layer below the layer of receptors[6].

There is debate on the relative ratios of CheA, CheW and receptors in the soluble ternary complexes. Immunoblotting experiments have established cellular stoichometries in the ratio of one receptor trimer of dimers for each CheA dimer and two CheW monomers[12]. However, analysis of the *in vitro* assembly of the signaling complex by electron microscopy, single particle image analysis [13,14]and scanning densitometry of polyacrylamide gels [15] have suggested slightly different ratios: one receptor trimer for each CheA monomer and 4 CheW monomers. These results are still inconsistent with a low stoichiometric complex suggested by binding experiments using radiolabeled proteins[16]. Also, there has not been extensive research on understanding the in-depth structural aspect of the CheA/CheW/Receptor complex. Though there are many studies that have probed interaction surfaces between CheW and receptor, there is only one published work based on a cysteine modification technique[17]that describes a receptor interaction surface on CheA. Apart from this, in Chapters 4 and 5 we proposed a new model of the ternary complex where the helical axis of a receptor dimer runs anti-parallel to the dimerization domain P3 in CheA/CheW complex. In this work, we aim to bridge the gap between the current low resolution images describing the arrangement of CheA and CheW in the hexagonal lattice and the wealth of experimental information obtained from *in vitro* and genetic studies which describe proposed interaction surfaces between any pair of proteins.

Our procedure of modeling is guided by the geometrical constraints of the hexagonal lattice, as well as the steric restraints from the size and shape of the individual protein components. Finally, we propose two models for the arrangement of CheA/CheW in chemoreceptor arrays which mainly differ in the orientation of CheW and associated P5 domains. In both the models ("close-packed" and "open-space"), the CheA/CheW molecules are placed such that the P3 domain sits at the center of alternate edges of the hexagon, and the receptor-interaction surface of CheW is

optimally oriented towards the receptor. Also, the P1 and P2 domains are oriented away from the signaling region of receptors and have considerable degrees of freedom.

6.2 RESULTS

In this work we have used PDB coordinates of structures determined for *T.maritima* proteins: CheAΔ289[18], the complex of CheW with the P4, P5 domain of CheA[7] and TM14 receptor[19]. Combination of the former two structures produced a model of CheAΔ289 bound to two CheW's which is used for further modeling in the lattice. Receptors from *T.maritima* crystallize as dimers, unlike trimers of dimers in *E.coli*[20]. We superimposed the structure of a single TM14 dimer on each of the Tsr dimers to obtain a trimer of dimers arrangement of TM14 receptors. Six of these trimers are then oriented to form a hexagon such that the 3- fold axis of each trimer is separated by 75 Å from the adjacent trimer. We found that the space between two trimers, along the line joining their 3-fold axis, is just sufficient to accommodate the dimerization domain of CheA. To start with, in an isolated hexagon, we placed a single CheAΔ289/CheW complex with the P3 domain aligned at the center of the line joining the two trimers. Based on the model of the ternary complex that we proposed in Chapter 4 and 5, we aligned the helical axis of P3 domain anti-parallel to the receptor axis. It should be noted that the alignment of P3 domains on the hexagon edge imposes symmetry in the lattice since a single CheA/CheW complex can interact symmetrically with adjacent hexagons. The stacking together of four helical bundles in this fashion has been seen in the structures of *T.maritima* receptors [7,19]. Also, any other type of alignment, for instance pushing the P3 domains inside the hexagon, leads to steric clashes of CheA/CheW with receptors. This orientation of CheW's brings the predicted receptor interaction surface close to one set of receptor trimers. (Figure 6.1)

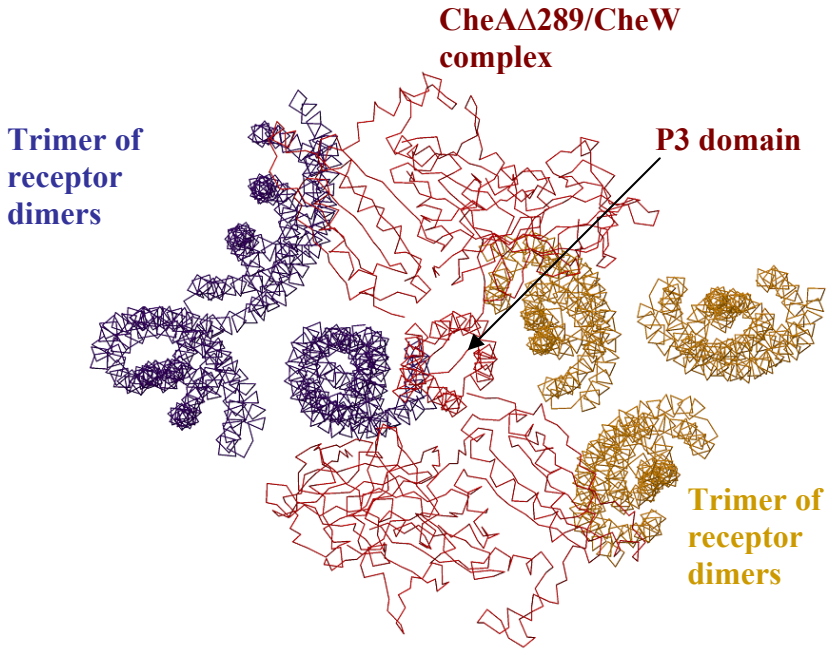

Figure 6.1. Alignment of CheAΔ289/CheW complex between two trimers of receptor dimers such that the P3 axis lies on the line joining the three-fold axis of each trimer. CheAΔ289/CheW complex is colored in red and two trimers of receptors are colored in indigo and mustard.

In each subunit, the N terminus of CheW (bound to the P5 domain) is in close proximity to at least one of the ends of the receptor dimers in the trimer unit. If we now superimpose the structures determined from crystallography and from Pulsed dipolar ESR (Chapter 4), we find that the latter aligns to the current CheA/CheW model to a greater extent. Positioning of CheA/CheW molecules at the center of all the edges of the hexagon results in severe steric clashes among receptors, CheW and CheA domains, hence this arrangement is ruled out. The situation improves dramatically if CheAΔ289/CheW molecules are placed only on alternate sides of the hexagon (Figure 6.2).

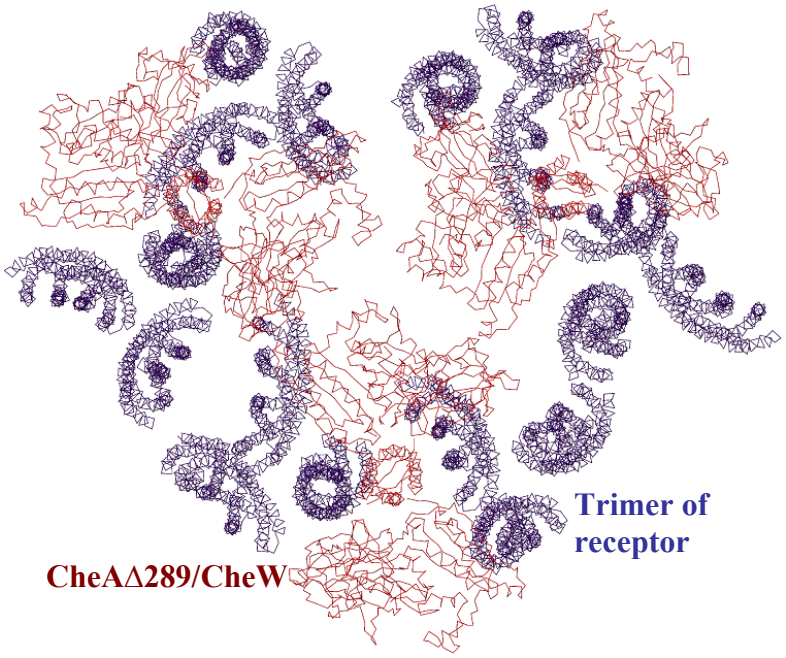

Figure 6.2. Arrangement of three molecules of CheAΔ289/CheW complex at the center of alternate edges in the hexagon formed by trimer of receptor dimers. All receptors are in colored in indigo and CheAΔ289/CheW molecules are in red.

The three sets of CheW and P4, P5 domains occupy most of the space inside the hexagon, hence we refer to this arrangement as the "close-packed" model. The three P5 domains directed towards the center of hexagon fall short of directly interacting with each other, leaving a small empty triangular (Figure 6.3) space at the center. Hence, the hydrophobic region near the subdomain 2 of the P5 domain remains exposed.

Now, starting from a single hexagon having an alternate arrangement of CheAΔ289/CheW molecules, we next attempt to build a two dimensional array. We observed that due to symmetry, the three sides of the hexagon along which there are no CheAΔ289/CheW molecules, form sides of three more hexagons that cannot accommodate any CheAΔ289/CheW complexes. Alternatively, every hexagon without

CheAΔ289/CheW molecules shares sides with six other hexagons, each having alternate arrangement of CheA/W molecules in their edges (Figure 6.4).

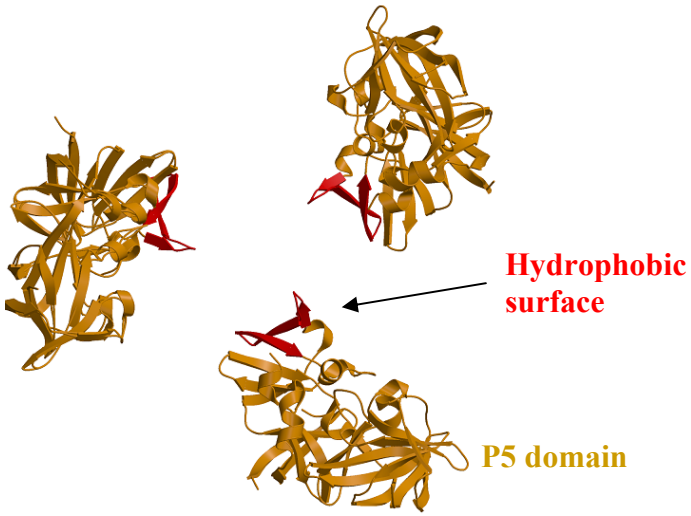

Figure 6.3. The orientation of three P5 domains in the "close-packed" model of hexagonal lattice. The surface on P5 domain highlighted in red is on the end of subdomain 2 and is hydrophobic in nature.

However, each trimer unit consistently has three nearest neighbors: two trimers and one CheA/CheW molecule. The CheA/CheW molecule is half as close as the other two trimers.

The CheAΔ289/CheW layer is about 75Å thick and if receptors are visualized as being vertical with the periplasmic domains at the top, then the bottom of this CheA/CheW layer lies in the plane containing the signaling tip region of receptor (Figure 6.5).

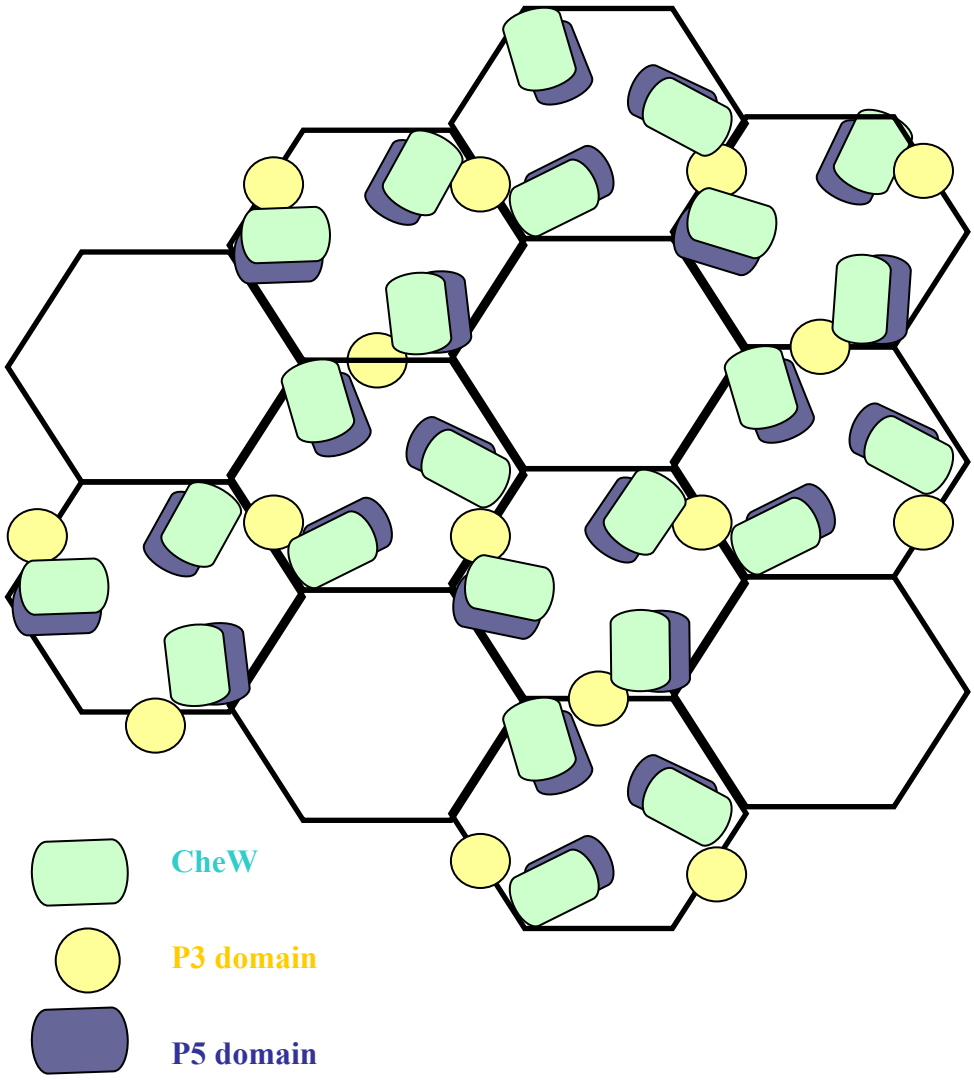

Figure 6.4. Schematic representation of hexagonal lattice in the “close-packed” model. P4 domains are oriented perpendicular to the plane of the lattice and are not shown. Trimer of receptor dimers sit on the vertex of every hexagon, and CheA/CheW molecules are oriented such that P3 domain sits on the center of alternate edges of hexagon. CheW and bound P5 domain are oriented inside the hexagon.

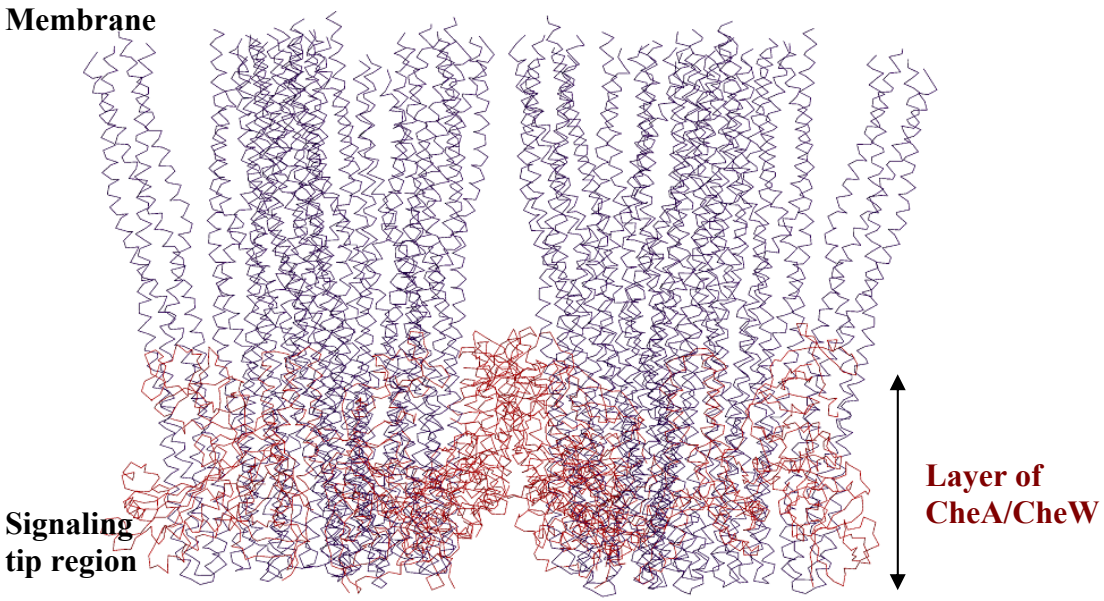

Figure 6.5. Layer of CheA and CheW lining the signaling tip region of chemoreceptors.

Due to molecular crowding in this layer, we propose that the P1 and P2 domains are located outside this plane, while being connected to the core CheA domains through long flexible linkers.

We propose a second model, where the orientation of CheW and the P5 domains in the hexagon allows for the interaction between hydrophobic ends of the P5 domains and the symmetric surface on the sub-domain 1 of CheW (Chapter 3). For simplicity, we refer to it as the "open-space" model. Here, in each CheA/CheW complex, both the P5 domains (bound to CheW) are rotated about the P4-P5 hinge such that plane containing CheW/P5 is approximately perpendicular to the P3 domain axis. A similar arrangement of CheW/P5 domains from the other two CheA/CheW complexes aligns the ends of the three CheW/P5 units very close to each other forming an approximate triangle. This arrangement results in considerable empty space at the center of the hexagon, hence we refer to it as the "open-space" model

(Figure 6.6). The proposed receptor interaction surface on CheW faces a set of receptor trimers in all the CheW/P5 units.

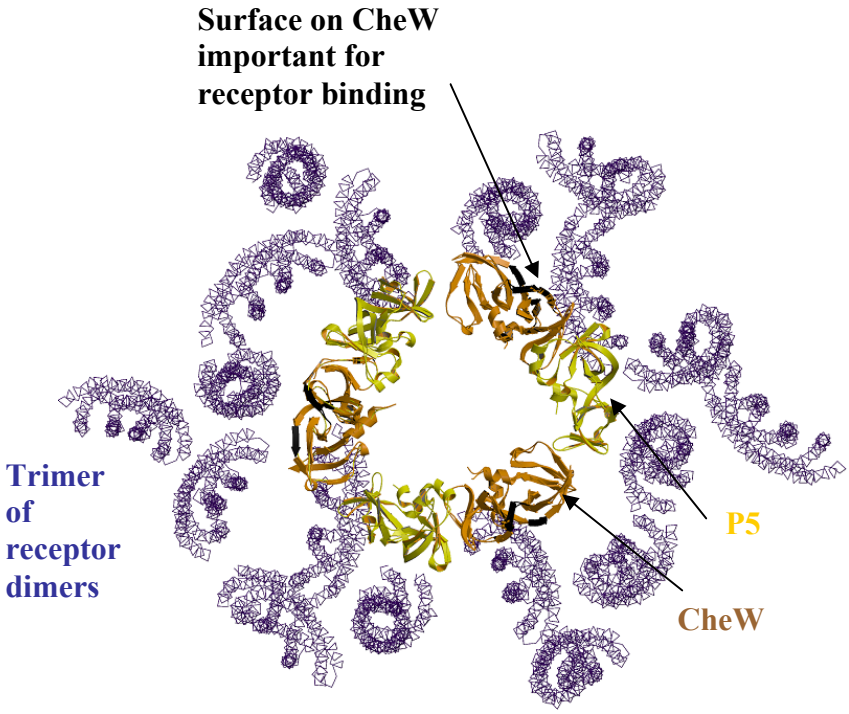

Figure 6.6. Arrangement of P5 domains and CheW in the "open-space" model. Trimer of receptors (indigo) form the vertices of the hexagon. CheW molecules (in mustard) while being bound to P5 domain (in yellow) form a ring type structure at the center of hexagon. The surface on CheW proposed to be important for receptor is marked in black.

The proximity constraint between the N-terminus of CheW and the signaling tip of receptors requires that this triangle sits in the plane containing the end/tip region of receptors. In this case, the P4 domains essentially move out of the plane, along with P1 and P2 domains. The main difference between our current model and the "closed-space" model is orientation of CheW and the P5 domains, while still maintaining alternate positioning of CheA/W molecules along the sides of each hexagon. This

implies that in the extended two dimensional array, the pattern of hexagons with and without CheA/CheW molecules does not change (Figure 6.7).

6.3 DISCUSSION

6.3.1 Overall arrangement of lattice

Chemoreceptors, CheA and CheW form dense, large-size arrays at the poles of the cell. The architecture of this network holds the key to understanding the remarkable features of chemotaxis such as sensitivity, gain and cooperativity. Electron microscopy detected an approximate hexagon pattern of arrays in *E.coli* cells over-expressing Tsr receptor. The core signaling unit in these hexagons has been determined to be a trimers of receptor dimers which agree well with the conclusions from numerous *in vitro* and *in vivo* experiments. Cryo-electron tomography on wild type *Caulobacter* cells has for the first time revealed information about the native state of arrays, as well as provided clues about the arrangement of CheA and CheW molecules in the lattice.

In *E.coli* cells overexpressing Tsr receptor, the lattice spacing of the hexagonal pattern of electron density is 75 Å which is quite different from the 120 Å found in wild type *Caulobacter* arrays. The reason behind this discrepancy is not known with certainty. We speculate that CheA and CheW proteins cause this longer separation by physically separating the two trimers. In this work, we have proposed two models of CheA/CheW/Receptor lattice ("open-space" and "close-packed") that are based on this idea. In each of them CheA/CheW molecules occupy center of alternate edges of the hexagon. In the EM analysis, additional density for CheA/CheW has been observed beneath alternate vertexes of the hexagon suggesting a stoichiometry of one receptor trimer for one CheA monomer and one CheW. However, due to low resolution of this

technique, it is difficult to know with certainty if the density is exactly beneath each vertex, or in-between two vertexes.

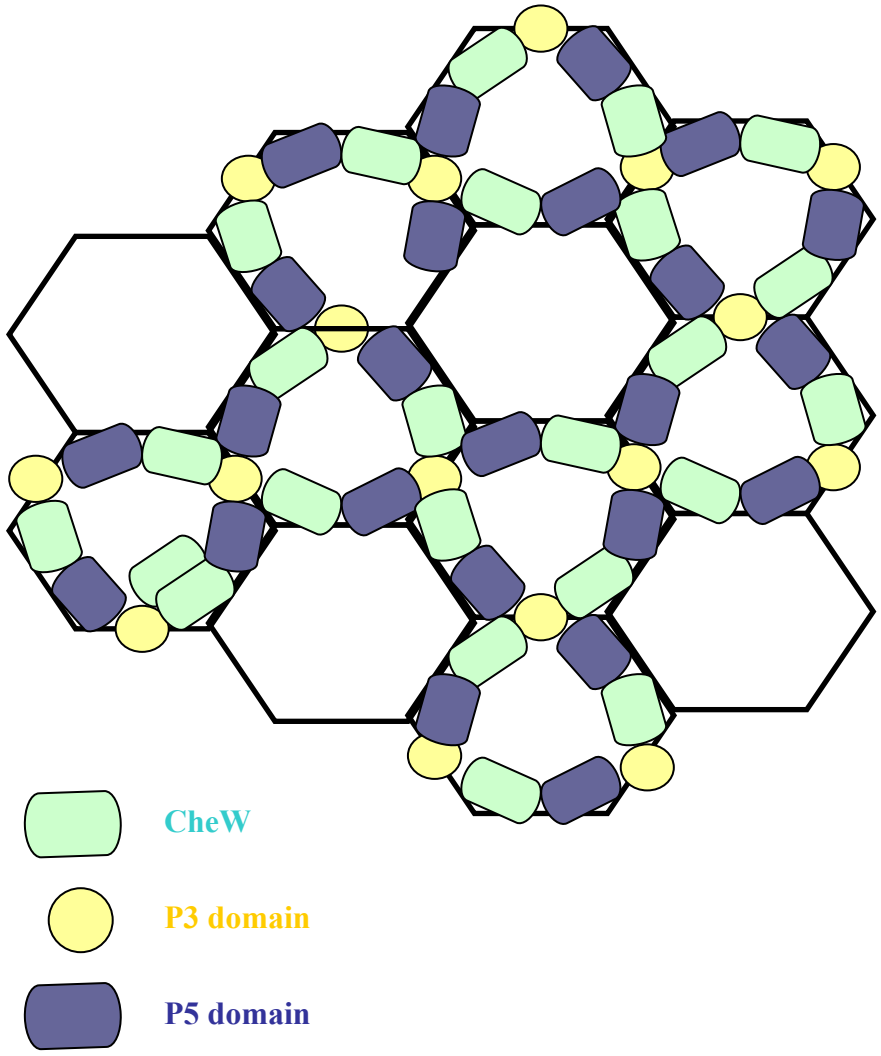

Figure 6.7. Schematic representation of hexagonal lattice in the "open-space" model. P4 domains are oriented perpendicular to the plane of the lattice and are not shown. Trimer of receptor dimers sit on the vertex of every hexagon, and CheA/CheW molecules are oriented such that P3 domain sits on the center of alternate edges of hexagon. CheW and bound P5 domain form a ring type structure inside the hexagon.

The latter scenario would agree well with our arrangement of CheA/CheW in the hexagon. This arrangement of CheA/W molecules imposes an additional symmetry in the two dimensional array which allows for the presence of hexagons that do not possess any CheA/CheW molecules.

6.3.2 Orientation of domains

The guidelines for determining the orientations of CheA domains and CheW were adopted from Chapter 4 and 5 where we proposed a structure of the ternary complex based on distance restraints from pulsed dipolar ESR spectroscopy. These were primarily: the antiparallel orientation of the P3 domain axis with respect to receptor axis, and the proximity of the N-terminus of CheW to the signaling tip of the receptor. Protection studies have identified two residues on P3 domain (roughly located at the N-terminal end and the hairpin region of P3) that directly interact with receptor. The arrangement of P3 domains in between two trimers does facilitate this interaction. The main difference between our two models is the orientation of CheW and associated P5 domains. However, in both models, the inter-subdomain region of CheW is oriented favorably to interact with the receptor. On the other hand, given the scarcity of experimental data on the orientation of the P4 and P5 domain with respect to receptor, the optimum orientation of these domains is still unclear. However, since CheW and P5 domain share a strong binding interaction, the orientation of the latter is somewhat predetermined by that of CheW. Protection studies have identified a single residue on the P4 and P5 domain that is crucial for receptor binding[17]. However, the residue on the P5 domain is buried, and hence unlikely to interact with the receptor. On the other hand, the residue on P4 resides on the face that directly orients towards the receptor in our model, hence agrees with this data. Moreover, interaction with two

other sites on P3 domain is also satisfied since the domain sits in the middle of two receptor trimers.

Cryo-electron tomography detected extra density for CheA and CheW roughly near the cytoplasmic end of the chemoreceptor array. A closer look at the extra density reveals that it spreads towards the center of the hexagon. In the "close-packed" model, the CheW, P4 and P5 domains from three CheA/CheW molecules indeed occupy the majority of space inside the hexagon, leaving a small empty space at the center. In contrast, in the "open-space" model, since CheW and the P5 domains line up along the sides of the hexagon, the alternate pattern of density may correspond to the position of P4 domains which come out of the plane containing tip region of receptors (Figure 6.8) The density from CheW and P5 domains perhaps becomes continuous with that of the receptors and hence may be difficult to detect.

Another difference between the two models is in the thickness of the CheAΔ289/CheW layer. In the open-space model, this layer is approximately 15 Å thinner since the CheW and P5 domains are oriented parallel to the plane formed by the signaling tips of receptors.

It should be noted that in both the models, the P1 and P2 domains protrude outwards from the layer of CheAΔ289/CheW and hence can be expected to have considerable freedom of motion. *In vitro* pulsed dipolar ESR studies (Chapter 4) and NMR experiments have also established that the P1 and P2 domains are fairly mobile and do not have stable interactions with the core CheA complex[21,22]. Auto-phosphorylation of CheA would require the P1 domains to reach up to CheA/CheW layer and interact with the P4 domains. The central empty space in the "open-space" model perhaps makes the two domains more accessible to each other. Also, steric reasons may prevent the P1 and P4 domains from the same subunits to interact with each other.

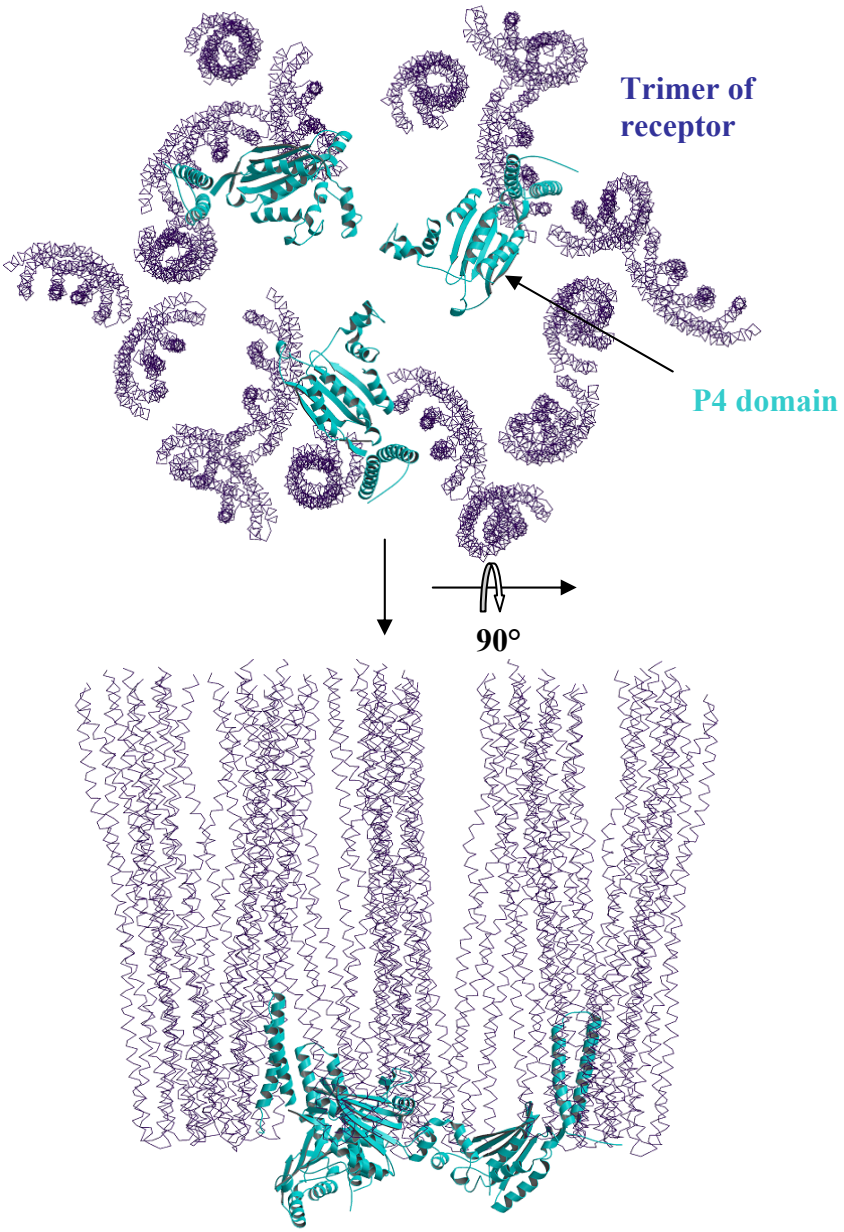

Figure 6.8. Orientation of P4 domains in the "open-space" model. All the other domains are deleted for clarity.

However, the “close-packed” model fails to account for the exposed hydrophobic region at the sub-domain 2 of P5 domains. Given the abundance of hydrophobic residues on this surface, it seems highly likely that this surface gets buried while interacting with other proteins. It has been reported that this region acts as an interface for associating CheAΔ289 molecules in the crystal lattice, as well as in the solution to some extent (chapter 3). The “open-space” model resolves this energetically unfavorable scenario by associating the exposed ends of the P5 domain and bound CheW from each CheA/CheW molecule with that of the neighboring molecule resulting in a triangle like pattern inside the hexagon. This is achieved by rotating the P5 domain (with CheW bound) about the P4-P5 hinge. The freedom of rotation of domains about the hinges has been previously attributed to the presence of different subunit conformations in the crystal structure of CheAΔ289 dimer.
The 75Å separation between the trimers does not allow them to directly interact with each other, unless they undergo dynamic motion. On the other hand, each trimer interacts with the CheA/W along the edge, or with domains located inside of the hexagon which perhaps give additional stability to the hexagon. A combination of these interactions may be responsible for propagation of signal throughout the array. The different nature of packing in these two types of hexagons may be responsible for local disorder seen in the chemoreceptor arrays. It is also possible that switching between these two forms of packing is the mode of regulation in chemotaxis.

REFERENCES

1. Maddock, J. R. & Shapiro, L. (1993). Polar location of the chemoreceptor complex in the Escherichia coli cell. *Science* **259**, 1717-1723.
2. Kentner, D., Thiem, S., Hildenbeutel, M. & Sourjik, V. (2006). Determinants of chemoreceptor cluster formation in Escherichia coli. *Molecular Microbiology* **61**, 407-417.
3. Zhang, P. J., Khursigara, C. M., Hartnell, L. M. & Subramaniam, S. (2007). Direct visualization of Escherichia coli chemotaxis receptor arrays using cryo-electron microscopy. *Proceedings of the National Academy of Sciences of the United States of America* **104**, 3777-3781.
4. Sourjik, V. & Berg, H. C. (2000). Localization of components of the chemotaxis machinery of Escherichia coli using fluorescent protein fusions. *Molecular Microbiology* **37**, 740-751.
5. Khursigara, C. M., Wu, X. W. & Subramaniam, S. (2008). Chemoreceptors in Caulobacter crescentus: Trimers of receptor dimers in a partially ordered hexagonally packed array. *Journal of Bacteriology* **190**, 6805-6810.
6. Briegel, A., Ding, H. J., Li, Z., Werner, J., Gitai, Z., Dias, D. P., Jensen, R. B. & Jensen, G. J. (2008). Location and architecture of the Caulobacter crescentus chemoreceptor array. *Molecular Microbiology* **69**, 30-41.
7. Park, S. Y., Borbat, P. P., Gonzalez-Bonet, G., Bhatnagar, J., Pollard, A. M., Freed, J. H., Bilwes, A. M. & Crane, B. R. (2006). Reconstruction of the chemotaxis receptor-kinase assembly. *Nature Structural & Molecular Biology* **13**, 400-407.

8. Shimizu, T. S., Le Novere, N., Levin, M. D., Beavil, A. J., Sutton, B. J. & Bray, D. (2000). Molecular model of a lattice of signalling proteins involved in bacterial chemotaxis. *Nature Cell Biology* **2**, 792-796.

9. Studdert, C. A. & Parkinson, J. S. (2004). Crosslinking snapshots of bacterial chemoreceptor squads. *Proceedings of the National Academy of Sciences of the United States of America* **101**, 2117-2122.

10. Ames, P., Studdert, C. A., Reiser, R. H. & Parkinson, J. S. (2002). Collaborative signaling by mixed chemoreceptor teams in Escherichia coli. *Proceedings of the National Academy of Sciences of the United States of America* **99**, 7060-7065.

11. Boldog, T., Grimme, S., Li, M. S., Sligar, S. G. & Hazelbauer, G. L. (2006). Nanodiscs separate chemoreceptor oligomeric states and reveal their signaling properties. *Proceedings of the National Academy of Sciences of the United States of America* **103**, 11509-11514.

12. Li, M. S. & Hazelbauer, G. L. (2004). Cellular stoichiometry of the components of the chemotaxis signaling complex. *Journal of Bacteriology* **186**, 3687-3694.

13. Wolanin, P. M., Baker, M. D., Francis, N. R., Thomas, D. R., DeRosier, D. J. & Stock, J. B. (2006). Self-assembly of receptor/signaling complexes in bacterial chemotaxis. *Proceedings of the National Academy of Sciences of the United States of America* **103**, 14313-14318.

14. Francis, N. R., Wolanin, P. M., Stock, J. B., DeRosier, D. J. & Thomas, D. R. (2004). Three-dimensional structure and organization of a receptor/signaling complex. *Proceedings of the National Academy of Sciences of the United States of America* **101**, 17480-17485.

15. Levit, M. N., Grebe, T. W. & Stock, J. B. (2002). Organization of the receptor-kinase signaling array that regulates Escherichia coli chemotaxis. *Journal of Biological Chemistry* **277**, 36748-36754.

16. Gegner, J. A., Graham, D. R., Roth, A. F. & Dahlquist, F. W. (1992). Assembly of an MCP receptor, CheW, and kinase CheA complex in the bacterial chemotaxis signal transduction pathway. *Cell* **70**, 975-982.

17. Miller, A. S., Kohout, S. C., Gilman, K. A. & Falke, J. J. (2006). CheA kinase of bacterial chemotaxis: Chemical mapping of four essential docking sites. *Biochemistry* **45**, 8699-8711.

18. Bilwes, A. M., Alex, L. A., Crane, B. R. & Simon, M. I. (1999). Structure of CheA, a signal-transducing histidine kinase. *Cell* **96**, 131-141.

19. Pollard, A. M., Bilwes, A. M. & Crane, B. R. (2009). The Structure of a Soluble Chemoreceptor Suggests a Mechanism for Propagating Conformational Signals. *Biochemistry* **48**, 1936-1944.

20. Kim, K. K., Yokota, H. & Kim, S. H. (1999). Four-helical-bundle structure of the cytoplasmic domain of a serine chemotaxis receptor. *Nature* **400**, 787-792.

21. McEvoy, M. M., delaCruz, A. F. A. & Dahlquist, F. W. (1997). Large modular proteins by NMR. *Nature Structural Biology* **4**, 9-9.

22. Zhou, H. J., McEvoy, M. M., Lowry, D. F., Swanson, R. V., Simon, M. I. & Dahlquist, F. W. (1996). Phosphotransfer and CheY-binding domains of the histidine autokinase CheA are joined by a flexible linker. *Biochemistry* **35**, 433-443.